

Technical Report Documentation Page

1. Report No. FHWA/TX-06/0-4835-1		2. Government Accession No.		3. Recipient's Catalog No.	
4. Title and Subtitle Evaluation of Non-Nuclear Methods for Compaction Control			5. Report Date July 2006		
			6. Performing Organization Code		
7. Author(s) Ellen M. Rathje, Stephen G. Wright, Kenneth H. Stokoe II, Ashley Adams, Ruth Tobin, Manal Salem			8. Performing Organization Report No. 0-4835-1		
9. Performing Organization Name and Address Center for Transportation Research The University of Texas at Austin 3208 Red River, Suite 200 Austin, TX 78705-2650			10. Work Unit No. (TRAIS)		
			11. Contract or Grant No. 0-4835		
12. Sponsoring Agency Name and Address Texas Department of Transportation Research and Technology Implementation Office P.O. Box 5080 Austin, TX 78763-5080			13. Type of Report and Period Covered Technical Report September 2003–August 2005		
			14. Sponsoring Agency Code		
15. Supplementary Notes Project performed in cooperation with the Texas Department of Transportation and the Federal Highway Administration.					
16. Abstract <p>This study evaluated currently available, non-nuclear devices as potential replacements for the nuclear gauge for soil compaction control. Devices based on impact methods, electrical methods, and stiffness methods were identified and evaluated through two field studies and two laboratory studies. Based on these studies, none of the devices tested is feasible to replace the nuclear gauge. Additionally, many of the devices do not provide a measure of water content, and thus would require another device to measure water content when water content is required for compaction control. Of the devices tested, two devices based on the measurement of electrical soil properties showed the most promise. However, improvements are required before these devices can be used in practice.</p>					
17. Key Words Compaction, Density, Water Content, Nuclear Gauge			18. Distribution Statement No restrictions. This document is available to the public through the National Technical Information Service, Springfield, Virginia 22161; www.ntis.gov.		
19. Security Classif. (of report) Unclassified		20. Security Classif. (of this page) Unclassified		21. No. of pages 144	
				22. Price	





## **Evaluation of Non-Nuclear Methods for Compaction Control**

Ellen M. Rathje  
Stephen G. Wright  
Kenneth H. Stokoe II  
Ashley Adams  
Ruth Tobin  
Manal Salem

---

CTR Technical Report:	0-4835-1
Report Date:	July 2006
Project:	0-4835
Project Title:	Assessment of Rapid Methods for Density Control of MSE Walls and Embankments
Sponsoring Agency:	Texas Department of Transportation
Performing Agency:	Center for Transportation Research at The University of Texas at Austin

Project performed in cooperation with the Texas Department of Transportation and the Federal Highway Administration.

Center for Transportation Research  
The University of Texas at Austin  
3208 Red River  
Austin, TX 78705

[www.utexas.edu/research/ctr](http://www.utexas.edu/research/ctr)

Copyright (c) 2007  
Center for Transportation Research  
The University of Texas at Austin

All rights reserved  
Printed in the United States of America

## **Disclaimers**

**Author's Disclaimer:** The contents of this report reflect the views of the authors, who are responsible for the facts and the accuracy of the data presented herein. The contents do not necessarily reflect the official view or policies of the Federal Highway Administration or the Texas Department of Transportation (TxDOT). This report does not constitute a standard, specification, or regulation.

**Patent Disclaimer:** There was no invention or discovery conceived or first actually reduced to practice in the course of or under this contract, including any art, method, process, machine manufacture, design or composition of matter, or any new useful improvement thereof, or any variety of plant, which is or may be patentable under the patent laws of the United States of America or any foreign country.

### **Engineering Disclaimer**

NOT INTENDED FOR CONSTRUCTION, BIDDING, OR PERMIT PURPOSES.

## **Acknowledgments**

The authors express appreciation to the following TxDOT personnel: Marcus Galvan (Project Director), members of the Project Monitoring Committee (Darlene Goehl, Mike Arellano, John Delphia, and Gregg Cleveland), and the Program Coordinator, Jeff Seiders.

# Table of Contents

<b>1. Introduction.....</b>	<b>1</b>
1.1 Research Objectives.....	1
1.2 Research Methodology .....	1
<b>2. Potential Methods for Compaction Control.....</b>	<b>3</b>
2.1 Introduction.....	3
2.2 Traditional Methods.....	3
2.3 Impact Methods .....	6
2.4 Electrical Methods .....	13
2.5 Stiffness Methods .....	20
2.6 Selection of Methods for Study .....	29
<b>3. Field Study 1.....</b>	<b>33</b>
3.1 Introduction.....	33
3.2 Material Description .....	33
3.3 Description of Field Testing .....	36
3.4 Equipment Calibration.....	38
3.5 Field Test Results.....	43
3.6 Summary.....	62
<b>4. Field Testing Program 2.....</b>	<b>65</b>
4.1 Introduction.....	65
4.2 Material Description .....	65
4.3 Equipment Calibration.....	67
4.4 Field Test Results.....	76
4.5 Summary.....	81
<b>5. Laboratory Testing Program.....</b>	<b>83</b>
5.1 Introduction.....	83
5.2 Material Description .....	83
5.3 Laboratory Testing Procedures .....	84
5.4 Equipment Calibration.....	86
5.5 Laboratory Test Results .....	90
5.6 Summary.....	97
<b>6. Practical Issues.....</b>	<b>99</b>
6.1 Introduction.....	99
6.2 Impact Methods .....	99
6.3 Electrical Methods .....	100
6.4 Stiffness Methods .....	101
6.5 Summary.....	102
<b>7. Stiffness of Compacted Soil Specimens.....</b>	<b>105</b>
7.1 Introduction.....	105
7.2 Background.....	105
7.3 Experimental Program .....	109

7.4 Experimental Results .....	111
7.5 Summary .....	118
<b>8. Conclusions and Recommendations.....</b>	<b>121</b>
8.1 Summary and Conclusions .....	121
8.2 Recommendations.....	123
<b>References.....</b>	<b>125</b>

## List of Figures

Figure 2.1. Rubber balloon apparatus.....	4
Figure 2.2. Schematic of nuclear gauge in (a) direct transmission and (b) backscatter modes.....	6
Figure 2.3. The PANDA dynamic cone penetrometer.....	7
Figure 2.4. Example of PANDA result displaying measured values, failure line, and tolerance line.....	9
Figure 2.5. Schematic of Clegg Impact Hammer (ASTM D5874).....	10
Figure 2.6. Determination of target CIV from testing at a range of water contents (ASTM D 5874).....	11
Figure 2.7. Schematic of standard DCP (ASTM D6951).....	12
Figure 2.8. Example of DCP field data.....	12
Figure 2.9. MDI field testing:.....	14
Figure 2.10. Example TDR waveform (Durham 2005).....	15
Figure 2.11. Effect of soil type on the TDR waveform (Durham 2005). ....	18
Figure 2.12. (a) Photograph of Electrical Density Gauge (GENEQ Inc. 2006), (b) plan view of EDG probe layout.....	19
Figure 2.13. Soil Quality Indicator (TransTech Systems 2004).....	20
Figure 2.14. Qualitative representation of dielectric spectrum (Drnevich et al. 2001). ....	20
Figure 2.15. PSPA components and data acquisition system.....	21
Figure 2.16. Schematic of GeoGauge (Humboldt 1999a).....	23
Figure 2.17. Field-measured seismic modulus versus GeoGauge (HSG) foundation stiffness.....	24
Figure 2.18. Field-measured dry unit weight versus GeoGauge (HSG) foundation stiffness from (a) Chen et al.( 1999) and (b) Ellis and Bloomquist (2003).....	25
Figure 2.19. Soil compaction supervisor sensor and control unit (MBW 2003).....	26
Figure 2.20. Soil stiffness versus number of passes of compaction equipment (Miller and Mallick 2003).....	27
Figure 2.21. Compaction monitoring using the SCS (Heitzler 1995). ....	28
Figure 2.22. Percent Standard Proctor compaction at SCS stop signal (Cardenas 2000).....	29
Figure 3.1. Grain-size distributions of materials selected for Field Study 1.....	34
Figure 3.2. Compaction curves for Soil I.....	35
Figure 3.3. Compaction curves for Soil II.....	35
Figure 3.4. Compaction curves for Soil III.....	36
Figure 3.5. Compacted field test pads for Field Study 1.....	37
Figure 3.6. Layout of test locations within field test pads.....	37
Figure 3.7. French soil classification system chart (Rivat 2005).....	39
Figure 3.8. Variation of CIV with water content for Soil I.....	40

Figure 3.9. Variation of CIV with dry unit weight for Soil I.....	41
Figure 3.10. Variation of CIV with water content for Soil II.....	41
Figure 3.11. Variation of CIV with dry unit weight for Soil II.....	42
Figure 3.12. Variation of CIV with water content for Soil III.....	42
Figure 3.13. Variation of CIV with dry unit weight for Soil III.....	43
Figure 3.14. Comparison of moist unit weights measured by the nuclear gauge and rubber balloon test for Soil I.....	44
Figure 3.15. Dry unit weights for Soil I measured by the nuclear gauge and rubber balloon test methods.....	44
Figure 3.16. CIV versus dry unit weight and water content for Soil I.....	46
Figure 3.17. PSPA Young's Modulus versus dry unit weight and water content for Soil I.....	46
Figure 3.18. PANDA dynamic cone resistance profiles for Soil I at locations 2 and 8.....	47
Figure 3.19. DCP profiles for Soil I at locations 2 and 8.....	48
Figure 3.20. Comparison of moist unit weights measured by the nuclear gauge and rubber balloon test for Soil II.....	49
Figure 3.21. Dry unit weights for Soil II measured by the nuclear gauge and rubber balloon test methods.....	49
Figure 3.22. CIV versus dry unit weight and water content for Soil II.....	50
Figure 3.23. PSPA Young's Modulus versus dry unit weight and water content for Soil II.....	51
Figure 3.24. PANDA dynamic cone resistance profiles for Soil II at locations 1 and 8.....	52
Figure 3.25. DCP profiles for Soil II at locations 1 and 8.....	52
Figure 3.26. Comparison of moist unit weights measured by the nuclear gauge and rubber balloon test for Soil III.....	54
Figure 3.27. Dry unit weights for Soil III measured by the nuclear gauge and rubber balloon test methods.....	55
Figure 3.28. CIV versus dry unit weight for Soil III.....	55
Figure 3.29. PSPA Young's Modulus versus dry unit weight for Soil III.....	55
Figure 3.30. PANDA dynamic cone resistance profiles for Soil III at locations 4 and 8.....	57
Figure 3.31. DCP profiles for Soil III at locations 4 and 8.....	57
Figure 3.32. CIV versus dry unit weight for Soil IV.....	58
Figure 3.33. PSPA Young's Modulus versus dry unit weight for Soil III.....	59
Figure 3.34. PANDA dynamic cone resistance profiles for Soil IV at locations 2 and 4.....	60
Figure 3.35. DCP profiles for Soil III at locations 4 and 8.....	60
Figure 3.36. CIV versus dry unit weight for Soil V.....	61
Figure 3.37. PSPA Young's Modulus versus dry unit weight for Soil V.....	62
Figure 4.1. Locations of field testing ( <a href="http://maps.google.com">http://maps.google.com</a> ).....	66
Figure 4.2. Grain size distributions of soils from Field Study 2.....	66
Figure 4.3. Standard Proctor compaction curves for the soils from Field Study 2.....	67
Figure 4.4. (a) Center rod being driven into the MDI calibration specimen, (b) MDI calibration specimen with the mold collar and multiple rod probe in place (Durham 2005).....	68
Figure 4.5. Representative MDI calibration waveform for poorly-graded sand.....	69

Figure 4.6. Representative MDI calibration waveforms for Taylor clay.....	70
Figure 4.7. MDI calibration data for Taylor clay.....	71
Figure 4.8. Representative MDI calibration waveforms for the low plasticity clay.....	72
Figure 4.9. MDI calibration data for the low plasticity clay.....	73
Figure 4.10. Representative MDI calibration waveforms for the sandy clay.....	74
Figure 4.11. MDI calibration data for the sandy clay.....	75
Figure 4.12. Comparison of (a) dry unit weight and (b) water content measured by the MDI, rubber balloon, and nuclear gauge for Taylor Clay.....	77
Figure 4.13. MDI waveform for measurement in Taylor Clay that resulted in a value of 48 pcf for dry unit weight and a water content of 10.7%. .....	78
Figure 4.14. Comparison of (a) dry unit weight and (b) water content measured by the MDI, rubber balloon, and nuclear gauge for low plasticity clay.....	79
Figure 4.15. Comparison of (a) dry unit weight and (b) water content measured by the MDI, rubber balloon, and nuclear gauge for the sandy clay.....	80
Figure 5.1. Grain size distribution of poorly graded sand used in laboratory testing.....	83
Figure 5.2. Grain size distribution of poorly graded sand used in laboratory testing.....	84
Figure 5.3. Laboratory test box.....	85
Figure 5.4. Location of compaction control tests within test specimens.....	86
Figure 5.5. MDI calibration data for the poorly graded sand.....	87
Figure 5.6. Failure and tolerance lines for the poorly graded sand obtained from the PANDA soil library (Sol-Solution 2006).....	89
Figure 5.7. Variation of CIV with water content for poorly graded sand.....	90
Figure 5.8. Variation of total unit weight with depth and horizontal location (points 1, 2, 4, and 5 are at the corners, point 3 is at the center).....	91
Figure 5.9. Comparison of (a) dry unit weight and (b) water content from rubber balloon testing, microwave oven, MDI, and EDG. ....	94
Figure 5.10. PANDA $q_d$ profiles for (a) specimen 1, test 1 and (b) specimen 6, test 1.....	95
Figure 7.1. Effect of compaction water content and dry density on matric suction for compacted Goose Lake clay (Olson and Langfelder, 1965).....	106
Figure 7.2. Matric suction values for specimens compacted at different dry unit weights and water contents (Gonzalez and Colmenares, 2006).....	106
Figure 7.3. Effect of degree of saturation on the small-strain shear modulus (Wu et al. 1984).....	107
Figure 7.4. Results of stiffness testing on compacted Waipio silt: (a) compaction curves, (b) dry unit weight versus stiffness, (c) stiffness versus water content, and (d) stiffness versus degree of saturation (Ooi and Pu 2003).....	108
Figure 7.5. Shear stiffness versus matric suction for London clay (Marinho et al., 1995).....	109
Figure 7.6. Schematic of piezoelectric transducer test up (Bringoli et al. 1996).....	110
Figure 7.7. Triaxial end platens designed for the test specimens.....	110
Figure 7.8. Measured shear wave velocities for specimens compacted at different values of water content and dry unit weight.....	111

Figure 7.9. Measured shear wave velocity versus (a) water content, (b) dry unit weight, and (c) degree of saturation. ....	113
Figure 7.10. Measured compression wave velocity versus (a) water content, (b) dry unit weight, and (c) degree of saturation.....	114
Figure 7.11. Measured matric suction for specimens compacted at different values of water content and dry unit weight.....	115
Figure 7.12. Measured values of matric suction versus water content. ....	116
Figure 7.13. Measured values of (a) shear modulus and (b) constrained modulus vs matric suction.....	117
Figure 7.14. Normalized values of (a) shear modulus and (b) constrained modulus vs matric suction.....	118

## List of Tables

Table 2.1. Compaction control devices selected for experimental studies .....	30
Table 2.2. Compaction control devices used in each experimental study. ....	31
Table 3.1. Five soil types selected for Field Study 1 (TxDOT 2004b).....	33
Table 3.2. TxDOT material gradations for retaining walls (TxDOT 2004b) .....	34
Table 3.3. List of devices tested on each test pad.....	38
Table 3.4. French soil classification of test soils .....	40
Table 3.5. Results for Soil I from compaction control devices .....	45
Table 3.6. Results for Soil II from compaction control devices .....	50
Table 3.7. Results for Soil III from compaction control devices.....	54
Table 3.8. Results for Soil IV from compaction control devices.....	58
Table 3.9. Results for Soil V from compaction control devices.....	61
Table 3.10. Summary of results from Field Study 1 .....	64
Table 4.1. MDI calibration coefficients for soils from Field Study 2.....	76
Table 4.2. Summary of results from Field Study 2.....	81
Table 5.1. Target compaction conditions for laboratory test specimens .....	85
Table 5.2. Recommended values of relative compaction and water content for EDG calibration in sandy soil (Electrical Density Gauge, LLC 2004).....	88
Table 5.3. Data set used to develop EDG soil model for the poorly graded sand .....	88
Table 5.4. Summary of PANDA measurements from laboratory test specimens .....	96
Table 5.5. CIV measurements from laboratory test specimens .....	97
Table 6.1. Comparison of Practical Issues for Compaction Control Devices .....	103



# **1. Introduction**

## **1.1 Research Objectives**

The performance of earth structures, such as earth retaining walls and embankments, is predominantly controlled by the engineering properties of the backfill. To ensure that the backfill has adequate strength and low compressibility, the soil is compacted with heavy compaction equipment. The criteria used to assess the field compaction of backfill materials are (1) achieving a specified minimum acceptable dry unit weight and (2) achieving a water content within a specified range. It is generally assumed that if the as-compacted backfill meets these criteria, the backfill and earth structure will perform satisfactorily. To assess compaction and the degree to which it meets the as-compacted backfill criteria, compaction control is performed in the field by measuring the dry unit weight and moisture content of the compacted fill. The nuclear gauge is the most common device used to make these measurements because it is very rapid and, thus, does not delay the construction schedule. However, due to increased regulatory restrictions and growing concerns over the safety of using a device with a nuclear source, there is an increased effort to find a possible alternative to the nuclear gauge for compaction control. The replacement device must accurately assess the properties of the compacted fill and do so in a timely manner that does not impact construction.

The goal of this study is to evaluate non-nuclear devices that are currently available and that could replace the nuclear gauge for soil compaction control. The specific application of this device is for the quality control of compaction of earth embankments and mechanically stabilized earth (MSE) wall backfill.

## **1.2 Research Methodology**

This research included several tasks aimed at achieving the objectives. First, a comprehensive literature review was conducted to identify available compaction control devices, understand the theoretical basis behind each device, and collect information on previous studies of each device. Generally, these devices fell into three broad categories: impact methods, electrical methods, and stiffness methods. Based on this literature review, which is discussed in Chapter 2, seven devices (three impact methods, three electrical methods, and one stiffness method) were selected for study in an experimental program.

The seven devices were evaluated through an experimental testing program that included two field studies (Chapter 3 and 4) and a laboratory study (Chapter 5). The first field study tested five of the seven devices on different soils representing typical soils used in Texas for the construction of embankments and retaining walls. Compacted stockpiles were constructed for use in this first field study. Testing included comparison of the results from the new compaction control devices with results from traditional nuclear gauge testing, rubber balloon testing, and oven-drying. The second field study tested the two additional devices, both of which were based on electrical methods. These devices were tested at three construction sites in central Texas. The laboratory study focused on testing the devices under controlled laboratory conditions. Specimens of sand were constructed in large laboratory test boxes at different compaction levels and each device was used to assess the compaction of soil in each box. After completion of the field and laboratory evaluations of the compaction control devices, each device was also assessed

based on various practical issues such as ease of use, calibration, and standardization (Chapter 6).

An additional laboratory study (Chapter 7) was performed on small-scale compacted clay specimens to assess the relationship between soil stiffness and compaction conditions (dry unit weight, water content). This experimental study included shear wave and compression wave velocity testing using piezoelectric bender elements and piezoelectric disks, respectively, in a triaxial cell. The shear and compression wave velocities were converted to shear moduli and constrained compression moduli, and related to the known dry unit weight and water content of the specimens. Additionally, pressure plate tests were performed on compacted clay specimens to measure the matric suction for different values of water content and dry unit weight.

## **2. Potential Methods for Compaction Control**

### **2.1 Introduction**

A literature review was performed to identify non-nuclear compaction control devices that are currently available for use. Nine devices were identified: three based on impact methods, three based on electrical methods, and three based on stiffness methods. This chapter describes the technical basis and procedures for using each compaction control device and discusses previous studies that evaluated each device. Additionally, the traditional methods used for compaction control are described. The selection of the devices for further investigation in this study is provided.

### **2.2 Traditional Methods**

Traditional methods of measuring soil unit weight and water content were employed as the standard for comparison for the methods being evaluated in this study. These traditional methods include rubber balloon unit weight measurement, oven-dry water content measurement, microwave-oven water content measurement, and nuclear gauge unit weight and water content measurement.

#### **2.2.1 Rubber Balloon Density**

The rubber balloon method (ASTM D2167) for measuring the in situ density of soil involves excavating a test hole in the compacted soil, weighing the excavated soil, and measuring the volume of the hole by inflating a balloon in the hole. The volume of the hole is assessed by measuring the volume of water required to inflate the balloon in the hole. The total unit weight is calculated by dividing the total weight of soil excavated from the hole by the volume of the hole. To obtain the dry unit weight of the soil, the water content of the soil must be determined by either the oven-dry water content method (ASTM D2216) or the microwave-oven dry water content method (ASTM D 4643).

The rubber balloon apparatus (Figure 2.1) consists of a metal base plate with a 4-in. diameter hole in the center and a water-filled calibrated vessel with a flexible, elastic, rubber balloon at the base. There is a valve on the side of the vessel that is attached to a pressure gauge so that an externally controlled pressure can be applied to the water to inflate the rubber balloon to measure the volume of the excavated hole.

To perform a unit weight measurement, the metal base plate is placed on a level testing location. The rubber balloon apparatus is placed on the base plate and pressurized so the rubber balloon inflates to fill the void between the ground surface and base plate. The volume indicated on the graduated vessel is recorded as the initial volume. The rubber balloon apparatus is removed from the base plate and a test hole is excavated beneath the 4- in. diameter hole in the plate. Typically, the hole is approximately 4 in. deep. The soil removed from the hole is placed in an air-tight bag and weighed. The rubber balloon apparatus is placed back on the base plate and pressurized until the rubber balloon is inflated to the same size as the test hole. The volume indicated on the graduated vessel is recorded as the final volume. The difference between the initial and final volumes is equal to the volume of the test hole. The in situ total unit weight is

calculated by dividing the weight of soil excavated from the test hole by the volume of the test hole. The rubber balloon method is described by the American Society for Testing and Materials (ASTM) as having an accuracy of  $\pm 1 \text{ lb/ft}^3$  (ASTM D2167).

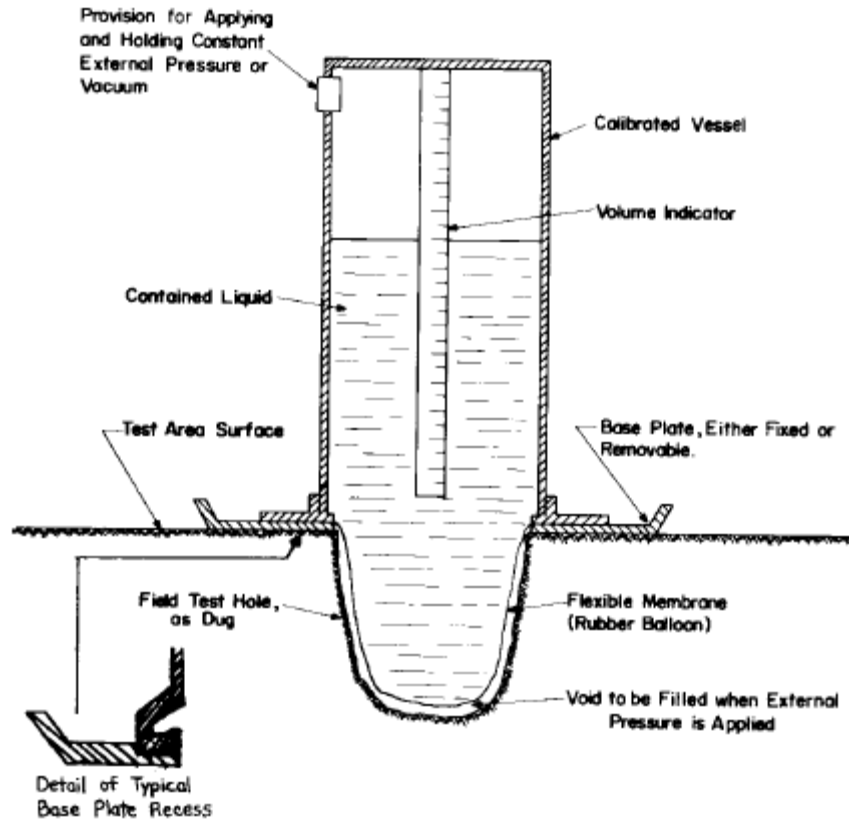


Figure 2.1. Rubber balloon apparatus

Each time the flexible rubber balloon is replaced, or at least once per year, the accuracy of the volume indicator must be checked through a calibration procedure (ASTM D 2167). This calibration involves inflating the rubber balloon inside a container of known volume, such as a standard Proctor compaction mold. The calibration determines the water pressure required to inflate the balloon to a known volume and ensures that the device is working properly. The rubber balloon should measure the volume of the calibration container to within 1 percent of the actual volume.

The rubber balloon method is most suitable for soils without significant amounts of rock or coarse materials because these materials may puncture the balloon. The method is not suitable for soils with appreciable organic content or for very soft soils, as these soils may deform when pressure is applied to the membrane during volume measurement. Also, unbound granular soils that cannot maintain an open hole are not suitable for this method.

### 2.2.2 Oven-Dry Water Content

The water content of soil can be easily measured by oven drying (ASTM D2216). The test is performed by first weighing a soil sample, placing it overnight in an  $110^{\circ}\text{C}$  ( $230^{\circ}\text{F}$ ) oven

to dry, and weighing the dried soil. The weight loss is assumed to be entirely water, and thus the soil water content can be calculated. The water content is determined by dividing the difference in weight of the soil before and after drying by the weight of the dry soil:

$$w = \frac{W_{cms} - W_{cds}}{W_{cds} - W_c} \cdot 100\% \quad (2.1)$$

where:

- w = water content (%)
- $W_{cms}$  = weight of the container and moist soil
- $W_{cds}$  = weight of the container and dry soil
- $W_c$  = weight of the container

### 2.2.3 Microwave Oven Water Content

The water content of a soil sample can also be determined by microwave oven heating (ASTM 4643). This method is best suited for soils with particles that pass through the #4 sieve. To perform the test, the weight of the empty container is recorded, and a minimum of 100 g (3.5 oz) of soil is placed in the container. The sample is placed in the microwave for a minimum of 3 minutes, after which it is mixed, weighed, and returned to the microwave for 1 minute. The soil is mixed and weighed again, and this procedure is repeated until there is less than a 1 percent difference between successive weight measurements. For routine testing of similar soils, a standardized amount of drying time can be established. The water content for this method is calculated using Equation 2.1.

### 2.2.4 Nuclear Gauge

The nuclear gauge (ASTM D2922) is currently the most widely used method to determine in situ unit weight and water content because of its simple operation, speed of measurement, and perceived accuracy. Concerns regarding certification and increased documentation for the nuclear gauge have created the desire to develop alternative methods to rapidly determine the unit weight and water content of compacted fill.

The nuclear gauge consists of a nuclear source, usually cesium or radium (ASTM D2922), a probe where the source is located, and a detector to measure the gamma ray attenuation through the soil. The nuclear gauge can be operated in two ways, the backscatter mode and the direct transmission mode (Figure 2.2). In the backscatter mode, the nuclear source and probe are both on the ground surface. For the direct transmission mode, a probe with the nuclear source is placed in the ground, while the detector remains on the ground surface.

To measure the unit weight of the soil, the nuclear source emits gamma ray photons through the soil. As the gamma rays travel through the soil, they are deflected and lose energy as they collide with electrons in the soil. The gamma detector measures the amount of photons received from the nuclear source. As the soil unit weight increases, the amount of photons reaching the detector decreases because of the increased number of collisions that occur during travel from the source to the detector. In both the direct transmission and backscatter methods, the gamma detector records the number of photons received from the source. The photon count is inversely proportional to the soil unit weight (Ayers and Bowen 1988).

The water content of the soil is measured by the nuclear gauge by emitting neutrons from the source. As the neutrons travel through the soil they collide with hydrogen atoms, which slow the neutrons down. Eventually, neutron thermalization occurs. Thermalization is defined as the

point at which the slowing of a neutron reaches a limit and additional collisions do not decrease the speed of the traveling neutron. The number of thermalized neutrons detected is related to the number of hydrogen atoms in the soil, which is related to the water content of the soil (Evet 2000).

The initial calibration of a nuclear gauge is performed using a reference block, consisting of magnesium, aluminum, granite, or limestone (ASTM D2922). Soil-specific calibration is not required, but a standardization check be performed before each day of operation (ASTM D2922). Standardization involves recording four repetitive readings on a reference block, computing their mean value, and comparing them to the current standardization count. This standardization ensures that the gauge is performing similarly on a day-to-day basis, as long as the daily standard counts fall within acceptable ASTM limits.

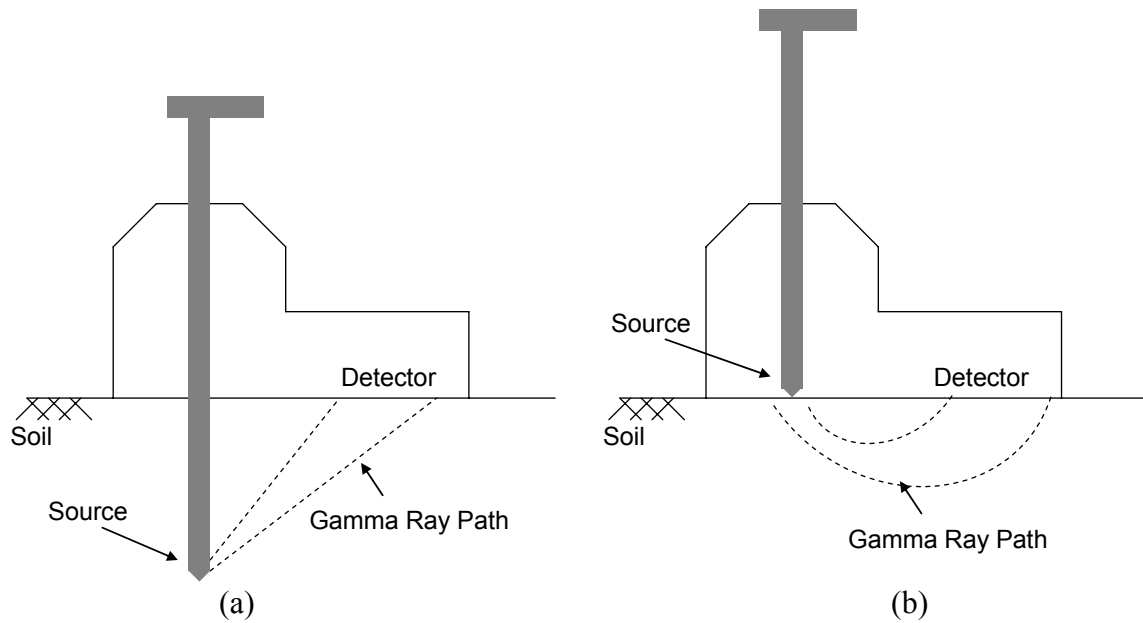


Figure 2.2. Schematic of nuclear gauge in (a) direct transmission and (b) backscatter modes.

## 2.3 Impact Methods

The impact methods considered in this study are similar in that the attempt to relate the resistance of the soil to impact to the in situ unit weight of the soil. The impact methods include the PANDA dynamic cone penetrometer, the Clegg Impact Hammer, and the standard dynamic cone penetrometer (DCP).

### 2.3.1 PANDA Dynamic Cone Penetrometer

The PANDA Dynamic Cone Penetrometer is used throughout Europe to monitor field compaction. This device measures the dynamic cone resistance ( $q_d$ ) of compacted soil versus depth. The test is performed by driving a cone rod into the soil with a fixed-weight hammer (Figure 2.3). The speed of hammer impact and the penetration depth for each blow are recorded. From the speed of hammer impact, the device calculates the amount of energy in each blow. The

penetration depth, energy per hammer blow, and device geometry measurements are used to calculate the dynamic cone resistance ( $q_d$ ) using (Langton 1999):

$$q_d = \left( \frac{1}{A} \right) \left( \frac{\frac{1}{2}MV^2}{1 + \frac{P}{M}} \right) \left( \frac{1}{x_{90^\circ}} \right) \quad (2.2)$$

where:

- $q_d$  = dynamic cone resistance
- $A$  = area of the cone
- $M$  = weight of hammer
- $V$  = speed of hammer impact
- $P$  = weight of struck weight or anvil
- $x_{90^\circ}$  = penetration of one hammer blow ( $90^\circ$  cone)

As the PANDA is being driven into the soil, the microprocessor records and displays a plot of  $q_d$  versus depth.



*Figure 2.3. The PANDA dynamic cone penetrometer*

For compaction control, measured values of  $q_d$  versus depth are plotted against pass/fail  $q_d$  curves from the PANDA soil library. These pass/fail curves were generated by the PANDA manufacturer through tests measuring density and dynamic cone resistance of natural soils at various compaction levels (Langton, 1999). Soils in the PANDA library are catalogued in terms of plasticity, grain size distribution, water content, and level of compaction. The PANDA soil library contains pass/fail  $q_d$  curves for eighteen natural soil types and three artificial soil types. Also provided are target  $q_d$  curves for two levels of compaction: Standard Proctor and Modified Proctor. For a given soil type and compaction energy, the PANDA library provides a failure  $q_d$  curve and a reference  $q_d$  curve. The region between the two curves is called the zone of tolerance (Langton, 1999). These curves can be plotted along with the measured  $q_d$  versus depth curve

obtained at a site (Figure 2.4). In Figure 2.4, the dashed line on the left is the failure line (92 percent Standard Proctor) and the dashed line on the right is the tolerance line (95 percent Standard Proctor). Portions of the field-measured  $q_d$  curve falling to the left of the failure line do not meet the selected compaction standards, while portions of the field-measured curve falling within the zone of tolerance or to the right of the tolerance line meet the selected compaction standards. However, the PANDA does not provide an exact measure of the relative compaction.

The PANDA can be used either during construction for lift-by-lift quality control or during post-construction for a full-depth profile. A complete site profile is useful for highlighting problem lifts or verifying post-construction compaction in utility trenches (Juran and Rousset, 1999). However, post-construction testing is not useful for large compaction projects, where identification of a poorly compacted layer at depth will require a significant volume of material to be removed and re-compacted.

Juran and Rousset (1999) conducted a field compaction study to determine the reliability, efficiency, advantages, and limitations of several compaction control devices, including the conventional nuclear gauge and the PANDA. Each device was used to assess the compaction quality/acceptance of five test trenches compacted with sandy backfill 5 ft thick. The five trenches were compacted differently, using different lift thicknesses (1 ft, 2.5 ft, and 5 ft) and numbers of passes (one and five passes per lift). For each trench, results from the PANDA were compared with nuclear gauge dry unit weight measurements and a specification of 95 percent relative compaction (RC) based on Standard Proctor. It should be noted that nuclear gauge measurements were performed on each lift, while the PANDA was used to profile the full depth of each trench after construction of the entire fill. Compared with the nuclear gauge, the PANDA either accurately identified layers not meeting the compaction specification or indicated that a layer did meet the specification when the nuclear gauge indicated it did not. This discrepancy between the PANDA and the nuclear gauge may have been caused by the fact that the PANDA was performed after all layers were compacted. Therefore, deeper layers that did not meet the 95 percent RC specification immediately after being placed may have been further densified by compaction of the layers above. Thus, if the PANDA is to be used to evaluate the compaction of fill as it is placed, a PANDA measurement should be performed on each lift and compared with direct unit weight measurements.

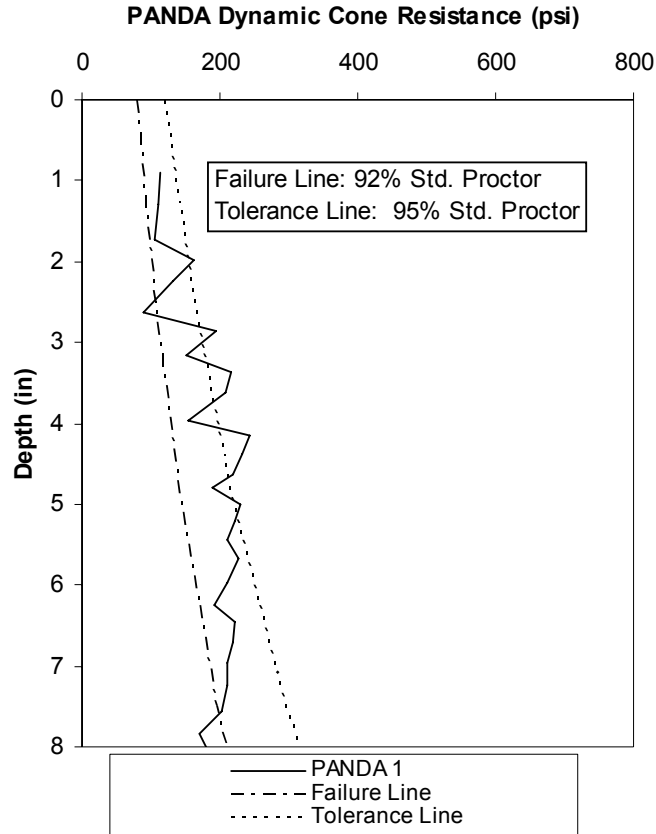


Figure 2.4. Example of PANDA result displaying measured values, failure line, and tolerance line.

### 2.3.2 Clegg Impact Hammer

The Clegg Impact Hammer was developed in Australia by Dr. Baden Clegg in the late 1960s to measure the strength/stiffness of soils by instrumenting a laboratory compaction hammer. The standard Clegg Impact Hammer consists of a 2-in. diameter, 10-lb hammer inside a guide tube. An accelerometer on the end of the hammer is attached to a digital display unit on the outside of the guide tube and measures the peak acceleration of the hammer during impact. A schematic of the Clegg is shown in Figure 2.5.

The operation of the Clegg Impact Hammer (ASTM D 5874) involves placing the device on a compacted lift of soil, raising the hammer 18 in., and allowing the hammer to free fall within the guide tube. The accelerometer measures the peak deceleration of the hammer during impact, and the display unit gives the peak acceleration value in tens of gravities (gravity =  $g = 32.2 \text{ ft/s}^2 = 9.81 \text{ m/s}^2$ ). Three additional blows, for a total of four blows, are applied with the hammer at the same testing location. The Clegg Impact Value (CIV) is the largest acceleration measured during the four blows. Testing has shown that the first two blows act as a seating mechanism, with CIV values increasing after the first few blows and remaining generally unchanged after four blows (ASTM D 5874). The CIV is roughly correlated to soil stiffness and strength, and thus larger values of CIV should indicate larger values of dry unit weight. ASTM D

5874 indicates that for field use, the coefficient of variation for the Clegg Impact Hammer is 4 percent for working conditions of high uniformity and 20 percent for highly variable conditions.

Using the Clegg Impact Hammer for compaction control involves setting a target CIV for the required compaction conditions (i.e., relative compaction for the specified compaction energy). ASTM D 5874 describes three laboratory methods that can be used to determine the target CIV. The laboratory methods involve (1) measuring the CIV at the optimum water content, (2) measuring the CIV at a range of water contents, or (3) measuring the CIV at a range of unit weights at the optimum water content. Each of these three methods utilizes compaction data from either a Standard Proctor or Modified Proctor compaction test. To set a target CIV for the optimum water content, a soil specimen is compacted in a Proctor mold at the optimum water content, the CIV is measured in the mold with the Clegg Impact Hammer, and this CIV is used as a minimum requirement for field compaction. To set a target CIV from a range of water contents, four specimens are compacted in Proctor molds at 100 percent relative compaction and at water contents that bracket the optimum water content. CIV values are measured for each specimen to produce a curve of CIV versus water content, and the target CIV is taken as the maximum (Figure 2.6). To set a target CIV from a range of unit weights, four specimens are compacted in Proctor molds at the optimum water content. Each specimen is compacted with a different number of blows to produce a range of unit weights representing approximately 90 percent to 100 percent relative compaction. The measured values of CIV are used to produce a curve of CIV versus relative compaction at optimum water content, where the target CIV is defined as the CIV at the required percent relative compaction for the site.

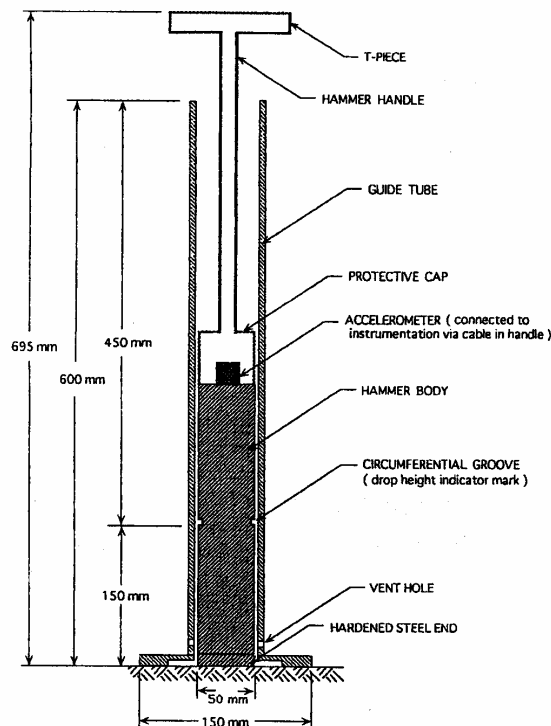


Figure 2.5. Schematic of Clegg Impact Hammer (ASTM D5874)

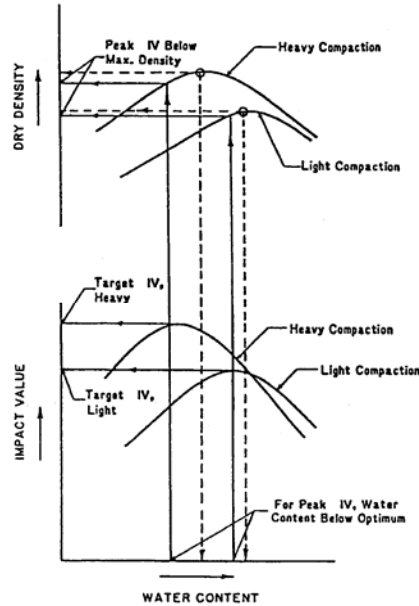


Figure 2.6. Determination of target CIV from testing at a range of water contents (ASTM D 5874)

Peterson and Wisler (2003) reported on a study by the New York State Electric & Gas Corporation that involved field comparisons between the Clegg Impact Hammer and traditional measurements of dry unit weight using the nuclear gauge. Fifteen measurements were performed at each of twelve trench backfill sites in Broome County, New York. The backfill material was crushed rock and gravel. Readings were taken after each lift was compacted to 90 percent Standard Proctor with a tamper. Target CIVs were based on 90 percent Standard Proctor dry unit weight. The study determined that the Clegg Hammer accurately identified 90 percent relative compaction for 84 percent of the measurements obtained (Peterson and Wisler 2003).

### 2.3.3 Standard Dynamic Cone Penetrometer

The Standard Dynamic Cone Penetrometer (DCP) is widely used to evaluate the in situ strength of pavement materials and subgrade soils (ASTM D 6951). The DCP measures the penetration rate (penetration distance per blow) of a cone as it travels through pavement or subgrade layers. The device is comprised of a steel drive rod, a disposable or permanent cone tip, and a 17.6-lb hammer and anvil assembly (Figure 2.7). A 10-lb hammer can be used for softer soils. One blow of the DCP occurs when the hammer is raised to the upper stop (22.6 in.) and released to fall on the anvil. A vertical scale is used to measure the relative displacement of the drive rod for each blow and measure the penetration rate in in./blow or mm/blow (Figure 2.8). ASTM D6951 provides a relationship between penetration rate and California Bearing Ratio (CBR) for pavement design. Typically, the variability in DCP penetration rate measurements is less than 2 mm/blow (ASTM D6951).

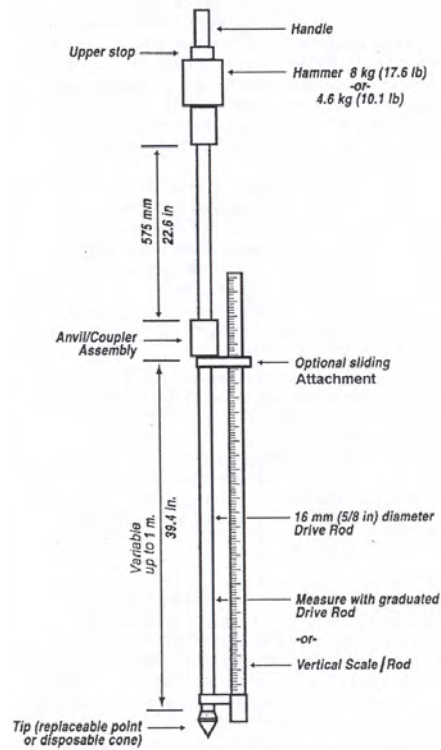


FIG. 1 Schematic of DCP Device

Figure 2.7. Schematic of standard DCP (ASTM D6951)

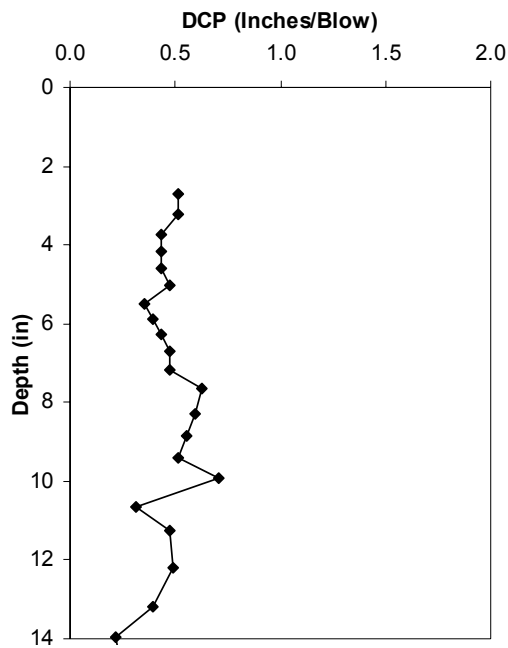


Figure 2.8. Example of DCP field data

It is important to maintain the verticality of the drive rod throughout DCP testing. However, materials with large rock particles may cause the rod to lose verticality. Additionally, large particles may result in large increases in penetration rate that are not representative of increases in density or stiffness. Thus, DCP testing should be limited to materials with a maximum particle size smaller than 2 in. (ASTM D6951).

DCP testing generally requires two people. One operator raises and drops the hammer, while the other operator measures relative displacement of the cone tip using the vertical scale. An electronic data recorder may be purchased to eliminate the second operator.

The Minnesota Department of Transportation (MnDOT) has conducted extensive research on the DCP and its applications in the construction industry. One of these studies, the Minnesota Road Research Project (Mn/ROAD) included more than 700 DCP tests on subgrade, sub base, and base materials (Burnham 1997). These tests were performed at active MnDOT construction sites, and the results were analyzed to determine limiting DCP penetration rates, in in./blow, that correspond to conditions of “adequate compaction”. These limiting values were determined to be 3 in./blow for silty/clayey material and 0.28 in./blow for granular materials (Burnham 1997). The researchers note that these limiting values do not take into account water content, and that changes in water content may affect DCP penetration rates. However, MnDOT specifications for compaction control with the DCP only reference limiting penetration indices, with no consideration of water content. The Mn/ROAD study was unable to find a direct correlation between DCP penetration rate and dry unit weight. The study also determined that DCP penetration rates were not valid over the top few in. of a compacted lift due to lack of confinement (Burnham 1997).

The Gas Technology Institute (GTI) conducted a research project investigating the effectiveness of several compaction devices, including the DCP (GTI 2004). Each device was evaluated for typical construction materials: sand, silty clay, and aggregate base. Field test trenches were constructed for testing. The GTI (2004) study concluded that, although the DCP was affordable and simple to use, it provided only very general post-compaction information, namely the existence of weak layers or layer boundaries. Because no soil-specific calibrations exist, the study found that the DCP penetration rate did not correlate well with dry unit weight or other compaction parameters. Additionally, the DCP provided unreliable data within the top 6 in. of most materials tested as a result of lack of confinement (GTI 2004).

## **2.4 Electrical Methods**

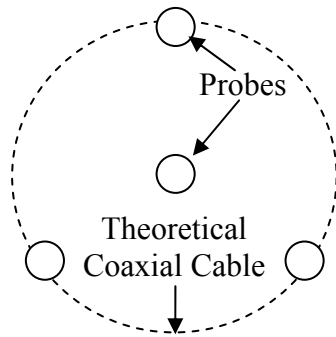
The electrical methods considered in this study attempt to relate the electrical properties of the soil to the in situ dry unit weight and water content of the soil. The electrical methods include the Moisture Density Indicator (MDI), the Electrical Density Gauge (EDG), and the Soil Quality Indicator (SQI). Another electrical-based method is being developed by Fratta et al. (2005), but it is not currently available for field testing.

### **2.4.1 Moisture Density Indicator**

The Moisture Density Indicator (MDI) uses time domain reflectometry (TDR) to assess the dry unit weight and water content of soil by measuring the apparent dielectric constant ( $K_a$ ) and bulk electrical conductivity ( $EC_b$ ) of the soil. These measurements are made using four, 10-in. long probes that are driven into the soil in the formation shown in Figure 2.9a. This configuration represents a coaxial cable with the center probe acting as the center cable, the three outer probes as the cable shielding, and the in situ soil acting as the insulator. An electromagnetic

wave is transmitted along the length of the soil probes, and it is reflected back along the same path. The data acquisition system measures and records the reflected signal.

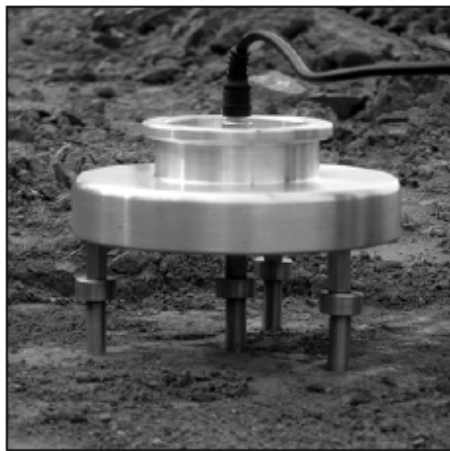
To conduct an MDI reading, the ground surface must be leveled. The probe template is placed on the ground and the four probes are driven into the ground using a mallet (Figure 2.9b). The probe template is removed and the coaxial head is placed on top of the four probes (Figure 2.9c). The coaxial head is connected to the MDI field carrying device, which is connected to a PDA (Figure 2.9d). Through the PDA software interface, the MDI records a TDR waveform. The software uses the TDR waveform and a soil-specific model, as described below, to compute and immediately display values of the in situ dry unit weight and water content of the soil tested.



(a)



(b)



(c)



(d)

*Figure 2.9. MDI field testing:  
(a) probe configuration, (b) probes being driven into the ground, (c) coaxial head placed on top of the soil probes, (d) field measurement being taken (Durham 2005).*

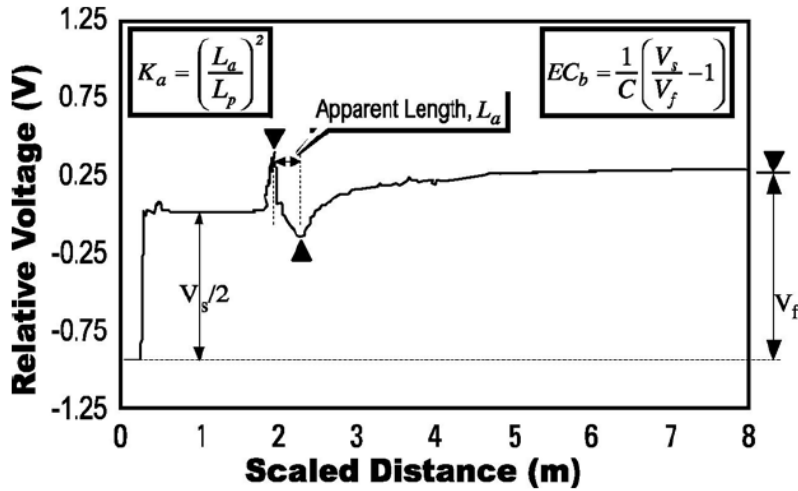


Figure 2.10. Example TDR waveform (Durham 2005).

The theoretical basis for the MDI is the measurement of the dielectric constant,  $K_a$ , and bulk electrical conductivity,  $EC_b$ , of the soil from a TDR waveform of relative voltage versus scaled distance (Figure 2.10).  $K_a$  is calculated from the first and second reflections in the TDR waveform (black triangles in Figure 2.10), which represent when the electromagnetic wave enters the soil and when it is reflected from the end of the soil probes, respectively. Specifically,  $K_a$  is calculated as (Yu and Drnevich 2004):

$$K_a = \left(\frac{L_a}{L_p}\right)^2 \quad (2.3)$$

where:

- $L_a$  = scaled horizontal distance between the first reflection and second reflection points in the TDR waveform
- $L_p$  = length of the soil probes

$EC_b$  represents the ability of the soil to attenuate electrical energy and it is calculated from the source voltage ( $V_s$ ) and final voltage ( $V_f$ ) in the TDR waveform using (Yu and Drnevich 2004):

$$EC_b = \frac{1}{C} \left(\frac{V_s}{V_f} - 1\right) \quad (2.4)$$

$$C = \frac{2\pi L_p R_s}{\ln\left(\frac{d_o}{d_i}\right)} \quad (2.5)$$

where:

$V_s$	=	source voltage or twice the step voltage
$V_f$	=	long term voltage level
$C$	=	constant related to probe configuration
$L_p$	=	length of probe in soil
$R_s$	=	internal resistance of the pulse generator
$d_o$	=	outer conductor diameter
$d_i$	=	inner conductor diameter

$K_a$  and  $EC_b$  are related to dry unit weight and water content through the following relationships (Yu and Drnevich 2004):

$$\sqrt{K_a} \frac{\rho_w}{\rho_d} = a + b \cdot w \quad (2.6)$$

$$\sqrt{EC_b} \frac{\rho_w}{\rho_d} = c + d \cdot w \quad (2.7)$$

where:

$a, b$	=	soil-specific calibration constants for $K_a$
$c, d$	=	soil-specific calibration constants for $EC_b$
$\rho_w$	=	density of water or unit weight of water
$\rho_d$	=	dry density of soil or dry unit weight of soil
$w$	=	water content of soil

To determine the calibration constants for a particular soil,  $K_a$  and  $EC_b$  are measured for several samples compacted in a compaction mold at a range of known water contents and dry unit weights. The measured data are plotted as  $\sqrt{K_a} \cdot \rho_w / \rho_d$  versus  $w$  and  $\sqrt{EC_b} \cdot \rho_w / \rho_d$  versus  $w$ , and a straight line is fit to the plotted data to determine soil constants  $a$ ,  $b$ ,  $c$ , and  $d$ .  $EC_b$  of the soil depends on the pore fluid conductivity and will change if the salinity in the pore fluid changes. Thus, the calibration constants  $c$  and  $d$  only apply to samples of the same soil with the same pore fluid as used during laboratory calibration. To account for differences between the pore fluid in the laboratory and the pore fluid in the field, a third calibration graph of  $EC_b^{0.5}$  versus  $K_a^{0.5}$  is constructed and soil constants  $g$  and  $f$  are determined by fitting a straight line through the data using:

$$\sqrt{EC_b} = f + g\sqrt{K_a} \quad (2.8)$$

where:

$f, g$	=	soil-specific calibration constants related to the soil type, density, and pore-fluid conductivity
--------	---	--

Equation (2.8) allows one to adjust the field  $EC_b$  based on the field-measured  $K_a$  so that the laboratory-evaluated calibration constants can be applied to the pore fluid present in the field. Because  $K_a$  and  $EC_b$  both depend on dry unit weight and water content, Equations 2.6 and 2.7 can be combined to evaluate  $f$  and  $g$  in terms of  $a$ ,  $b$ ,  $c$ , and  $d$ .

$$f = \frac{b \cdot c - a \cdot d}{b} \quad (2.9)$$

$$g = \frac{d}{b} \quad (2.10)$$

To account for differences between the electrical conductivity of the pore fluid in the field and the pore fluid in the laboratory used during calibration, the following procedure is used to develop adjusted values of  $K_a$  and  $EC_b$  ( $K_{a,adj}$ ,  $EC_{b,adj}$ ) from the field measured values of  $K_a$  and  $EC_b$  ( $K_{a,field}$ ,  $EC_{b,field}$ ).  $K_a$  is insensitive to changes in pore fluid such that  $K_{a,adj}$  is set equal to  $K_{a,field}$  (Equation 2.11).  $K_{a,field}$  is used with Equation 2.8 to calculate  $EC_{b,adj}$  for the soil (Equation 2.12).

$$K_{a,adj} = K_{a,field} \quad (2.11)$$

$$EC_{b,adj} = (f + g\sqrt{K_{a,field}})^2 \quad (2.12)$$

where:

- $K_{a,field}$  = field measured dielectric constant
- $K_{a,adj}$  = adjusted dielectric constant
- $EC_{b,adj}$  = adjusted bulk electrical conductivity

Based on Equation (2.11) and (2.12), it is clear that during field MDI testing, only the dielectric constant ( $K_a$ ) is measured and the electrical conductivity ( $EC_b$ ) is derived from the  $K_a$  measurement. Thus, the field  $EC_b$  is never measured. After this adjustment, the values  $K_{a,adj}$  and  $EC_{b,adj}$  are used in Equations (2.6) and (2.7) to solve simultaneously for the field dry unit weight and water content.

One last consideration regarding the MDI is the impact of soil type on the TDR waveform. In highly plastic clays, the attenuation of the electromagnetic wave can be so large that the MDI is unable to detect the second reflection of the electromagnetic wave (Yu and Drnevich 2004). Figure 2.11 shows representative waveforms for different soil types: sand, low plasticity silt, and low plasticity clay. These waveforms reveal that the second reflection point in the TDR waveform diminishes with increasing soil plasticity.

Yu and Drnevich (2004) report that MDI testing is limited to soils that have 30 percent or less, by weight, retained on the No. 4 sieve, and a maximum particle size of 0.75-in. Frozen soils cannot be tested. Additionally, there may also be problems obtaining accurate measurements in high plasticity clays because of the attenuation of the electromagnetic wave (Figure 2.11).

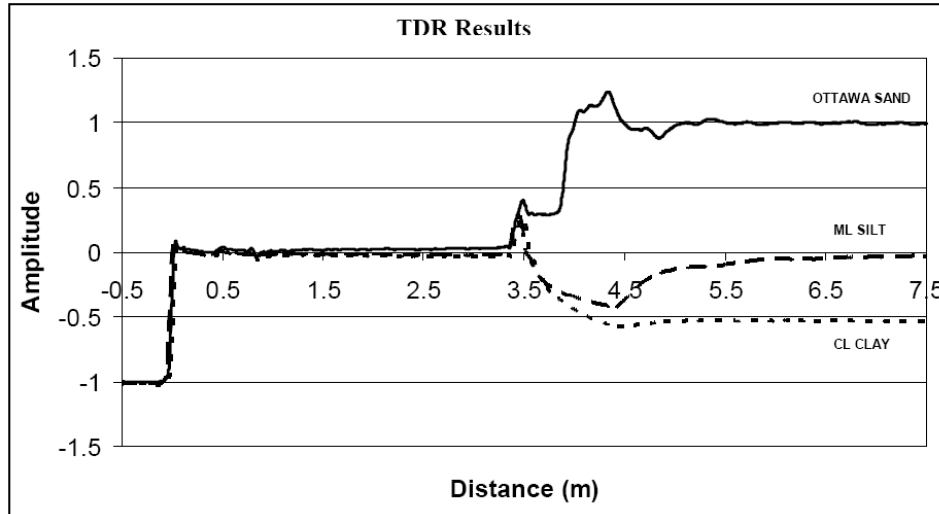


Figure 2.11. Effect of soil type on the TDR waveform (Durham 2005).

#### 2.4.2 Electrical Density Gauge

The Electrical Density Gauge (EDG) measures the electrical dielectric properties of soil using high frequency radio waves. The measured properties are used with a soil-specific calibration model and algorithm to compute the dry unit weight and water content of the soil (GENEQ Inc. 2006). A detailed description regarding the theoretical basis for the EDG is not currently available.

The soil-specific calibration for the EDG is performed by performing electrical measurements in soil compacted over a range of known dry unit weights and water contents. The dry unit weight and moisture content of each soil sample used in the calibration are measured by other methods, such as the rubber balloon test for unit weight and oven drying for water content. The EDG develops a “Soil Model” using the electrical measurements and the direct measurements of dry unit weight and water content. However, the form of the model and the model parameters are not reported.

To operate the EDG, four 6-in. metal probes are placed in the soil in a square formation and attached to the EDG apparatus (Figure 2.12). Four electrical measurements are obtained at one location after the probes are inserted. The electrical connectors are placed on two of the probes that are diagonally across from each other, such as probes A and D in Figure 2.12b, and an electrical measurement is taken. The connector locations are reversed on the same probes and another measurement is taken. The connectors are attached to the other two probes (e.g., B and C) for another measurement. The connector locations are reversed on these probes and a fourth and final measurement is taken.

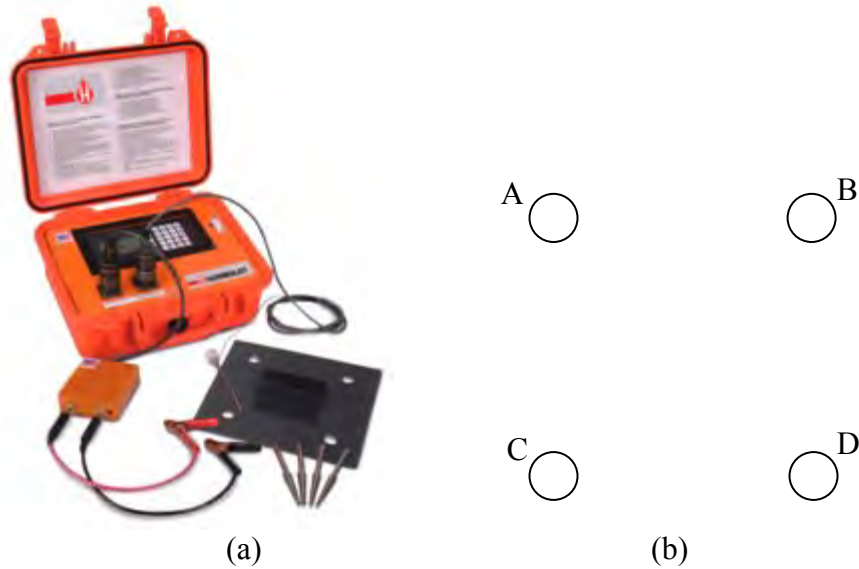


Figure 2.12. (a) Photograph of Electrical Density Gauge (GENEQ Inc. 2006), (b) plan view of EDG probe layout.

### 2.4.3 Soil Quality Indicator

The Soil Quality Indicator (SQI) is currently being developed by TransTech Systems as a sister device to the patented Pavement Quality Indicator. The SQI measures the relative dielectric permittivity ( $\epsilon_R$ ) of a soil matrix over the frequency range of 1 kHz to 10 MHz (TransTech Systems 2004) using a circular measurement plate and associated electronics (Figure 2.13). The relative dielectric permittivity ( $\epsilon_R$ ) is the ratio of the dielectric permittivity of a material to the dielectric permittivity of air. Dielectric permittivity is a basic electrical parameter that relates the electric field density with the electric flux density (Drnevich et al. 2001). In soil,  $\epsilon_R$  is frequency dependent and a plot of  $\epsilon_R$  versus frequency is called the dielectric spectrum (Figure 2.14).

Over the frequency range used in the SQI measurement,  $\epsilon_R$  is affected most by the Maxwell-Wagner effect (TransTech Systems 2004). The Maxwell-Wagner effect is a reduction in  $\epsilon_R$  above a measured relaxation frequency due to the fact that soil consists of different constituents (soil, water, air) with different dielectric properties (Drnevich et al., 2001). The value of  $\epsilon_R$  above and below the relaxation frequency, as well as the location of the relaxation frequency, are a function of the physical properties of the soil (e.g., density, water content).

Drnevich et al. (2001) attempted to develop a rigorous analytical model that uses the inherent physical and electrical properties of the soil to predict the dielectric spectrum. This model was used to evaluate the physical soil properties from a measured dielectric spectrum. However, this approach was not successful because of non-unique solutions (Drnevich et al. 2001). The SQI uses an empirical approach to relate features in the measured dielectric spectrum (e.g.,  $\epsilon_R$  at the highest test frequency,  $\epsilon_R$  at 100 kHz, Maxwell-Wagner relaxation frequency) to the physical soil properties. An artificial neural network trained with calibration data is used to compute the dry unit weight and water content of the soil from the features in the dielectric spectrum (TransTech Systems 2004).



Figure 2.13. Soil Quality Indicator (TransTech Systems 2004).

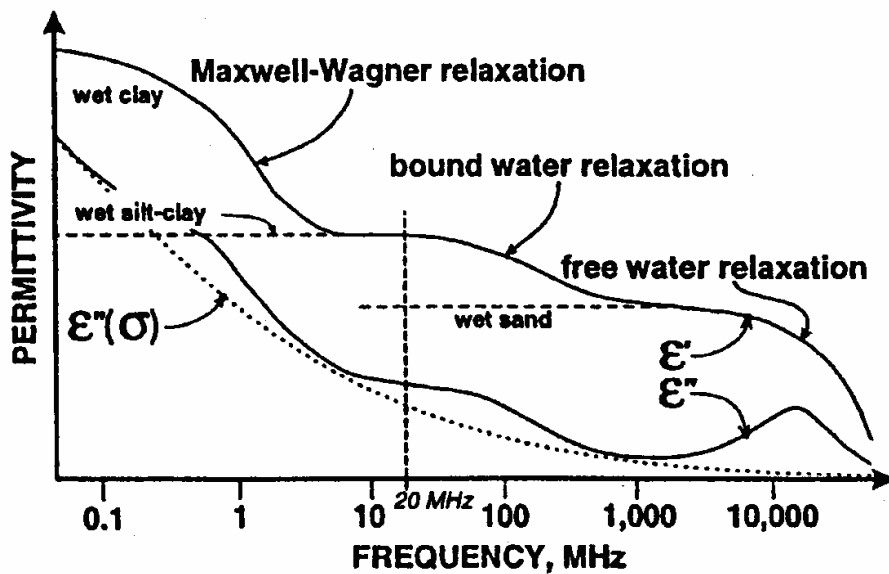


Figure 2.14. Qualitative representation of dielectric spectrum (Drnevich et al. 2001).

## 2.5 Stiffness Methods

Stiffness methods attempt to relate the stiffness of the soil to its in situ dry unit weight. The stiffness methods considered in this study include the Portable Seismic Property Analyzer (PSPA), the GeoGauge, and the Soil Compaction Supervisor (SCS).

### 2.5.1 Portable Seismic Property Analyzer

The Portable Seismic Property Analyzer (PSPA) is a modified version of the Seismic Pavement Analyzer (SPA), which was first developed as a prototype in 1993 at the University of

Texas at El Paso. The SPA was developed to test both flexible and rigid pavements for early signs of distress and to provide general quality control during pavement construction. The SPA measures the elastic properties (i.e., Young's Modulus,  $E$ , and Shear Modulus,  $G$ ) and layer thicknesses of the pavement system, including the asphalt, concrete, and subgrade, using five seismic techniques (Nazarian et al. 1997): Ultrasonic Body Wave (UBW), Ultrasonic Surface Wave (USW), Impact Echo (IE), Impulse Response (IR), and Spectral Analysis of Surface Waves (SASW). A portable version of the large, trailer-mounted SPA is the Portable Seismic Pavement Analyzer (PSPA), also called the Portable Seismic Property Analyzer. The PSPA is more suitable for compaction control, as it can be moved from location to location easily by the operator. For soil compaction control, only the USW function of the PSPA is used, measuring the Young's Modulus of the soil.

The PSPA consists of two receivers (geophones), one wave source, and a data acquisition system (Figure 2.15). The wave source is coupled with the two receivers on adjustable pneumatic rods. The adjustment of the rods changes the receiver spacing, and thus, the depth of the material tested by the PSPA. The tilt and pitch along the rod can be adjusted to assist in seating the source and receivers. The data acquisition system connects the hardware of the PSPA to a computer for the reduction and analysis of the measured data.



*Figure 2.15. PSPA components and data acquisition system.*

To conduct a PSPA measurement, the rods are adjusted for the desired measurement depth, and then the receivers and source are placed gently on the soil surface. Good contact at the receiver/soil interface is integral to achieving good measurements. The software in the data acquisition system initiates wave generation from the source and records wave forms from the two receivers. Indicator lights in the software inform the operator if adequate contact with the soil has been achieved. The software reduces the wave records and phase differences to compute an average Young's modulus over the depth tested.

The USW method performed by the PSPA is based on seismic wave propagation and the measurement of dispersion of high frequency surface waves (Gucunski and Maher 2002). Essentially, the USW method is simply the spectral analysis of surface waves (SASW) applied at high frequencies. SASW assumes that the soil is a layered half-space, through which elastic waves propagate. The PSPA source generates high frequency surface waves that propagate

horizontally and are measured by the two receivers. The recorded motions are used to compute the Rayleigh wave velocity ( $V_R$ ) at different frequencies. The variation of  $V_R$  with frequency is called dispersion and the velocities at different frequencies represent the variation of  $V_R$  with depth. The shear modulus ( $G$ ) can be related to  $V_R$  through the shear wave velocity ( $V_s$ ) using:

$$G = \rho \cdot V_s^2 = \rho(C \cdot V_R)^2 \quad (2.13)$$

$$C = 1.135 - 0.182 \cdot \nu \quad (2.14)$$

where:

$$\begin{aligned} \rho &= \text{total mass density} \\ \nu &= \text{Poisson's ratio of soil (assumed)} \end{aligned}$$

The Young's modulus ( $E$ ) can be related to the shear modulus ( $G$ ) using Poisson's ratio:

$$E = [2 \cdot (1 + \nu)] \cdot G \quad (2.15)$$

The PSPA software displays  $E$  versus depth and computes an average  $E$  over the depth measured.

### 2.5.2 GeoGauge

The GeoGauge, originally known as the Humboldt Stiffness Gauge, was developed in the mid 1990s by the Humboldt Manufacturing Company as a direct soil stiffness measurement device. The GeoGauge consists of an external case housing an electro-mechanical shaker, upper and lower velocity sensors, a power supply, and a control and display unit. A rigid foot with annular ring is fixed at the base of the case (Figure 2.15).

The GeoGauge measures soil stiffness by vibrating its rigid foot, producing vertical harmonic excitations, and measuring the applied force ( $P$ ) and the resulting vertical velocity of the plate. The velocity is converted to vertical displacement ( $x$ ). This method of operation is comparable to a dynamic plate load test (Nelson and Sondag, 1999). Forces and displacements are induced through vibration at a range of frequencies between 100 and 190 Hz. The average stiffness ( $K$ ) over the frequency range is computed as:

$$K = \frac{P}{x} \quad (2.16)$$

where:

$$K = \text{foundation stiffness}$$

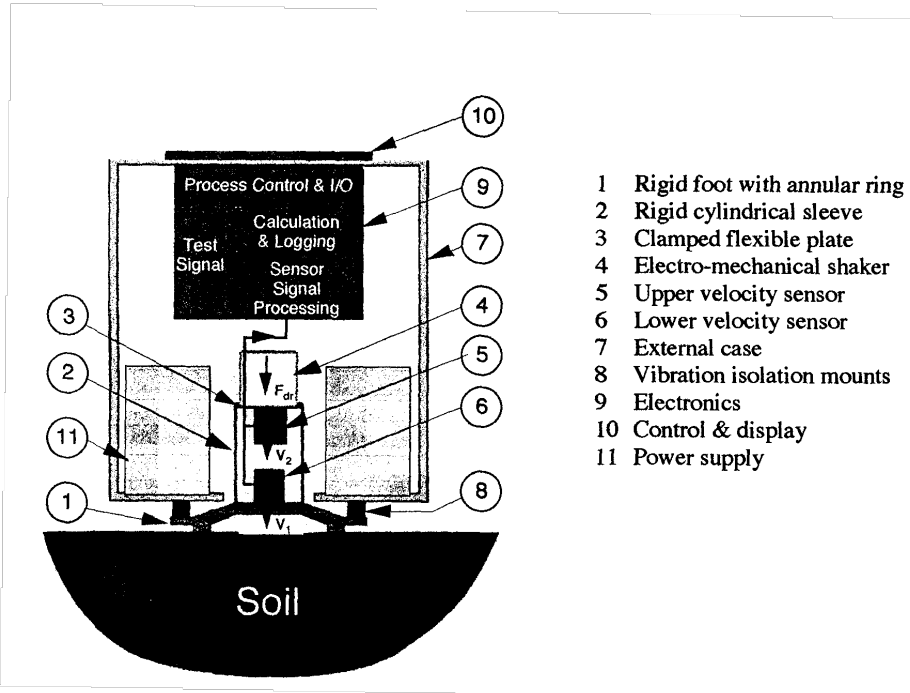


Figure 2.16. Schematic of GeoGauge (Humboldt 1999a).

This measured foundation stiffness can be related to the Young's modulus ( $E$ ) and shear modulus ( $G$ ) of the soil. The relationship between foundation stiffness ( $K$ ) and soil stiffness ( $E$  or  $G$ ) can be derived assuming a rigid ring on a linear elastic, homogeneous, isotropic half space (Lenke et al. 1999), yielding the following relationships:

$$G \approx \frac{K(1-\nu)}{3.54R} \quad (2.17)$$

$$E \approx \frac{K(1-\nu^2)}{1.77R} \quad (2.18)$$

where:

- $\nu$  = Poisson's ratio of soil (assumed)
- $R$  = outside radius of the ring foot

GeoGauge field measurements are obtained by placing the device on top of a compacted lift, making sure to create the recommended soil-foot contact over at least 60 percent of the foot area (Humboldt, 1999a). If the testing surface is rough or the 60 percent contact area is difficult to achieve, a thin layer of sand or local fines should be placed under the ring to ensure good contact. The footing also can be pushed slightly into the lift layer for additional contact. The GeoGauge measures the stiffness of the soil over a depth range of approximately 4 to 8 in., and most accurately measures foundation stiffness values ( $K$ ) in the range of 200 to 1,500 k/ft (3 to 22 MN/m) and soil moduli within the range of 550 to 4,000 ksf (26 to 193 MPa). Humboldt is

working to develop new devices with broader ranges of measurement capabilities to accommodate both softer and stiffer soils.

Several research studies have been performed to assess the accuracy of the GeoGauge. A field study by Chen et al. (1999) evaluated the correlation between the foundation stiffness ( $K$ ) measured by the GeoGauge and the dry unit weight measured by the nuclear gauge. This study also compared the foundation stiffness measured by the GeoGauge with soil stiffness measurements from seismic methods (e.g., PSPA). The study found that the GeoGauge stiffness (labeled HSG in Figure 2.17) correlated well with the seismic modulus (Figure 2.17), while the relationship between GeoGauge stiffness and measured dry unit weight was very poor (Figure 2.18a). In another study by Ellis and Bloomquist (2003), almost no correlation was found between dry unit weight and GeoGauge stiffness (Figure 2.18b).

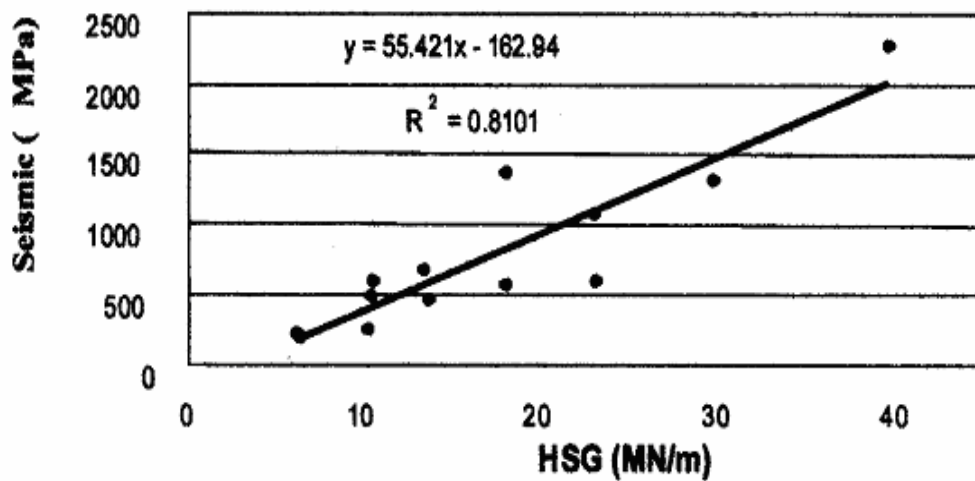
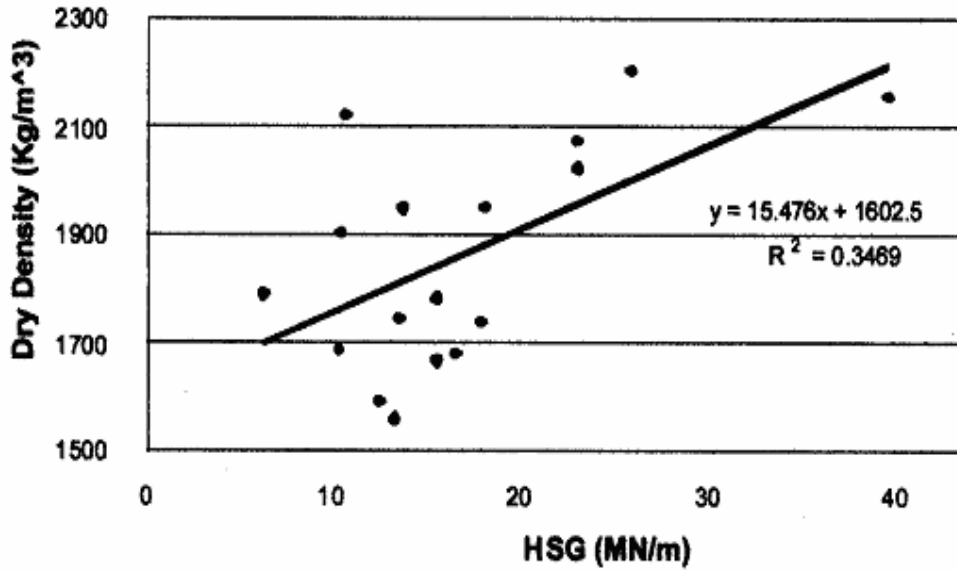
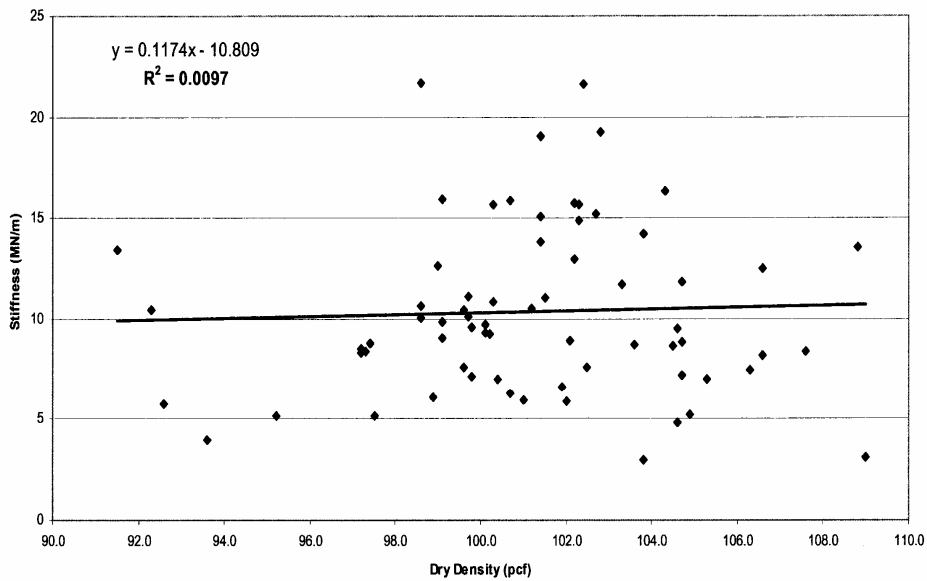


Figure 2.17. Field-measured seismic modulus versus GeoGauge (HSG) foundation stiffness (Chen et al. 1999).



(a)



(b)

Figure 2.18. Field-measured dry unit weight versus GeoGauge (HSG) foundation stiffness from (a) Chen et al. (1999) and (b) Ellis and Bloomquist (2003)

Problems with the field use of the GeoGauge have been reported in several studies, including Simmons (2000), Miller and Mallick (2003), and Ellis and Bloomquist (2003). Many of these problems centered on the seating at the soil-foot interface. The recommended 60 percent contact area is difficult to achieve in practice, and the addition of leveling sand, as recommended by the manufacturer, was shown to significantly alter the measurements depending on the thickness of sand used (Simmons, 2000). Several studies reported that interference from vibrations from passing vehicles, compaction equipment, or trains caused the GeoGauge to malfunction (Simmons, 2000, Miller and Mallick, 2003). The repeatability of measurements at

one specific testing point or site was difficult to achieve in some instances, resulting in a reported high degree of variability in measured GeoGauge stiffnesses (Simmons, 2000, Ellis and Bloomquist, 2003). Ellis and Bloomquist (2003) also investigated potential GeoGauge equipment modifications and procedural alterations to improve the GeoGauge measurements. Most recommendations from this study centered on improving the soil-ring interface.

### 2.5.3 Soil Compaction Supervisor

The Soil Compaction Supervisor (SCS) is a compaction control device that has been used in the construction industry for utility excavation backfills (MBW 2003). New interest lies in adapting the SCS for general highway projects. The SCS system consists of a disposable sensor that is buried in the soil and a battery powered hand-held control unit. The sensor and control unit are connected by a cable (Figure 2.19). The sensor includes piezoelectric transducers that detect vibrations generated by compression waves in the soil (Heirtzler et al., 1995). In the field, compression waves are generated from compaction efforts, such as manual compaction (hammer) for small sites or vibratory compaction for larger projects. The amplitudes of the compression waves in the soil increase as the stiffness and density of the soil increases during the compaction process. Therefore, tracking the compression wave amplitude as compaction progresses allows one to track changes in soil stiffness and density.

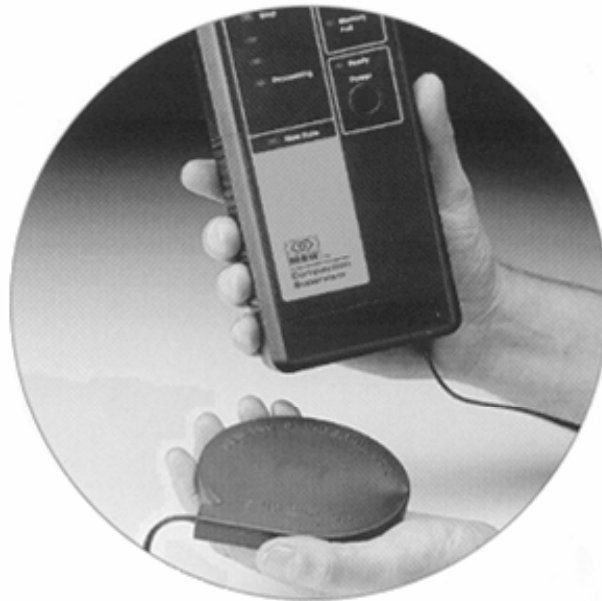


*Figure 2.19. Soil compaction supervisor sensor and control unit (MBW 2003).*

The transducers located within the disposable sensor produce a voltage in response to the amplitude of the compression waves and this voltage is transmitted via cable to the SCS control unit. As compaction proceeds and soil density and stiffness increase, the transmitted voltage, or wave amplitude, increases. At some point during the compaction process, the stiffness of the soil will no longer increase with increasing compactive efforts or passes of the equipment (Figure 2.20). At this point, additional passes of the compaction equipment will not increase its stiffness, and one may assume that compaction is complete. The basis of the SCS is to identify when this asymptotic value of stiffness has been reached through the continuous monitoring of voltages

from SCS sensors embedded at the base of the soil layer. If the voltages are increasing over time, additional passes are needed for the lift and the control unit displays a succession of green lights to the operator. As the voltages produced in the sensor beneath the compacted layer reach an asymptotic value, the SCS control unit displays a red light to the operator, indicating that compaction is complete for that particular lift.

In practice, an SCS sensor is placed beneath the first lift of loosely-placed fill (Figure 2.21). Each sensor can provide readings through approximately 4 ft. of soil; therefore several disposable sensors may be required for fills of thickness greater than 4 ft. A narrow trench is excavated from the sensor to the perimeter of the lift to accommodate the SCS cable. This prevents damage from compaction equipment and allows QA/QC personnel to remain a safe distance from machinery during compaction. Compaction equipment should begin operations within 8 to 10 ft. from the sensor because SCS measurements depend on the proximity of the source of vibrations. After the equipment passes over the sensor and measurements have begun, the SCS control unit displays a blinking green “processing” light. After the compaction process for the lift begins to generate increased stiffness and/or density as indicated by large wave amplitudes measured by the SCS sensor, a succession of two additional “compaction indicator” green lights appear. After the lift has been compacted fully under the field conditions, the red “stop” light is illuminated on the SCS control unit.

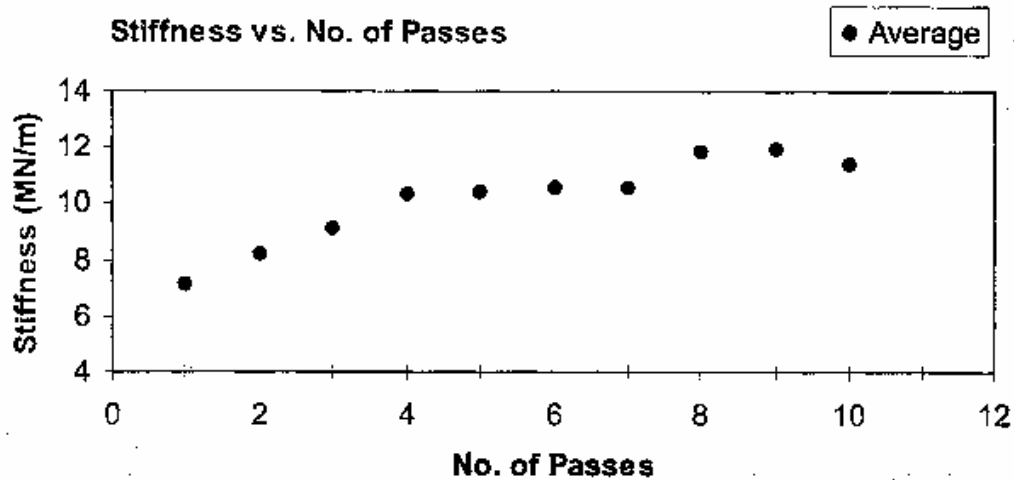


Figure 2.20. Soil stiffness versus number of passes of compaction equipment (Miller and Mallick 2003).

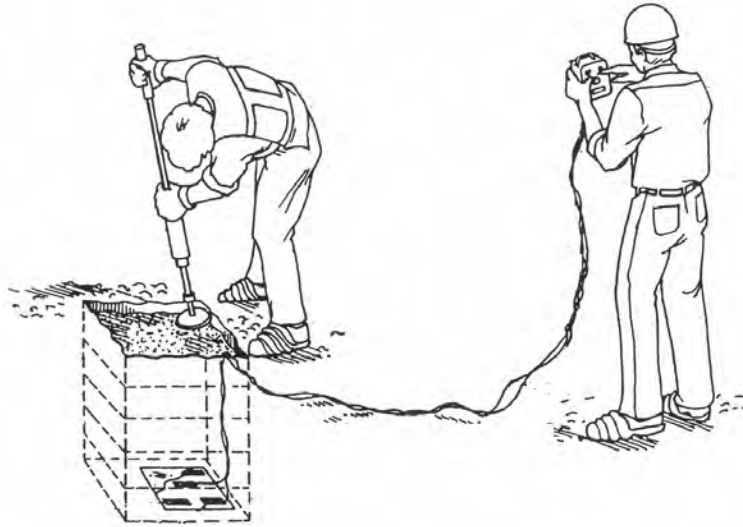


Figure 2.21. Compaction monitoring using the SCS (Heirtzler 1995).

The basis of SCS operation is the development of asymptotic wave amplitudes, and this hypothesis was verified by Cardenas (2000). In this study, four different soils were compacted using various compaction methods and at a variety of water contents and lift thicknesses. Each test soil was compacted in lifts, with nuclear gauge unit weight and water content measurements performed after each complete pass of compaction machinery. The SCS was used to monitor compaction during each lift until the red *stop* signal was displayed. After the SCS red light signal, additional passes of compaction machinery were completed to assess the changes in unit weight after the *stop* signal. Nuclear gauge unit weight and water content measurements were taken after two (RD+2) and four (RD+4) additional passes were completed after the *stop* signal. Average unit weight measurements obtained after the SCS had displayed the red *stop* signal indicated that there was less than a 2 percent increase in density with additional compactive effort.

The Cardenas (2000) study also sought to verify that when the SCS displays the red *stop* signal, at least 95 percent Standard Proctor dry unit weight is achieved under adequate compaction conditions. Compaction curves were developed for Standard Proctor effort to identify the maximum dry unit weight and optimum water content for each of the soils tested. Nuclear gauge measurements obtained after the SCS displayed the *stop* signal verified at least 95 percent Standard Proctor relative compaction for all of the soils tested except for a low plasticity clay (Figure 2.22). This soil was determined to have been compacted overly wet of optimum for all lifts and therefore did not represent adequate compaction conditions (Cardenas, 2000).

The Juran and Rousset (1999) field compaction study discussed in Section 2.3.1 also included an evaluation of the SCS. In this study, each compaction control device was used to assess the compaction quality/acceptance of five test trenches compacted with sandy backfill, 5-ft thick. For these tests, the SCS generally displayed the red *stop* signal, although direct measurement of the unit weight using the nuclear gauge indicated less than 95 percent Standard Proctor relative compaction.

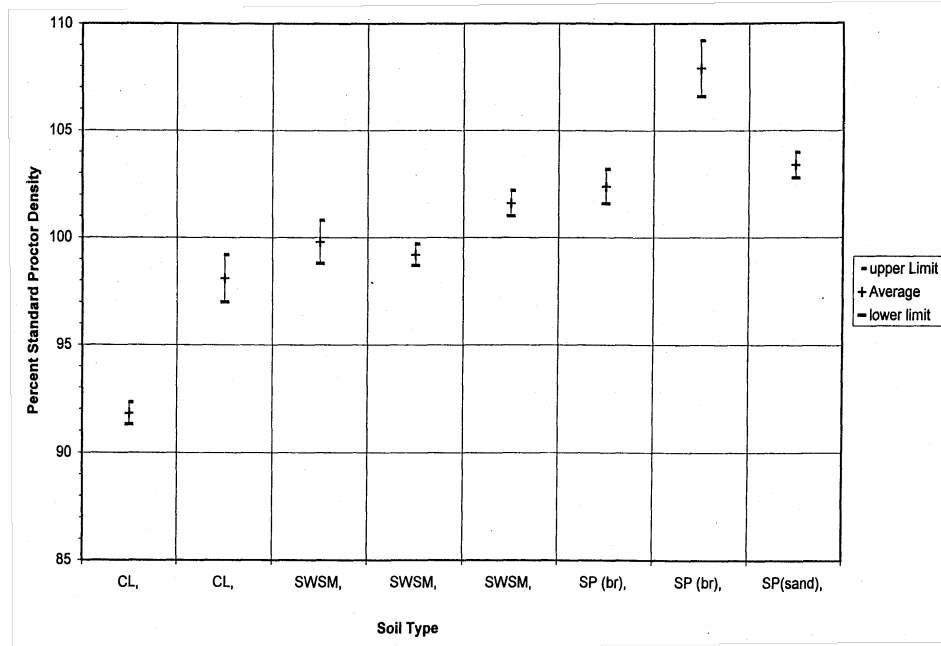


Figure 2.22. Percent Standard Proctor compaction at SCS stop signal (Cardenas 2000).

## 2.6 Selection of Methods for Study

Nine non-nuclear compaction control devices were identified and considered for this study. Three devices are based on impact testing: the PANDA dynamic cone penetrometer, the Clegg Impact Hammer, and the standard dynamic cone penetrometer (DCP). Three devices are based on measuring the electrical properties of soil: the Moisture Density Indicator (MDI), the Electrical Density Gauge (EDG), and the Soil Quality Indicator (SQI). Finally, three devices measure the stiffness properties of soil: the Portable Seismic Property Analyzer (PSPA), the GeoGauge, and the Soil Compaction Supervisor (SCS).

Based on an evaluation of the technical basis of each compaction control method and results from previous testing, seven of the nine identified devices were initially selected for use in the experimental program in this study (Table 2.1). The two devices that were not selected for further study are the GeoGauge and the SCS. The GeoGauge was not selected because of the previously identified technical problems related to seating and repeatability. The SCS was not selected because of its weak theoretical basis and the lack of evidence of prior success.

**Table 2.1. Compaction control devices selected for experimental studies.**

<b>Compaction Control Device</b>	<b>Selected for Study</b>
PANDA	X
Clegg	X
DCP	X
MDI	X
EDG	X
SQI	X
PSPA	X
GeoGauge	
SCS	

The compaction control devices listed in Table 2.1 were evaluated through two field studies and one laboratory study. Field Study 1 focused on evaluating the five devices that were available during the first year of this study (Table 2.2), while Field Study 2 focused on two electrical devices (MDI, EDG) that became available during the second year of this study. The Laboratory Study investigated the two electrical devices (MDI, EDG), as well as the PANDA and Clegg Impact Hammer, under controlled compaction conditions in large-scale laboratory specimens.

Problems during field testing were encountered for two of the devices (SQI and EDG). The SQI was selected for study and it was used to collect data during Field Study 1. Soil samples were sent to the SQI manufacturer (TransTech Systems) to develop soil-specific calibrations so that SQI field measurements of dry unit weight and water content could be compared with direct measurements of these parameters by traditional methods. However, these calibrations were not performed by TransTech due to technical problems. Without these calibrations, the SQI field data could not be converted into dry unit weights and water contents. Thus, the accuracy of the SQI could not be evaluated in this study.

Calibration of the EDG requires several direct measurements of dry unit weight and water content to develop a “Soil Model”. These measurements must be made in the field because a laboratory calibration procedure has not been developed for the device. During Field Study 2, time constraints due to the construction schedule precluded the development of “Soil Models” in the field, and thus the device could not be evaluated.

**Table 2.2. Compaction control devices used in each experimental study.**

<b>Compaction Control Device</b>	<b>Field Study 1</b>	<b>Field Study 2</b>	<b>Laboratory Study</b>
PANDA	X		X
Clegg	X		X
DCP	X		
MDI		X	X
EDG		X <sup>(2)</sup>	X
SQI	X <sup>(1)</sup>		
PSPA	X		
GeoGauge			
SCS			

- Notes: (1) SQI was initially selected for study but calibration could not be performed.
- (2) EDG was selected for use in field study 2, but field difficulties precluded its assessment.



## 3. Field Study 1

### 3.1 Introduction

Field study 1 was conducted during the summer of 2004 and intended to include the five compaction control devices available at the time: the PANDA, the Clegg Impact Hammer, the standard DCP, the SQI, and the PSPA (Table 2.2). However, because of the calibration issues discussed in Chapter 2, the SQI could not be evaluated in this study. Five soils were selected to evaluate the remaining four devices. These soils represent typical soils used in Texas for the construction of embankments (two soils) or as backfill for retaining walls (three soils). This chapter describes the soils used, the construction of the field test pads, and the results from field testing.

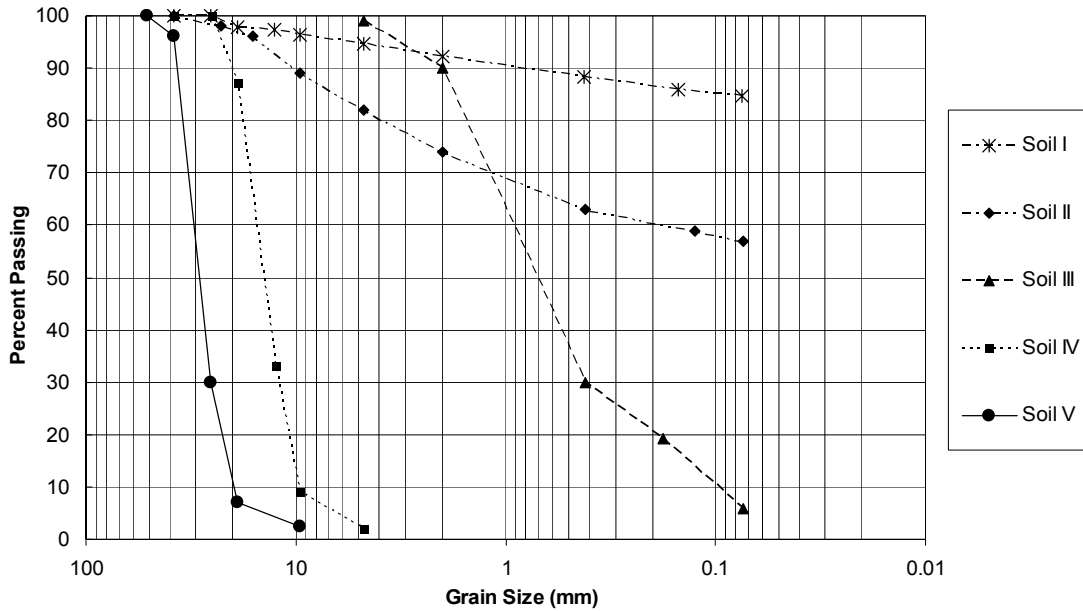
### 3.2 Material Description

Five soils were obtained for field testing. Two of these soils were clayey soils that are typical of embankment construction in Texas. The other three soils were typical select backfill materials used in retaining wall construction.

Two clayey soils, a high plasticity clay (Soil I, PI = 31) and a low plasticity clay (Soil II, PI = 17), were selected to represent typical embankment materials available in the central Texas region. The grain size distributions of these materials are shown in Figure 3.1. While there are no specific requirements for embankment materials in the TxDOT Standard Specifications (TxDOT 2004a), the CL and CH soils are native to the region and were obtained from active TxDOT construction sites in June 2004.

**Table 3.1. Five soil types selected for Field Study 1 (TxDOT 2004b)**

<b>Label</b>	<b>Soil Type</b>
<b>I</b>	High plasticity clay-CH
<b>II</b>	Low plasticity clay-CL
<b>III</b>	Well-graded sand-SW (TxDOT Type B)
<b>IV</b>	Poorly graded gravel-GP (TxDOT Type A)
<b>V</b>	Poorly graded gravel-GP (TxDOT Type D)



Proctor maximum dry unit weight for Soil I is approximately 116 pcf at an optimum water content of about 14.9 percent.

Figure 3.3 displays the compaction curves from Soil II (CL). Again, the compaction curves exhibit classic shapes with distinct peaks. The Standard Proctor maximum dry unit weight for Soil II is approximately 103 pcf at an optimum water content of about 19.5 percent. The Modified Proctor maximum dry unit weight for Soil II is approximately 113 pcf at an optimum water content of about 15.0 percent.

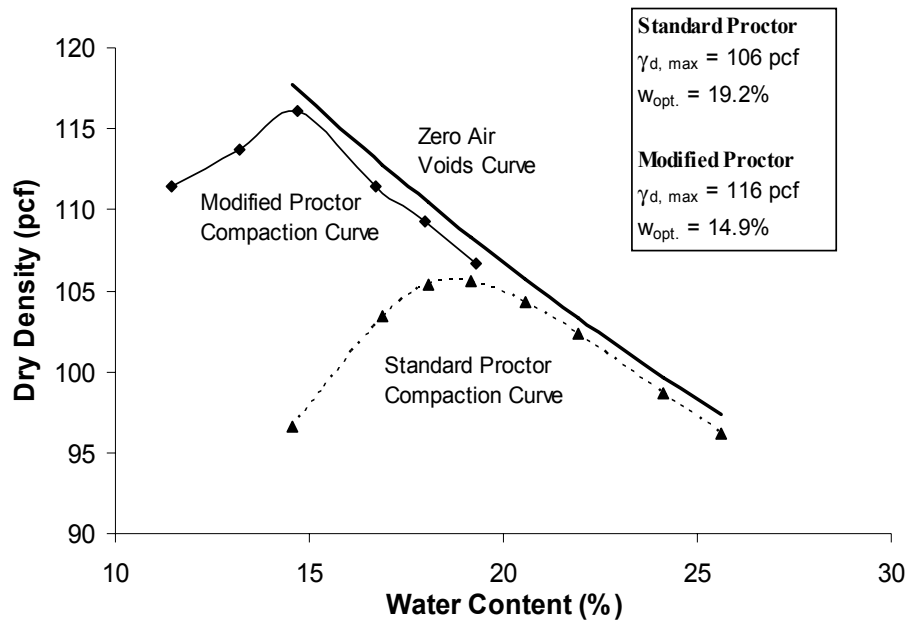


Figure 3.2. Compaction curves for Soil I

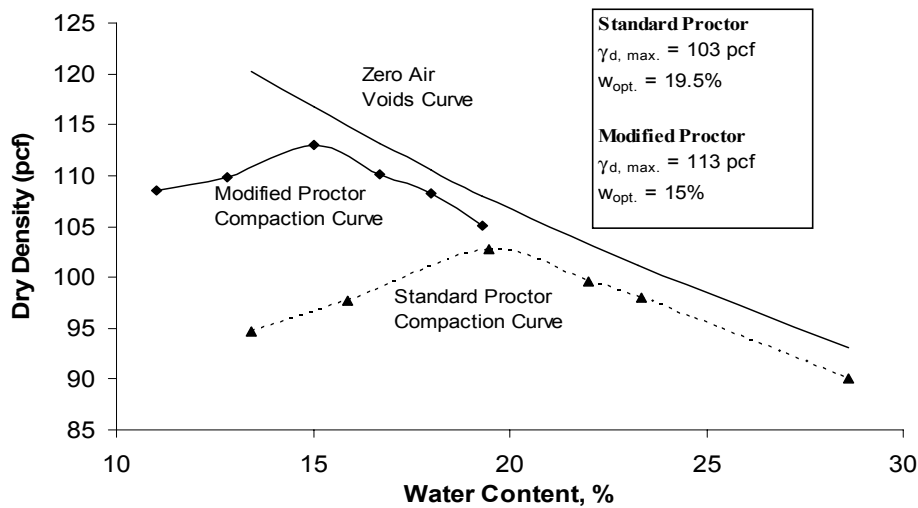


Figure 3.3. Compaction curves for Soil II

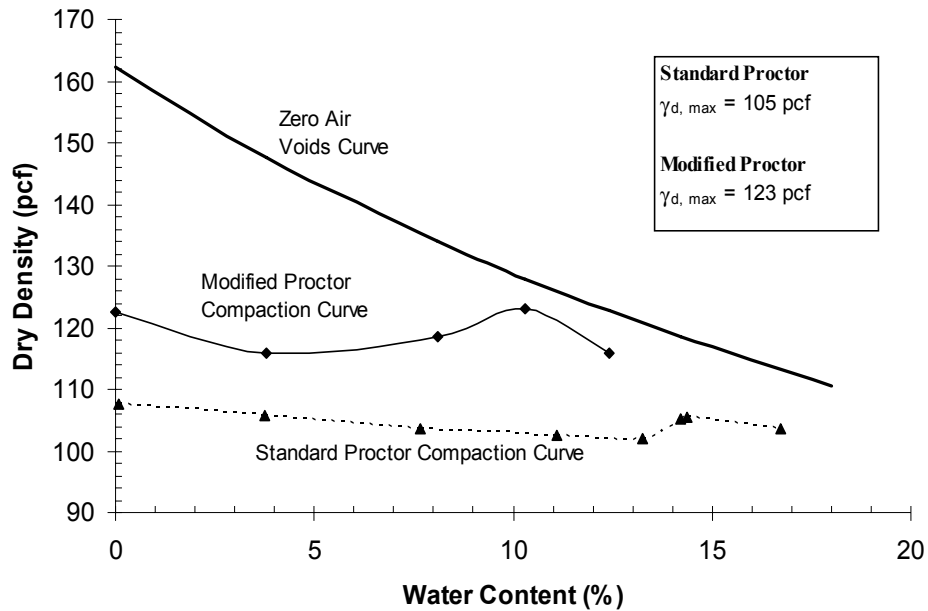


Figure 3.4. Compaction curves for Soil III

Figure 3.4 displays the compaction curves for Soil III, the well-graded sand (SW). These compaction curves display only a minor effect of water content on dry unit weight, which is typical for coarse-grained materials. Based on these curves, the Standard Proctor maximum dry unit weight is approximately 105 pcf and the Modified Proctor maximum dry unit weight is approximately 123 pcf. Soil IV was compacted at 0 percent water content and Standard Proctor compactive effort, with the resulting dry unit weight approximately equal to 104 pcf.

### 3.3 Description of Field Testing

To evaluate the compaction control device for the five test soils, five test pads were constructed. Each test pad was approximately 40 ft long, 25 ft wide, and averaged 12 in. deep (Figure 3.5). The test pads were constructed outdoors at a TxDOT facility in Austin, Texas and were placed in 6-in. compacted lifts on top of existing fill material. No moisture control was used in placement or compaction of the granular materials (Soils III, IV, and V); however, water was added to the two fine-grained soils (Soils I and II) in an attempt to achieve approximately the optimum water content. While strict compaction requirements (e.g., specific values of relative compaction) were not needed for device comparisons to be meaningful, a minimum level of compaction was desired so that all devices would be operating within typical limits.

For the test pads composed of granular soils (Soils III, IV, and V), each 6-in. lift was compacted via ten to fifteen passes of a 25,000-lb. front-end loader or large dump truck. For the test pads composed of fine-grained soils (Soils I and II), each lift was compacted by five to ten passes with a 25,000-lb. front-end loader and then rolled with a 17,000-lb. pneumatic roller for twenty to thirty additional passes. The test pads for Soils I and II were covered with plastic sheeting for moisture retention.



Figure 3.5. Compacted field test pads for Field Study 1

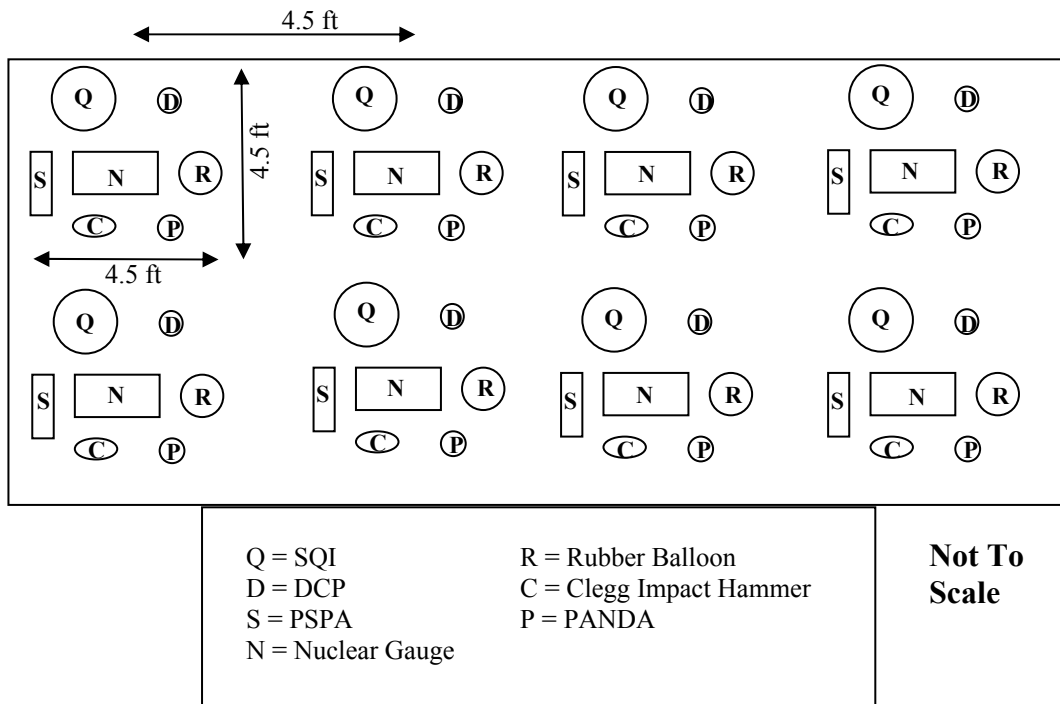


Figure 3.6. Layout of test locations within field test pads

Each device was tested at eight locations on each of the test pads. Each test location encompassed an area approximately 4.5 ft by 4.5 ft, separated by approximately 4.5 ft on center (Figure 3.6). The two traditional methods (rubber balloon, nuclear gauge) and five test devices (PANDA, Clegg Impact Hammer, DCP, SQI, and PSPA) were tested in a side-by-side manner.

Each device was tested within approximately 1 ft. of the nuclear gauge test location (Figure 3.6). As previously noted, although the SQI was tested in the field, soil-specific calibration could not be performed and thus no meaningful measurements of dry unit weight or water content can be reported.

Some of the compaction control devices could not be used on Soils IV and V due to particle size limitations (Table 3.3). The nuclear gauge was used on all of the soils; however, the direct transmission mode was used for Soils I, II, and III, while the backscatter mode was used for Soils IV and V. The rubber balloon test was not performed on Soils IV and V because the large particles precluded an accurate assessment of the hole volume (ASTM D2167). The PANDA and DCP were not performed on Soil V because particles larger than 2 in. adversely influence the results (ASTM 6951).

**Table 3.3. List of devices tested on each test pad**

<b>Compaction Control Test</b>	<b>Soils I, II, III</b>	<b>Soil IV</b>	<b>Soil V</b>
Nuclear Gauge	X	X	X
Rubber Balloon	X		
PANDA	X	X	
Clegg	X	X	X
DCP	X	X	
SQI	X <sup>(1)</sup>	X <sup>(1)</sup>	X <sup>(1)</sup>
PSPA	X	X	X

Notes: (1) SQI was selected for study but calibration could not be performed and thus no results can be reported.

### 3.4 Equipment Calibration

#### 3.4.1 PANDA Dynamic Cone Penetrometer

The PANDA Dynamic Cone Penetrometer software has a built-in soil library containing failure and tolerance lines (i.e., acceptance curves) for different types of soils. If the acceptance curves from the PANDA software are used to evaluate the compaction level in the field, no soil-specific calibration is necessary. However, to use the acceptance curves from the PANDA soil library, the soil must be classified according to the French soil classification system (Rivat, 2005).

In the French soil classification system, soils are first divided into natural and artificial soils. Artificial soils are defined as gravel-sized particles that are generated by crushing; all other soils are considered natural soils. Natural soils are divided into sub-categories based on maximum particle size, as shown in Figure 3.7. The top chart is used for soils with a maximum particle size less than or equal to 2 in. (50 mm), while the bottom chart is used for soils with a maximum particle size larger than 2 in. (50 mm). For soils with a maximum particle size less than or equal to 2 in. (50 mm), the final soil class is defined based on the percent passing the #200 sieve, the percent passing the #10 sieve, and the plasticity index (labeled  $I_p$  in Figure 3.7) of the soil. Alternatively, the Methylene blue test can be used instead of the plasticity index. For soils with a maximum particle size larger than 2 in. (50 mm), the final soil class is defined based on the percent passing sieve #200, the plasticity index, and the particle shape.

The four soils evaluated by the PANDA device were classified according to the French soil classification system (Figure 3.7) and these classifications are listed in Table 3.4. Based on its significant fines content (passing the #200 sieve) and plasticity index of 31, Soil I is classified as A<sub>3</sub>. Based on its significant fines content and plasticity index of 17, Soil II is classified as A<sub>2</sub>. Soil III is classified as B<sub>2</sub> because less than 12 percent passes the #200 sieve, more than 70 percent passes the #10 sieve (Figure 3.1), and the soil is moderately plastic (PI > 1). Finally, Soil IV is classified as D<sub>2</sub> because less than 12 percent passes the #200 sieve, less than 70 percent passes the #10 sieve (Figure 3.1), and the soil is non-plastic.

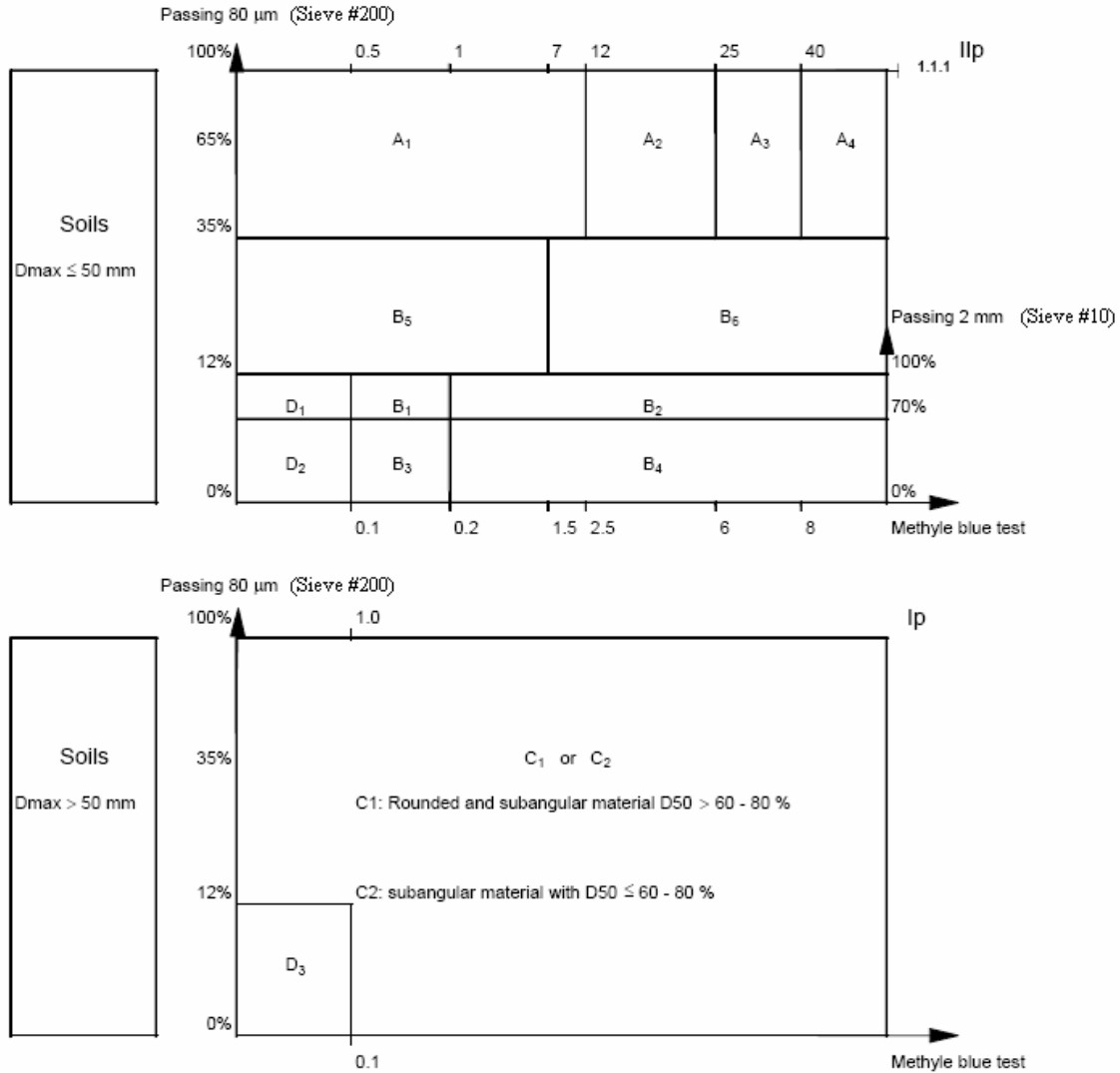


Figure 3.7. French soil classification system chart (Rivat 2005).

**Table 3.4. French soil classification of test soils**

Label	French Soil Class
I	A <sub>3</sub>
II	A <sub>2</sub>
III	B <sub>2</sub>
IV	D <sub>2</sub>

### 3.4.2 Clegg Impact Hammer

The Clegg Impact Hammer provides measurements of the Clegg Impact Value (CIV) during field testing. Laboratory values of CIV must be measured in soil specimens compacted in compaction molds to determine target CIV values for a given material and required relative compaction (ASTM D 5784). Laboratory testing was performed to evaluate the target CIV for Soils I, II, and III. Soils IV and V contain particles that are too large for laboratory compaction testing, thus negating use of the Clegg Impact Hammer.

In accordance with ASTM D 5784, the relationship between CIV and water content is used to identify a target CIV. The target CIV is chosen as the maximum value obtained over the range of water contents tested. To better understand the impact of dry unit weight alone on the CIV, CIV testing was performed at a constant water content and variable dry unit weight.

The measured CIV for Standard Proctor compactive effort are plotted versus water content for Soil I in Figure 3.8. The CIV decreases as the water content increases from dry of optimum (optimum water content = 19.2 percent) to wet of optimum. Based on the maximum CIV in Figure 3.8, the target CIV for Soil I for Standard Proctor compactive effort is 7.1. Figure 3.9 displays measured CIV versus dry unit weight for specimens compacted at a water content of approximately 24 percent. The CIV increases slightly from 2.5 to 3.0 over the range in dry unit weight from 94.5 to 100.5 pcf. This increase is much smaller than observed in Figure 3.8, indicating that the CIV is influenced more by water content than dry unit weight in this clayey soil.

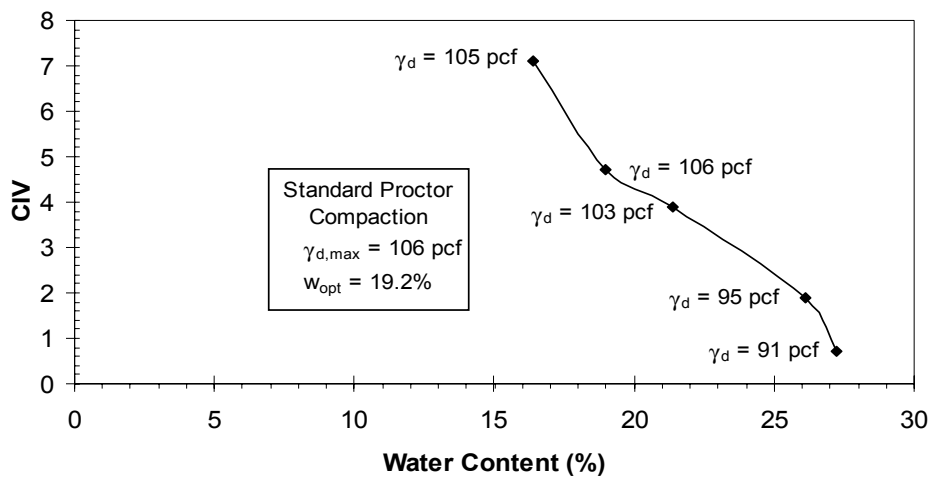


*Figure 3.8. Variation of CIV with water content for Soil I*

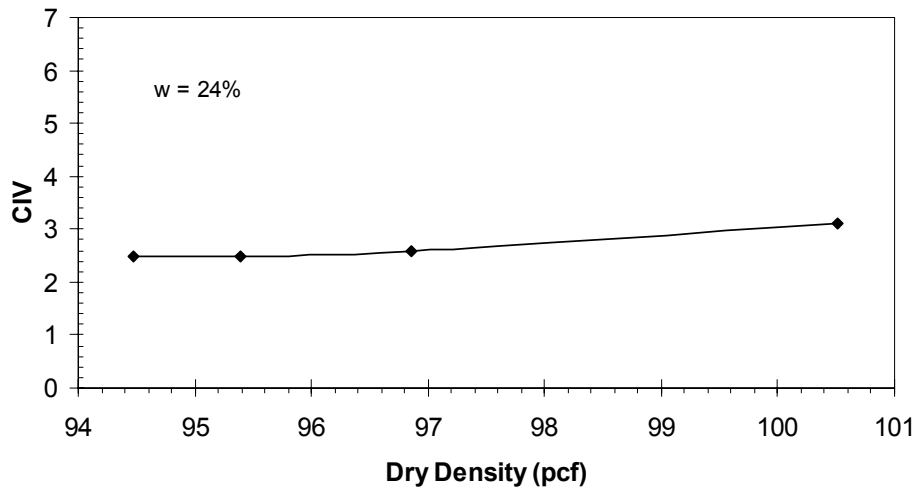


Figure 3.9. Variation of CIV with dry unit weight for Soil I

The measured CIV for Standard Proctor and Modified Proctor compactive efforts are plotted versus water content for Soil II in Figure 3.10. Again, the CIV decreases as the water content increases. The CIV is approximately 17.6 at a water content of 5 percent and becomes less than 2.0 at water contents greater than approximately 20 percent. At water contents greater than 25 percent no CIV was recorded because the soil was so soft and the hammer compressed the soil so much that the hammer hit the stops on the device and did not record a value. Based on the maximum CIV in Figure 3.10, the target CIV for Soil II for Standard Proctor compactive effort is 7.9 and for Modified Proctor compactive effort is 17.6. Figure 3.11 displays measured CIV versus dry unit weight for specimens compacted at a water content of approximately 21 percent. Similar to the results from Soil I, the CIV only increases slightly over the dry unit weight range of 94 to 104 pcf. Thus, it appears that for clayey soils, CIV is most influenced by water content.

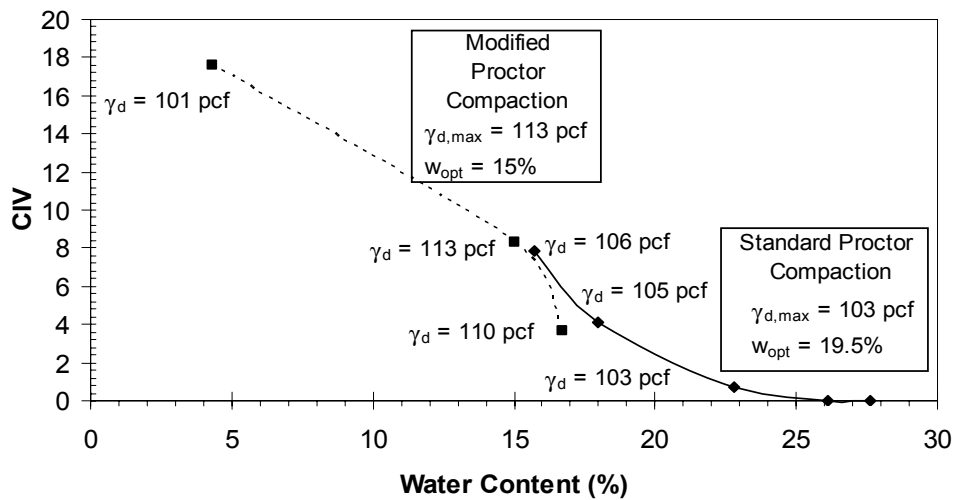


Figure 3.10. Variation of CIV with water content for Soil II

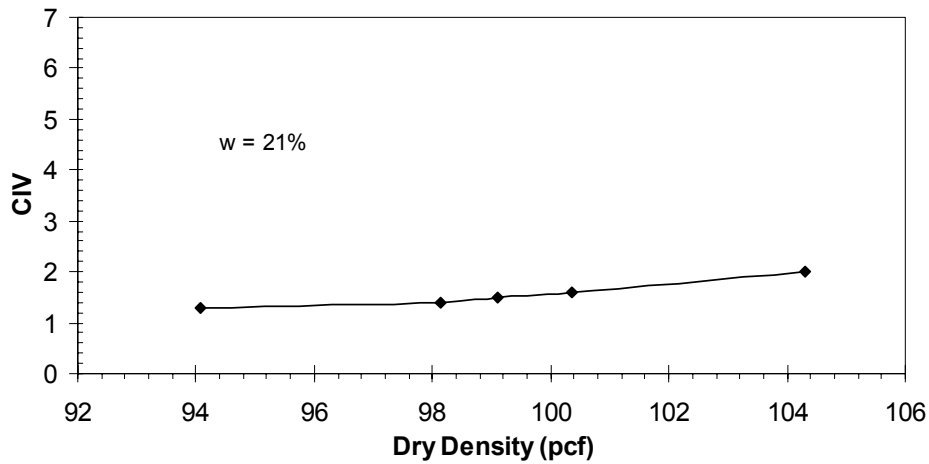


Figure 3.11. Variation of CIV with dry unit weight for Soil II

The measured CIV for Standard Proctor and Modified Proctor compactive efforts are plotted versus water content for Soil III in Figure 3.12. Soil III is well-graded sand and its CIV is not significantly influenced by water content. However, it appears the dry unit weight has a more significant influence, as evidenced by the larger CIV recorded for specimens constructed to larger dry unit weights using Modified Proctor compactive effort. Based on the maximum CIV in Figure 3.12, the target CIV for Soil III for Standard Proctor compactive effort is about 21 and for Modified Proctor compactive effort it is about 35. Figure 3.13 displays measured CIV versus dry unit weight for specimens compacted at a water content of approximately 4 percent. These data indicate that the dry unit weight influences the CIV significantly over the dry unit weight range of 80 to 115 pcf. The most significant increases occur at dry unit weights greater than about 100 pcf.

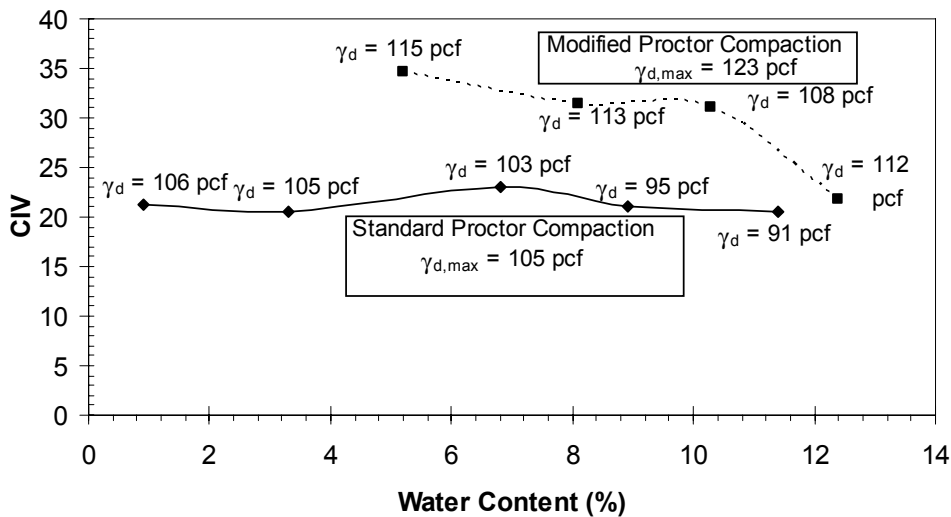


Figure 3.12. Variation of CIV with water content for Soil III

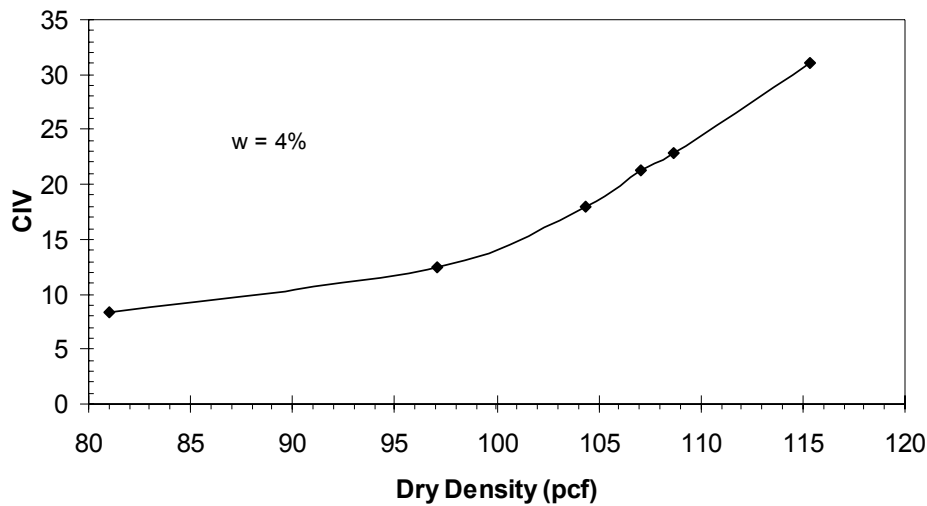


Figure 3.13. Variation of CIV with dry unit weight for Soil III

### 3.4.3 Other Devices

Soil-specific calibration was not performed for the DCP and PSPA. The results from field testing for these devices were used to evaluate whether a strong relationship exists between measured dry unit weight/water content and the results from the DCP (penetration resistance) and PSPA (soil stiffness). Additionally, the general compaction control criteria developed for the DCP by MnDOT (Burnham 1997) and discussed in Chapter 2 will be compared with the field results.

## 3.5 Field Test Results

### 3.5.1 Soil I

Before considering the results from the new compaction control devices, the moist unit weights and water contents measured by the nuclear gauge were compared with those measured by the rubber balloon and oven drying methods. Moist unit weight was compared rather than dry unit weight because the devices make direct measurements of moist unit weight and rely on separate measurements of water content to compute dry unit weight.

Figure 3.14 compares the moist unit weights measured by the nuclear gauge with the moist unit weights measured by rubber balloon for Soils I (CH). Here, the moist unit weights measured by the nuclear gauge were about 15 percent smaller than the moist unit weights measured by the rubber balloon. There was not a systematic difference between the nuclear gauge and oven-dry water contents, although differences as large as +/-10 percent were observed (Adams 2004). These results indicate that there are potential discrepancies between moist unit weights measured by the nuclear gauge and rubber balloon methods. To assess which unit weights were more accurate, the dry unit weights from the nuclear gauge and rubber balloon test methods were plotted versus water content along with the compaction curves for Soil I (Figure 3.15). The dry unit weights from the rubber balloon plot above the zero air voids curve, which indicates that the rubber balloon values are not realistic. It appears there were some problems

performing the rubber balloon tests in the field, such that the hole volumes were not accurately measured. Thus, even for traditional methods, differences in unit weight measurements can exist as a result of operator error. Because of these problems with the unit weight measurements from the rubber balloon test method, the dry unit weights and water contents measured by the nuclear gauge were used as the basis for comparison with the new compaction control devices.

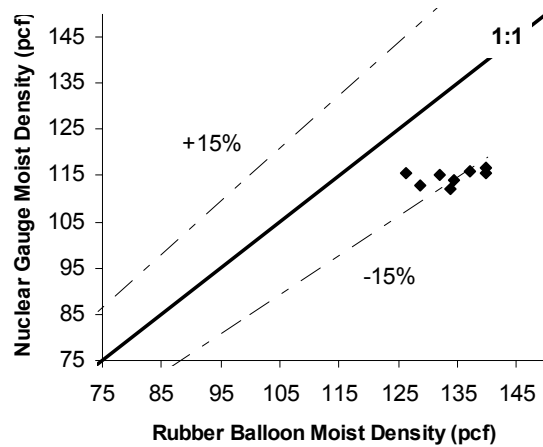


Figure 3.14. Comparison of moist unit weights measured by the nuclear gauge and rubber balloon test for Soil I

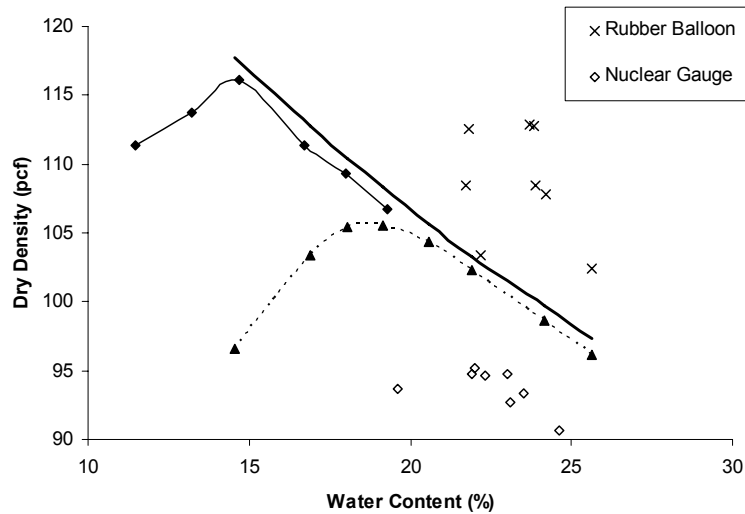


Figure 3.15. Dry unit weights for Soil I measured by the nuclear gauge and rubber balloon test methods.

Table 3.5 summarizes the results from the compaction control devices at the eight test locations for Soil I. Unfortunately, the clay was not compacted well, such that the percent Standard compaction, as measured by the nuclear gauge, ranged from only 85 to 90 percent. The measured CIV are plotted versus dry unit weight and water content (as determined by the nuclear

gauge) in Figure 3.16. Most of the CIV are between 2 and 6 and do not vary systematically with dry unit weight or water content. One measured CIV was above 12 and this value corresponded to the location with the smallest water content. This result confirms what was shown in Figure 3.10; for clayey soils CIV is most affected by water content. The target CIV for Soil I is 7.1, based on the measurement made at 16.5 percent water content (Figure 3.8). Seven of the eight CIV measurements fall below the target CIV, indicating poor compaction. However, the target CIV was measured at a water content that is smaller than the water content in the field. Because water content affects CIV significantly for clayey soils, it is not reasonable to compare CIV obtained at different water contents. Nonetheless, the CIV accurately identified seven of the eight test locations as poorly compacted.

The measured Average Young's Moduli from the PSPA for Soil I are plotted versus dry unit weight and water content in Figure 3.17. Similar to the CIV, there is no clear trend between the PSPA Young's Modulus either dry unit weight or water content. Most of the Young's Moduli from the PSPA range between 7 and 11 ksi, with one large value of 16 ksi. This larger value was measured at location 8 (Table 3.5), the same location where the large CIV was measured and the location of the smallest water content. This result indicates that small-strain stiffness is significantly influenced by water content. This issue is further discussed in Chapter 7.

Figure 3.18 displays dynamic cone resistance ( $q_d$ ) profiles from the PANDA device for Soil I at locations 2 and 8 (Table 3.5). The failure and tolerance lines provided by the PANDA software for 92 percent and 95 percent Standard Proctor are also shown. These locations represent locations with similar dry unit weights, different water contents, and different results from the CIV and PSPA testing. At location 2, the  $q_d$  values fall well below the failure line, indicating poor compaction. The  $q_d$  values are slightly larger at location 8, but still fall below the failure line in the top 8 in. The  $q_d$  value increases dramatically below 8 in., but this result is due to the soil underlying the test pad. The results from the other locations were similar to those shown in Figure 3.18, and thus the PANDA accurately identified each test location as poorly compacted at less than 92 percent Standard Proctor (Table 3.5).

**Table 3.5. Results for Soil I from compaction control devices**

$\gamma_{d, \text{max. std.}} = 106 \text{ pcf}$ $W_{\text{opt. std.}} = 19.2\%$									
Test Location	$\gamma_{d, \text{Nuclear Gauge}}$ (pcf)	$W_{\text{nuclear gauge}}$ (%)	% Standard Compaction	Average CIV	Pass/Fail Target CIV (CIV=7.1)	Average PSPA Young's Modulus (ksi)	PANDA % Standard Compaction	Average DCP Penetration Rate (in/bl)	Pass/Fail MnDOT DCP Criterion (3.0 in/bl)
1	93.3	23.5	88	2.5	Fail	11	<92%	2.8	Pass
2	95.2	22.0	90	3.1	Fail	9	<92%	3.5	Fail
3	94.8	21.9	89	2.5	Fail	8	<92%	3.7	Fail
4	92.7	23.1	87	2.1	Fail	8	<92%	3.1	Fail
5	90.6	24.6	85	4.1	Fail	7	<92%	2.2	Pass
6	94.7	23.0	89	3.5	Fail	7	<92%	4.9	Fail
7	94.6	22.3	89	5.6	Fail	9	<92%	4.1	Fail
8	93.7	19.6	88	12.3	Pass	16	<92%	2.0	Pass

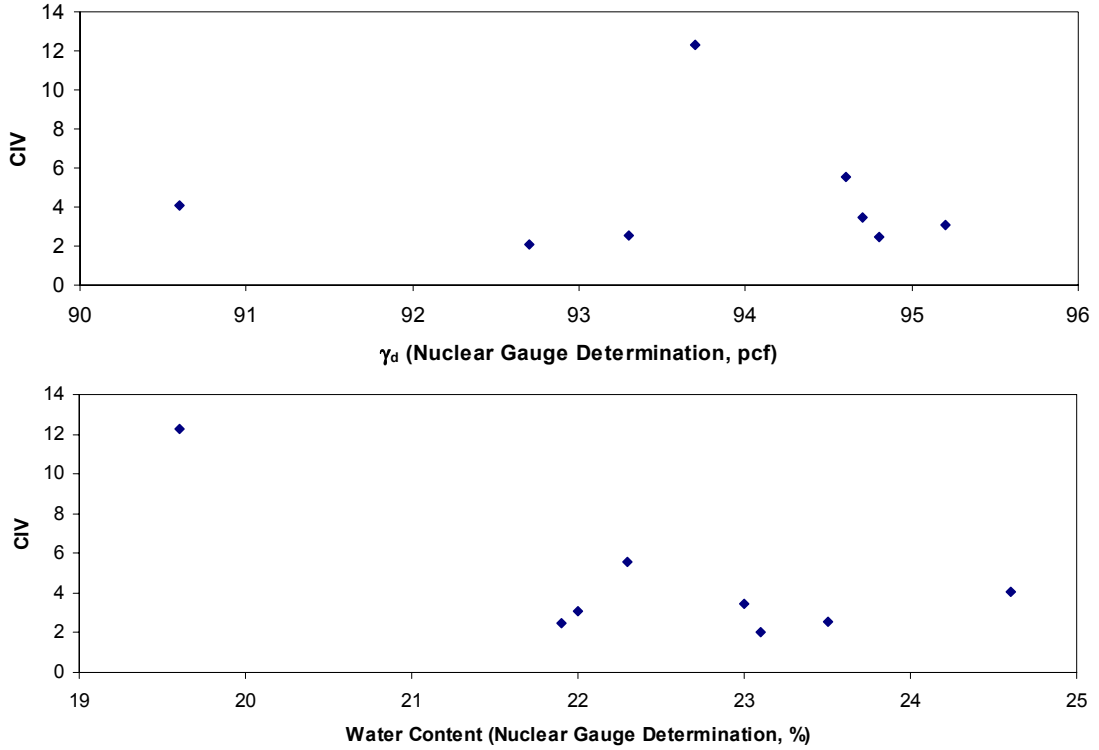


Figure 3.16. CIV versus dry unit weight and water content for Soil I

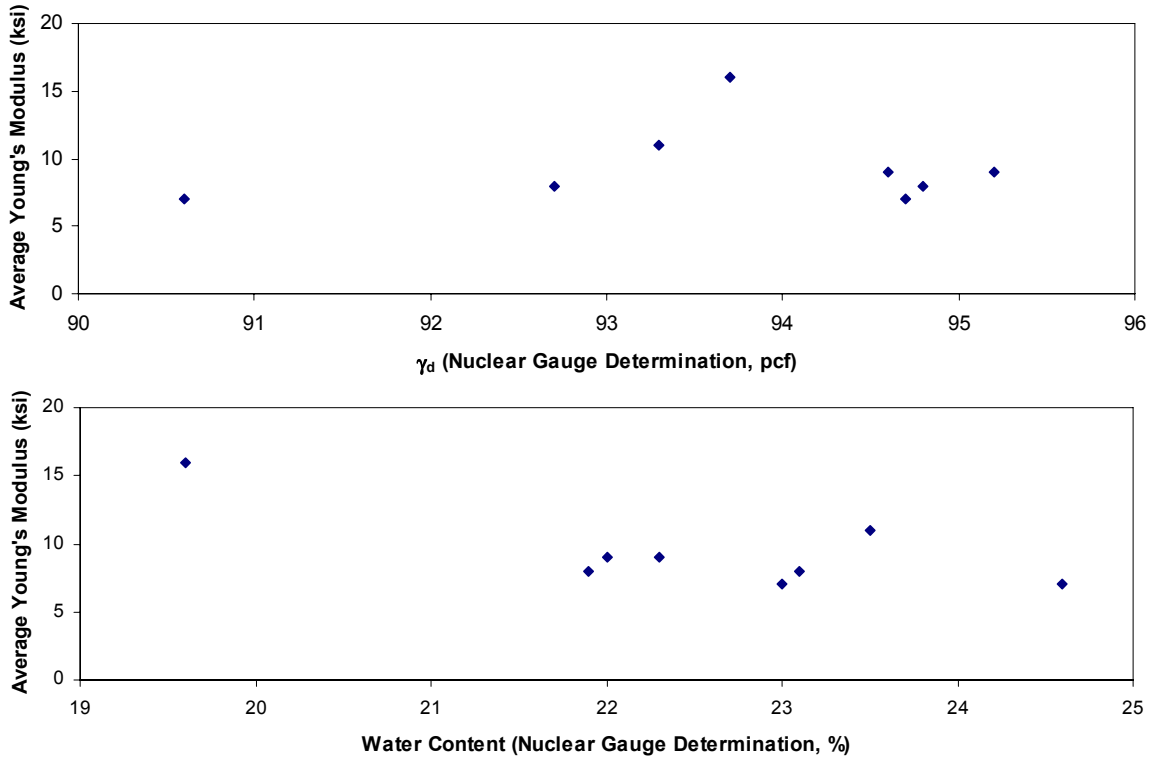


Figure 3.17. PSPA Young's Modulus versus dry unit weight and water content for Soil I

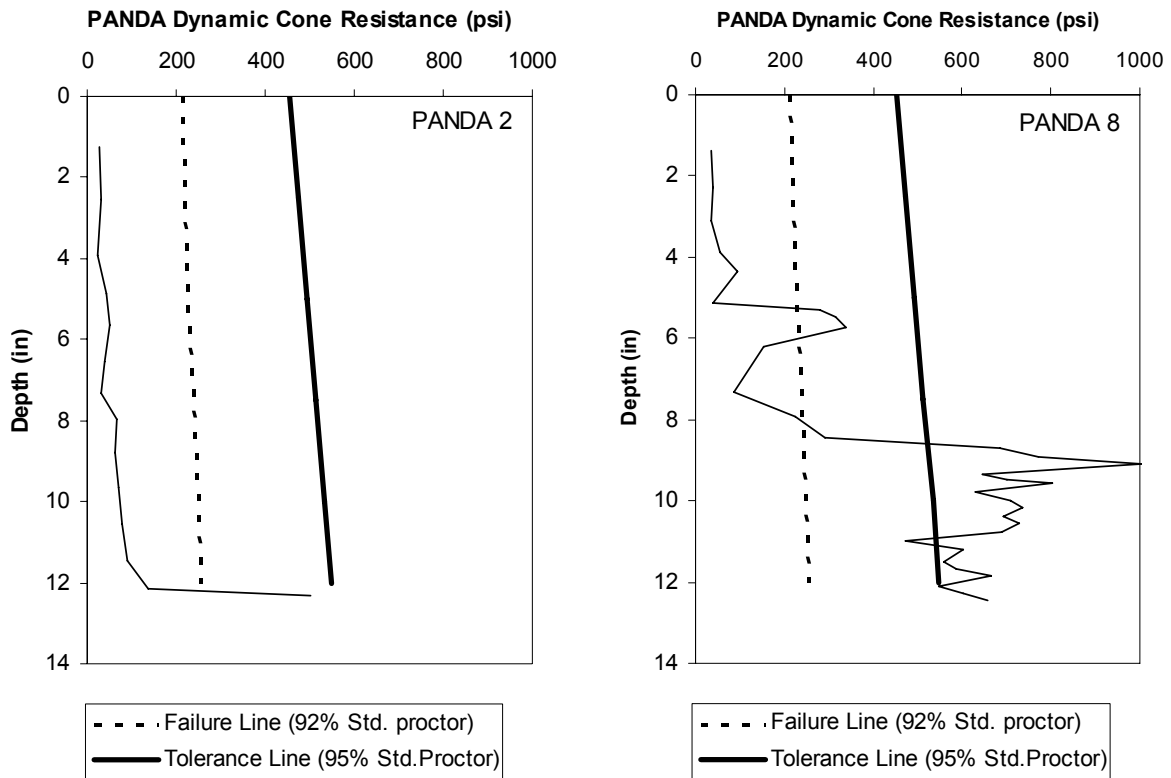


Figure 3.18. PANDA dynamic cone resistance profiles for Soil I at locations 2 and 8.

Figure 3.19 displays DCP profiles (penetration rate in in./blow versus depth) for Soil I at locations 2 and 8 (Table 3.5). At location 2, the DCP penetrated over 4 in. during its first blow and penetrated approximately 2 in./blow at deeper depths. At location 8, the DCP penetrated between 1.5 and 2.5 in./blow over the top 8 in. before the underlying soil was encountered. The MnDOT DCP compaction criterion for clayey soils is 3 in./blow or less. Averaging the DCP penetration rate over the top 6 in., location 2 has an average penetration rate of 3.5 in./blow, while location 8 has an average value of 2.0 in./blow. Based on the MnDOT criterion, location 2 fails the compaction criterion and location 8 passes. Table 3.5 displays the average DCP penetration rate for the 8 test locations and shows that locations 1, 5, and 8 meet the criterion, although based on their dry unit weights, these locations are poorly compacted.

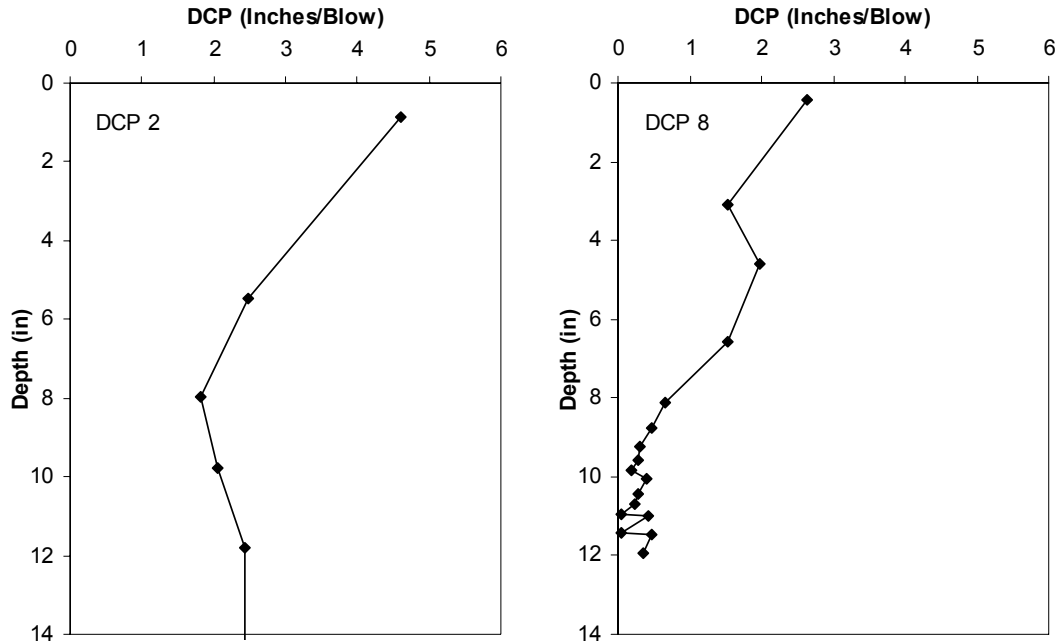


Figure 3.19. DCP profiles for Soil I at locations 2 and 8.

### 3.5.2 Soil II

Similar to Soil I, the moist unit weights and water contents measured by the nuclear gauge were compared with those measured by the rubber balloon and oven drying methods. For Soil II (CL), the moist unit weights measured by the nuclear gauge again were smaller than those from the rubber balloon (Figure 3.20). When plotting the dry unit weights from the nuclear gauge and rubber balloon/oven-drying methods versus water content (Figure 3.21), only two points from the rubber balloon fall above the zero air voids curve. Although all of the rubber balloon results cannot be discarded based on their location relative to the zero air voids curve, the nuclear gauge dry unit weights and water contents will be used as the basis for comparison, making the results for Soil II consistent with those for Soil I.

Table 3.6 summarizes the results from the compaction control devices at the eight test locations for Soil II. Most of the test locations were compacted to between 91 and 96 percent Standard relative compaction, except for location 1, which was compacted to only 84 percent. The measured CIV are plotted versus dry unit weight and water content (as determined by the nuclear gauge) in Figure 3.22. The CIV range from 2.5 and 7.1, and do not vary systematically with dry unit weight. There is a slight reduction in CIV with increasing water content, but there is significant scatter in this trend. The target CIV for Soil II is 7.9, based on the measurement made at 16 percent water content (Figure 3.10). All of the field values of CIV fall below this value, indicating poor compaction. Although this result is in agreement with the measured values of dry unit weight and percent Standard compaction, it is not recommended that one compare CIV values obtained at different water contents for clayey soils because water content affects CIV more than dry unit weight for clayey soils (Figures 3.10, 3.11).

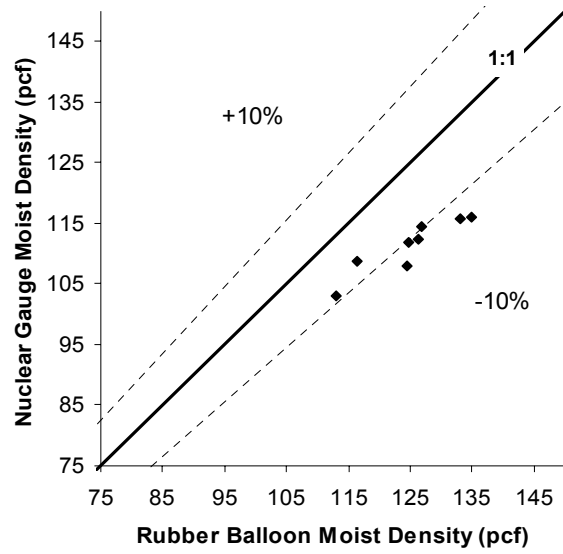


Figure 3.20. Comparison of moist unit weights measured by the nuclear gauge and rubber balloon test for Soil II.

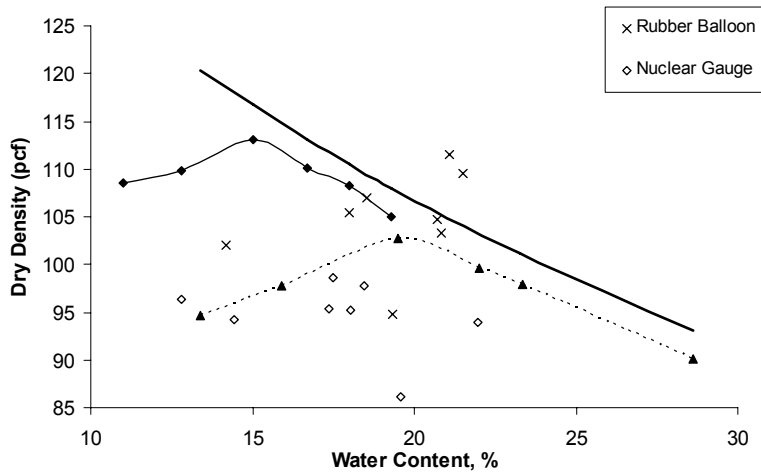
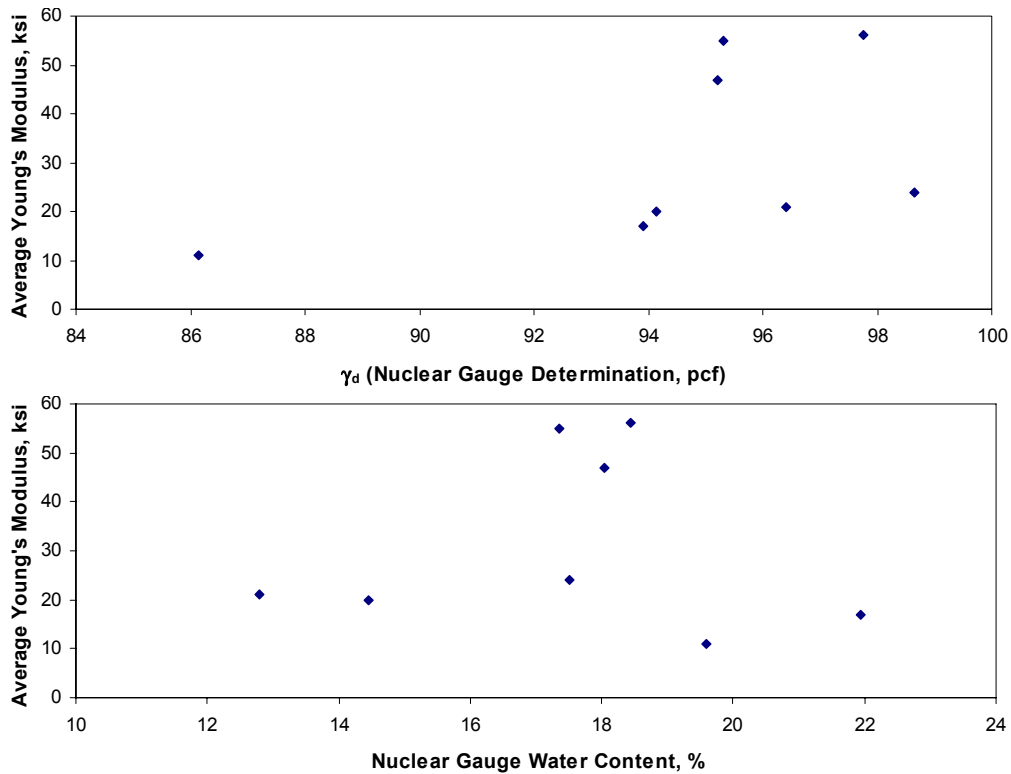


Figure 3.21. Dry unit weights for Soil II measured by the nuclear gauge and rubber balloon test methods

**Table 3.6. Results for Soil II from compaction control devices**

$\gamma_d, \text{max. std.} = 103 \text{ pcf}$									
$W_{\text{opt. std.}} = 19.5\%$									
Test Location	$\gamma_d$ , Nuclear Gauge (pcf)	$W_{\text{nuclear gauge}}$ (%)	% Standard Compaction	Average CIV	Pass/Fail Target CIV (CIV=7.9)	Average PSPA Young's Modulus (ksi)	PANDA % Standard Compaction	Average DCP Penetration Rate (in/bl)	Pass/Fail MnDOT DCP Criterion (3.0 in/bl)
1	86.2	19.6	84	6.7	Fail	11	<92%	6.9	Fail
2	94.2	14.5	91	7.1	Fail	20	<92%	2.4	Pass
3	93.9	22.0	91	2.5	Fail	17	<92%	3.0	Pass
4	95.2	18.1	92	4.2	Fail	47	<92%	5.0	Fail
5	97.8	18.5	95	4.1	Fail	56	<92%	3.7	Fail
6	98.7	17.5	96	6.3	Fail	24	<92%	2.0	Pass
7	95.3	17.4	93	3.6	Fail	55	<92%	1.2	Pass
8	96.4	12.8	94	4.7	Fail	21	<92%	1.2	Pass



*Figure 3.22. CIV versus dry unit weight and water content for Soil II.*

The measured Average Young's Moduli from the PSPA for Soil II are plotted versus dry unit weight and water content in Figure 3.23. Similar to the CIV results, there is no clear trend between the Young's Moduli from the PSPA and dry unit weight. For the locations with dry unit weights between 94 and 99 pcf, the Young's Moduli range from less than 20 ksi to more than 50 ksi. The measured water contents do not explain the differences in measured Young's Moduli and plotting Young's Modulus versus saturation resulted in a similar trend as Figure 3.23. It is surprising that the Young's Moduli for Soil II do not vary systematically with water content or saturation. This result may indicate some variability between the water content at the nuclear gauge measurement locations and the PSPA measurement locations.

Figure 3.24 displays PANDA dynamic cone resistance ( $q_d$ ) profiles for Soil II at locations 1 and 8 (Table 3.6). These two profiles are shown for illustrative purposes. The failure and tolerance lines provided by the PANDA software for 92 percent and 95 percent Standard Proctor are also shown. Locations 1 and 8 represent locations with different dry unit weights (86 pcf versus 96 pcf, respectively) and different water contents (19.6 percent versus 12.8 percent, respectively), as listed in Table 3.6. For both locations, the  $q_d$  values fall well below the failure line, indicating poor compaction. Table 3.6 summarizes the compaction results from the PANDA device for the all eight locations. None of the eight locations tested by the PANDA indicated compaction above 92 to 95 percent Standard compaction (Table 3.6), al though the field measurements indicated that locations 4 through 8 were compacted to at least 92 percent relative compaction.

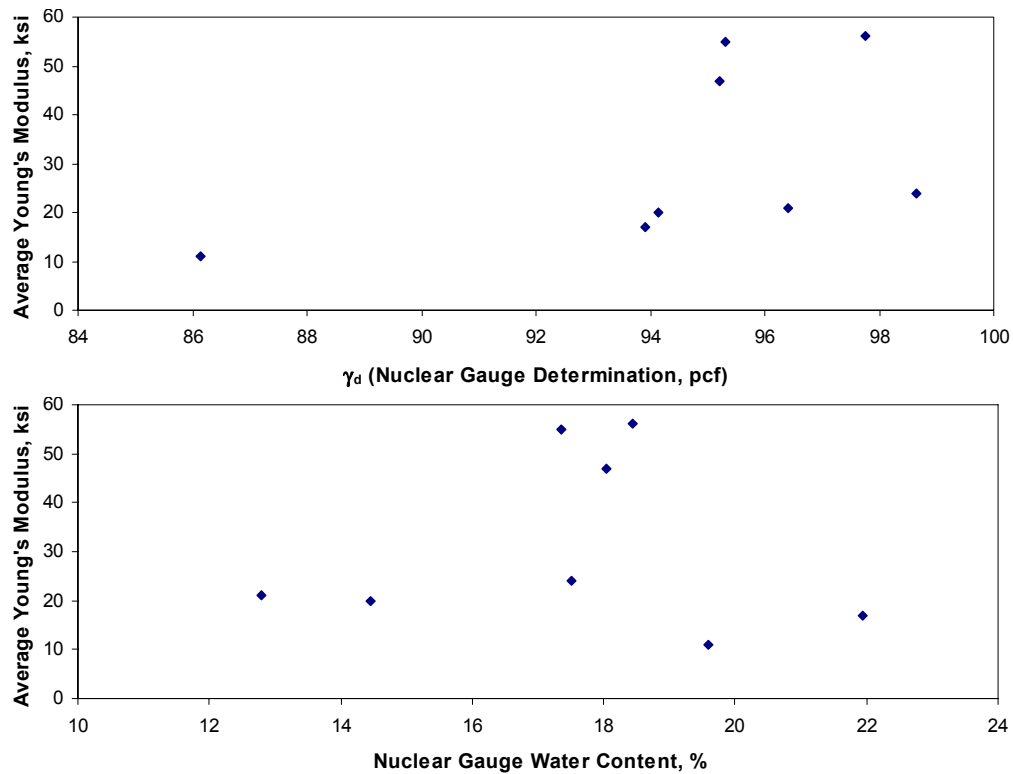


Figure 3.23. PSPA Young's Modulus versus dry unit weight and water content for Soil II.

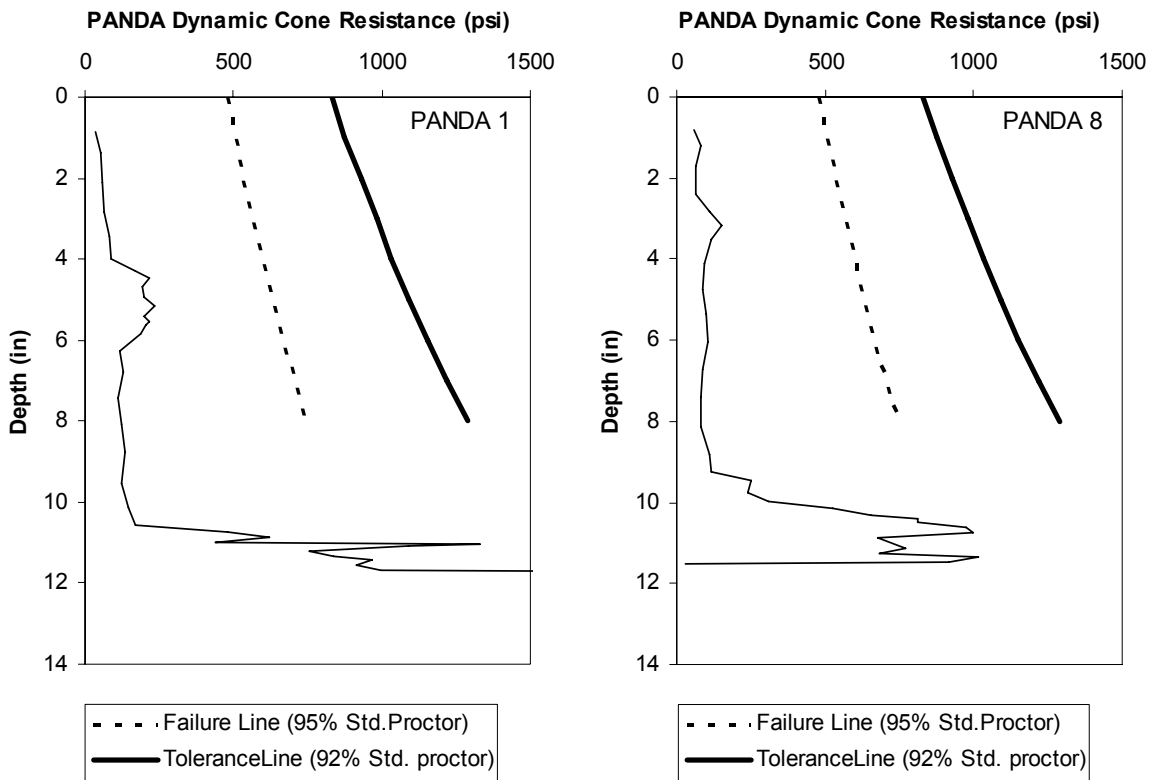


Figure 3.24. PANDA dynamic cone resistance profiles for Soil II at locations 1 and 8.

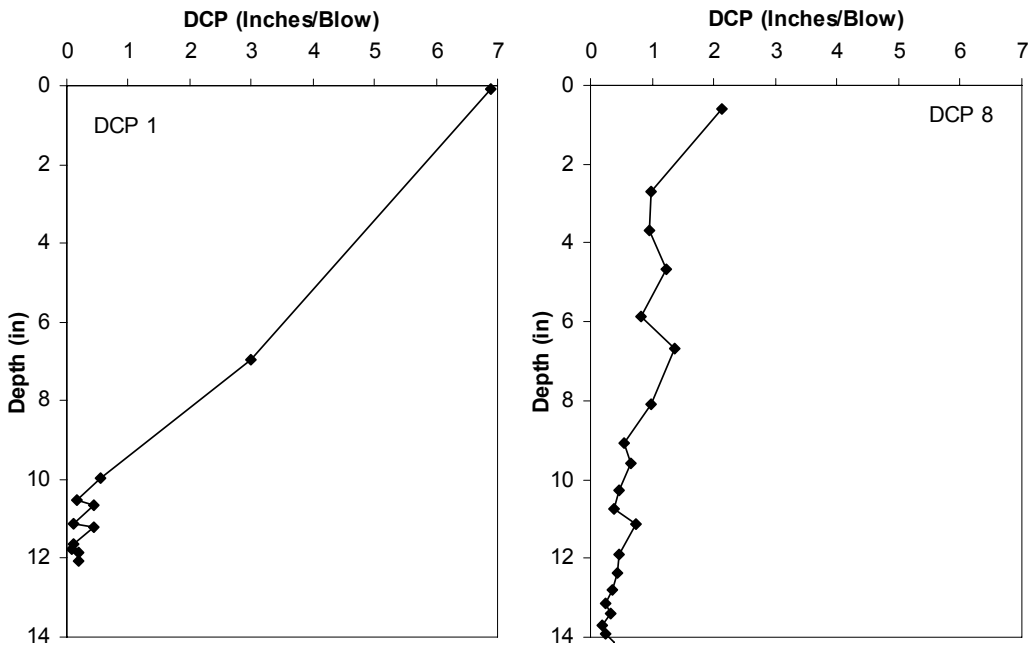


Figure 3.25. DCP profiles for Soil II at locations 1 and 8.

Figure 3.25 displays DCP profiles (penetration rate in in./blow versus depth) for Soil II at locations 1 and 8 (Table 3.6). These two locations are again being used for illustrative purposes. At location 1, the DCP penetrated almost 7 in. during its first blow and penetrated at total of 10 in. in two blows. Below a depth of 2 in., the penetration rate reduced to less than 1.0 in./blow because the underlying soil was reached. At location 8, the DCP penetrated less than about 1.0 in./blow over most of the top 10 in. before the underlying soil was encountered. The MnDOT DCP compaction criterion for clayey soils is 3 in./blow. Averaging the DCP penetration rate over the top 6 in., location 1 has an average penetration rate of 6.9 in./blow, while location 8 has an average value of 1.2 in./blow. Based on the MnDOT criterion, location 1 fails the compaction criterion and location 8 passes. Table 3.6 displays the average DCP penetration rate for the 8 test locations and shows that locations 2, 3, 6, 7, and 8 pass the criterion. These assessments accurately identify the well-compacted locations of 6, 7, and 8 (assuming 92 percent relative compaction to be adequate), but miss well-compacted locations 4 and 5.

### 3.5.3 Soil III

The moist unit weights and water contents measured by the nuclear gauge were compared with those measured by the rubber balloon and oven drying methods for Soil III (SW). The moist unit weights measured by the nuclear gauge again were smaller than those from the rubber balloon (Figure 3.26). When plotting the measured dry unit weights versus water content from the nuclear gauge and rubber balloon/oven-drying methods (Figure 3.27), none of the points from the rubber balloon fall above the zero air voids curve because the water contents were less than 10 percent. Nonetheless, the dry unit weights and water contents from the nuclear gauge will be used as the basis for comparison to make the results for Soil III consistent with the other soils.

Table 3.7 summarizes the results from the compaction control devices at the eight test locations for Soil III. Unfortunately, this sandy soil was not compacted well and the resulting values of percent relative Standard compaction ranged from only 82 to 94 percent. The measured CIV are plotted versus dry unit weight (as determined by the nuclear gauge) in Figure 3.28. The CIV are not plotted versus water content because the Clegg calibration for Soil III (Figure 3.12) showed that CIV is not sensitive to water content in this sandy soil and because the water content range in the field was small (3.3 to 5.6 percent). The CIV range from 3.4 and 23, and the values generally increase with increasing dry unit weight. The target CIV for Soil III is 21, which is the average value measured at 100 percent Standard Proctor compaction (Figure 3.12). All of the field values of CIV fall below this value except for location 4, indicating poor compaction (less than 100 percent Standard relative compaction). The measured Young's Moduli from the PSPA for Soil III are plotted versus dry unit weight in Figure 3.29. Similar to the CIV results, there is a clear increase in Young's Modulus with increasing dry unit weight. The Young's Moduli range from about 15 ksi to more than 35 ksi.

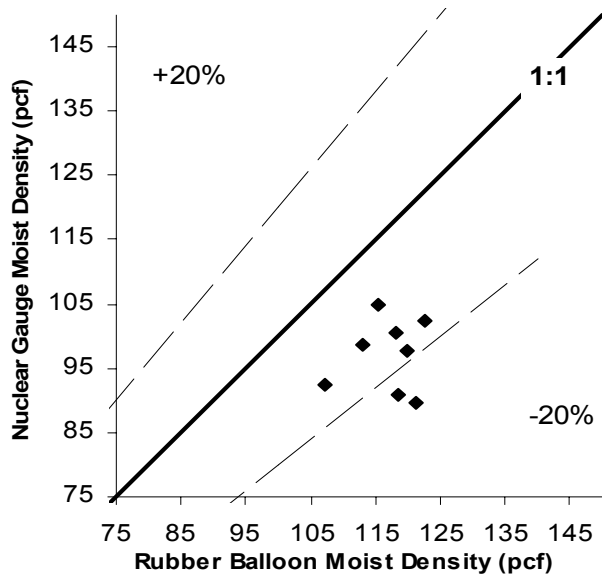


Figure 3.26. Comparison of moist unit weights measured by the nuclear gauge and rubber balloon test for Soil III

Table 3.7. Results for Soil III from compaction control devices

$\gamma_{d, \text{max, std.}} = 105 \text{ pcf}$									
Test Location	$\gamma_d$ , Nuclear Gauge (pcf)	$W_{\text{nuclear gauge}}$ (%)	% Standard Compaction	Average CIV	Pass/Fail Target CIV (CIV=21)	Average PSPA Young's Modulus (ksi)	PANDA % Standard Compaction	Average DCP Penetration Rate (in/bl)	Pass/Fail MnDOT DCP Criterion (0.28 in/bl)
1	86.6	3.3	82	7.3	Fail	15	92-95	0.8	Fail
2	98.7	5.6	94	14.5	Fail	35	>95	0.6	Fail
3	95.5	5.5	91	18.6	Fail	35	>95	0.4	Fail
4	96.5	4.2	92	23.0	Pass	23	>95	0.5	Fail
5	94	3.9	90	8.5	Fail	33	<92	1.1	Fail
6	93.8	4.4	89	11.4	Fail	26	>95	0.5	Fail
7	88.7	4.4	84	13.2	Fail	27	>95	0.6	Fail
8	86.2	3.4	82	3.4	Fail	15	<92	1.2	Fail

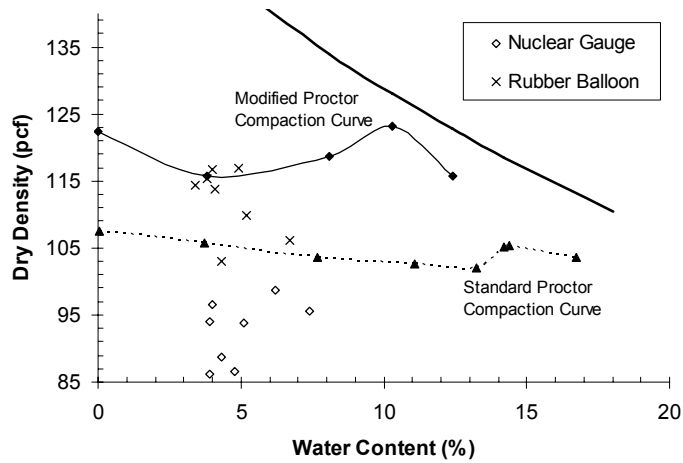


Figure 3.27. Dry unit weights for Soil III measured by the nuclear gauge and rubber balloon test methods

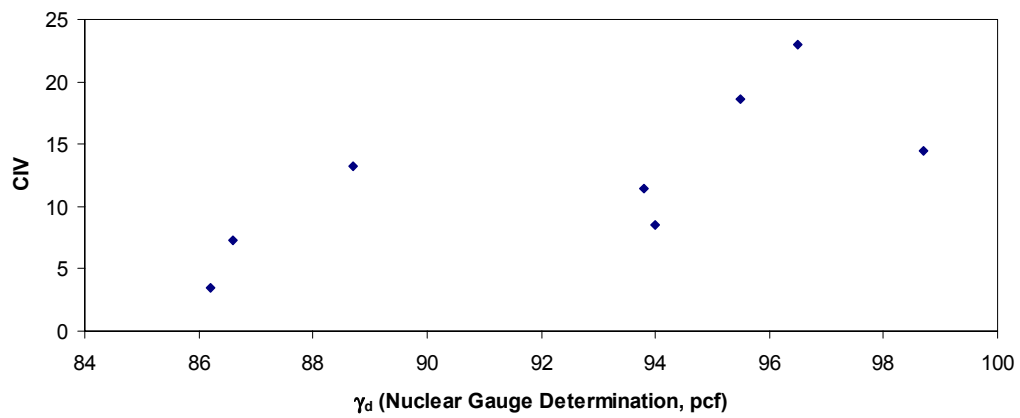


Figure 3.28. CIV versus dry unit weight for Soil III.

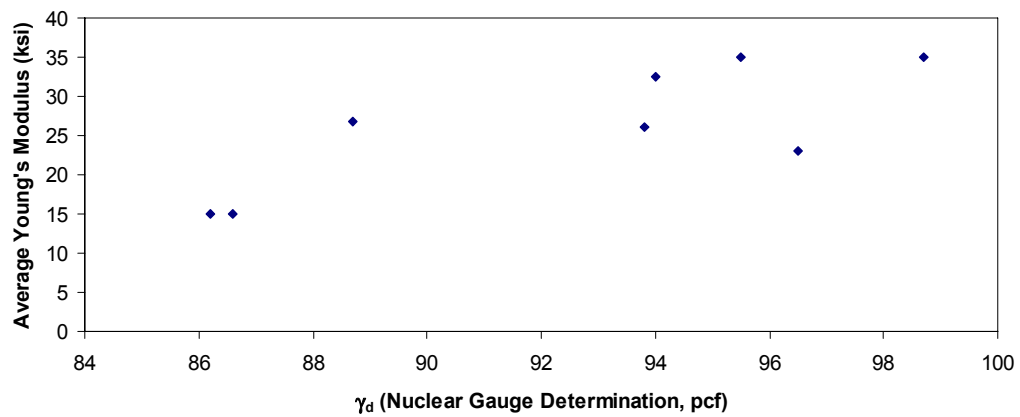


Figure 3.29. PSPA Young's Modulus versus dry unit weight for Soil III.

Figure 3.30 displays dynamic cone resistance ( $q_d$ ) profiles from the PANDA device for Soil III at locations 4 and 8 (Table 3.7). These two locations are shown for illustrative purposes. The failure and tolerance lines provided by the PANDA software for 92 percent and 95 percent Standard Proctor are also shown for this soil. These locations represent locations with different dry unit weights (96.5 pcf versus 86.2 pcf, respectively) and percent Standard compaction (92 percent versus 82 percent, respectively). For location 4, the  $q_d$  values fall well above the tolerance line at depths between 1 and 8 in., indicating adequate compaction over these depths. However, this assessment does not agree with the nuclear gauge measurement of relative compaction (92 percent, Table 3.7). At location 8, the  $q_d$  values over the top 6 in. fall significantly below the tolerance line, which indicates poor compaction. This assessment agrees with the nuclear gauge measurement of relative compaction (86 percent, Table 3.7). Table 3.7 lists the PANDA assessments of compaction for the other test locations. The PANDA profiles indicated that most of the locations had adequate compaction above 95 percent Standard Proctor, although the nuclear gauge indicated that most of these locations had less than 92 percent Standard relative compaction. Thus, the PANDA did not assess the compactness of Soil III accurately.

Figure 3.31 displays DCP profiles of penetration rate in in./blow versus depth for Soil III at locations 4 and 8 (Table 3.7). At location 4, the DCP penetration rate was about 0.5 in./blow over the top 10 in., while at location 8 the DCP penetrated more than 1.5 in. during its first blow and averaged about 1.0 in./blow between depths of 4 and 10 in. The MnDOT DCP compaction criterion for sandy soils is 0.28 in./blow. Averaging the DCP penetration rate over the top 6 in., location 4 has an average penetration rate of 0.5 in./blow, while location 8 has an average value of 1.2 in./blow. Based on the MnDOT criterion, locations 4 and 8 both fail the compaction criterion. Table 3.7 displays the average DCP penetration rate for the 8 test locations and shows that none of the locations pass the criterion.

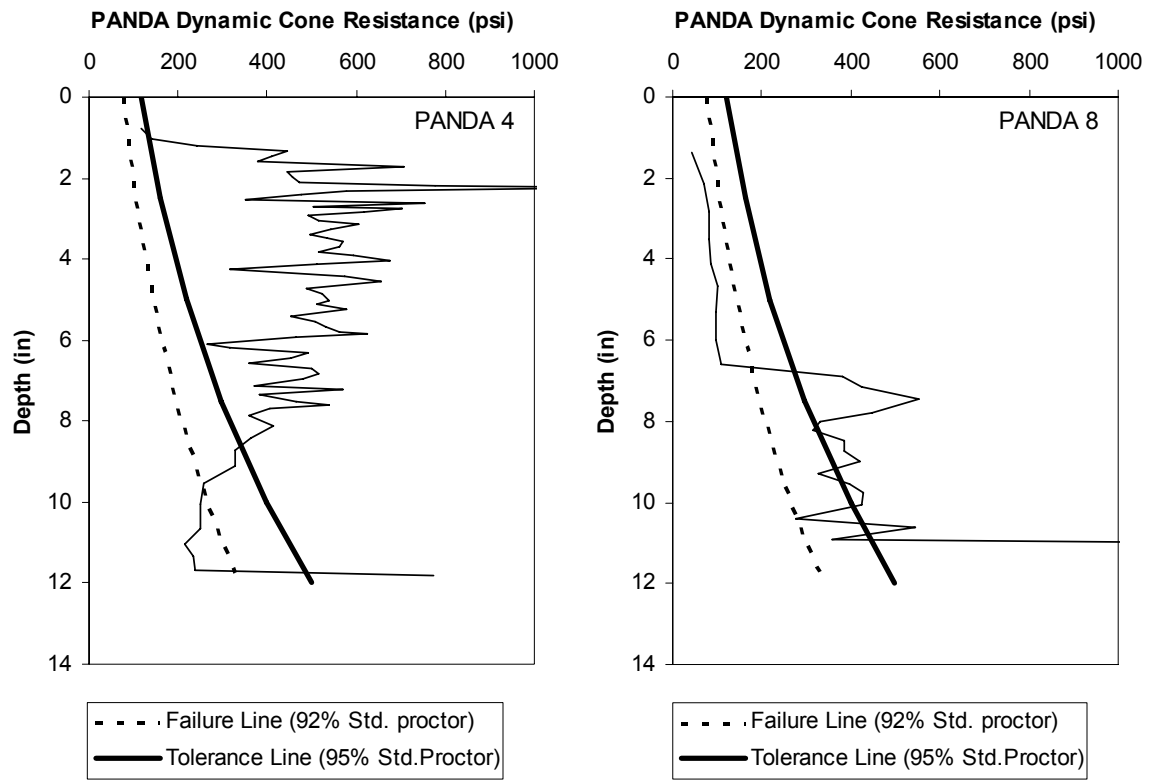


Figure 3.30. PANDA dynamic cone resistance profiles for Soil III at locations 4 and 8.

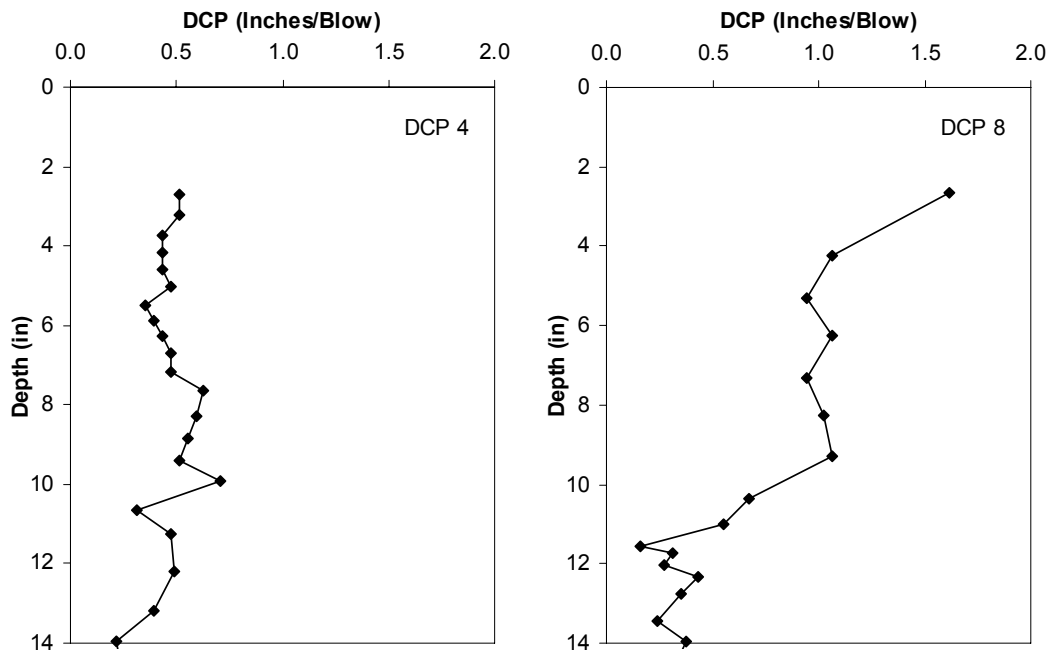


Figure 3.31. DCP profiles for Soil III at locations 4 and 8.

### 3.5.4 Soil IV

Because Soil IV (GP) contains a significant amount of large particles, only nuclear gauge testing was performed and was used as the basis for comparison for the test results. Table 3.8 summarizes the results from the compaction control devices at the eight test locations for Soil IV. The Standard relative compaction for the test locations ranged from 90 to 98 percent, with all of the water contents around 1.5 percent.

The measured CIV are plotted versus dry unit weight (as determined by the nuclear gauge) in Figure 3.32. The CIV are not plotted versus water content because the CIV should not be sensitive to water content in this sandy soil and because there was only no variability in the field values of water content. The CIV range from about 7 to 10, with no clear relationship with respect to the dry unit weight. No target CIV was defined for Soil IV because the large particle sizes precluded laboratory evaluation of CIV. The measured average Young's Moduli from the PSPA for Soil IV are plotted versus dry unit weight in Figure 3.33. The Young's Moduli range from about 25 ksi to more than 75 ksi, which are larger than the values measured for Soils I (CH), II (CL), and III (SW). From Figure 3.33 it appears that the Young's Moduli decrease with increasing dry unit weight, but that trend is influenced by the two large values at dry unit weights of about 93 pcf. If these data are excluded, there is no clear trend between Young's Modulus and dry unit weight for the data in Figure 3.33.

**Table 3.8. Results for Soil IV from compaction control devices**

$\gamma_{d, \text{max, std.}} = 104 \text{ pcf}$								
Test Location	$\gamma_d$ , Nuclear Gauge (pcf)	$w_{\text{nuclear gauge}}$ (%)	% Standard Compaction	Average CIV	Average PSPA Young's Modulus (ksi)	PANDA % Standard Compaction	Average DCP Penetration Rate (in/bl)	Pass/Fail MnDOT DCP Criterion (0.28 in/bl)
1	99.8	1.6	96	7.6	47	>98.5%	0.9	Fail
2	101.9	1.5	98	9.9	33	>98.5%	0.8	Fail
3	102.0	1.2	98	10.3	55	>98.5%	1.0	Fail
4	98.2	1.3	94	7.3	27	96-98.5%	1.2	Fail
5	98.6	1.6	95	8.9	48	>98.5%	1.3	Fail
6	93.9	1.6	90	9.0	71	96-98.5%	0.8	Fail
7	93.2	1.8	90	8.9	79	>98.5%	0.7	Fail
8	95.1	1.7	91	6.9	48	98.5%	0.6	Fail

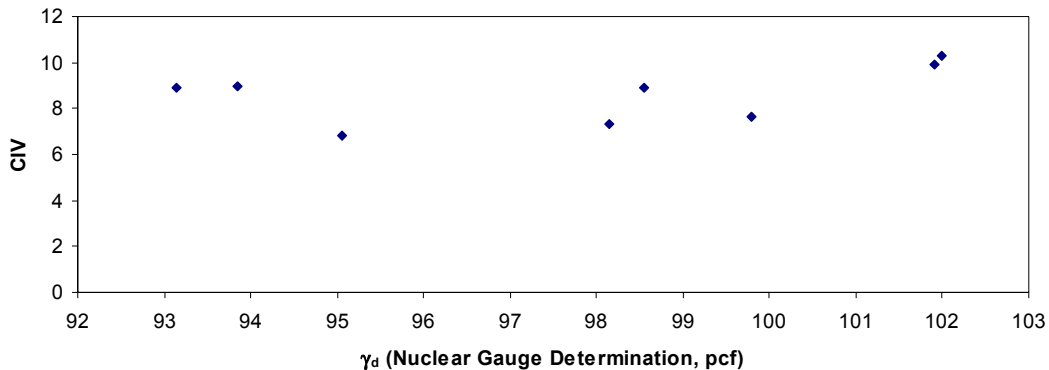


*Figure 3.32. CIV versus dry unit weight for Soil IV.*

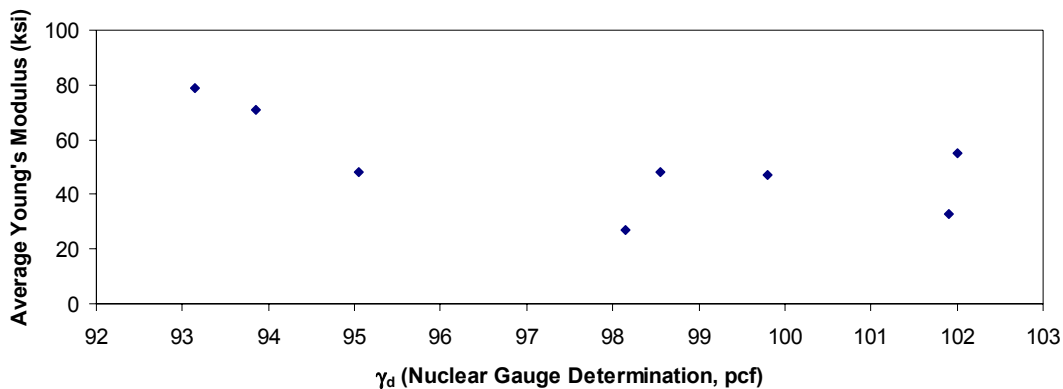


Figure 3.33. PSPA Young's Modulus versus dry unit weight for Soil III.

Figure 3.34 displays PANDA dynamic cone resistance ( $q_d$ ) profiles for Soil IV at locations 2 and 4 (Table 3.8). The two locations are displayed for illustrative purposes. The failure and tolerance lines provided by the PANDA software for 96 percent and 98.5 percent Standard Proctor are also shown for this soil. These locations represent locations where the cone resistances were high and low, respectively (Table 3.8). For location 2, the  $q_d$  values fall well above the tolerance line at depths between 1 and 10 in., indicating adequate compaction over these depths. The smaller values close to the ground surface are most likely the result of poor confinement. The compaction assessment from the PANDA (i.e., adequate compaction) agrees with the nuclear gauge measurement of relative compaction (98 percent, Table 3.8). At location 4, the  $q_d$  values over the top 4 in. are close to the failure line, but exceed the tolerance line over depths from 4 to 8 in. The percent Standard compaction from the nuclear gauge was 94 percent. The nuclear gauge measurement was made via the backscatter mode, due to the soil's large particle size, and thus represents the dry unit weight closer to the ground surface. The  $q_d$  profiles shown in Figure 3.34 certainly reveal that location 2 is better compacted than location 4, but it is not clear that an accurate value of relative compaction would be assigned for the locations. Table 3.8 lists the PANDA assessments of compaction for the other test locations. Based on the PANDA measurements, the relative compaction at each test location is greater than 96 percent. However, the measured dry unit weights indicate smaller values of relative compaction (Table 3.8).

Figure 3.35 displays DCP profiles (penetration rate in in./blow versus depth) for Soil IV at locations 2 and 4 (Table 3.8). At location 2, the DCP penetration rate was over 2.0 in./blow at the ground surface, most likely due to poor confinement, but decreased to less than 1.0 in./blow at depths greater than 4 in. At location 4 the DCP again penetrated more than 2.0 in. during its first blow and averaged less than 1.0 in./blow at larger depths. It is difficult to identify different compaction levels between the two locations shown in Figure 3.35. The MnDOT DCP compaction criterion for granular soils is 0.28 in./blow. Averaging the DCP penetration rate over the top 6 in., location 2 has an average penetration rate of 0.8 in./blow, while location 4 has an average value of 1.2 in./blow. Based on the MnDOT criterion, locations 2 and 4 both fail the compaction criterion. Table 3.8 displays the average DCP penetration rate for the eight test locations and shows that none of the locations pass the criterion.

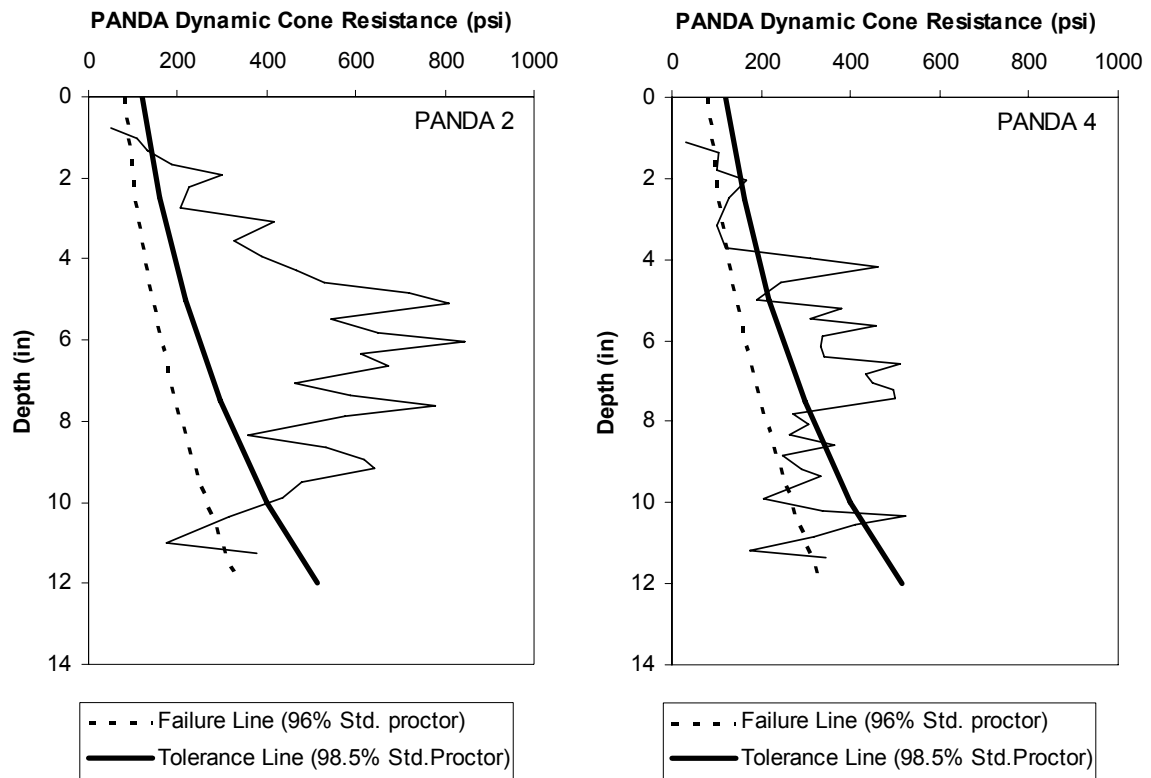


Figure 3.34. PANDA dynamic cone resistance profiles for Soil IV at locations 2 and 4.

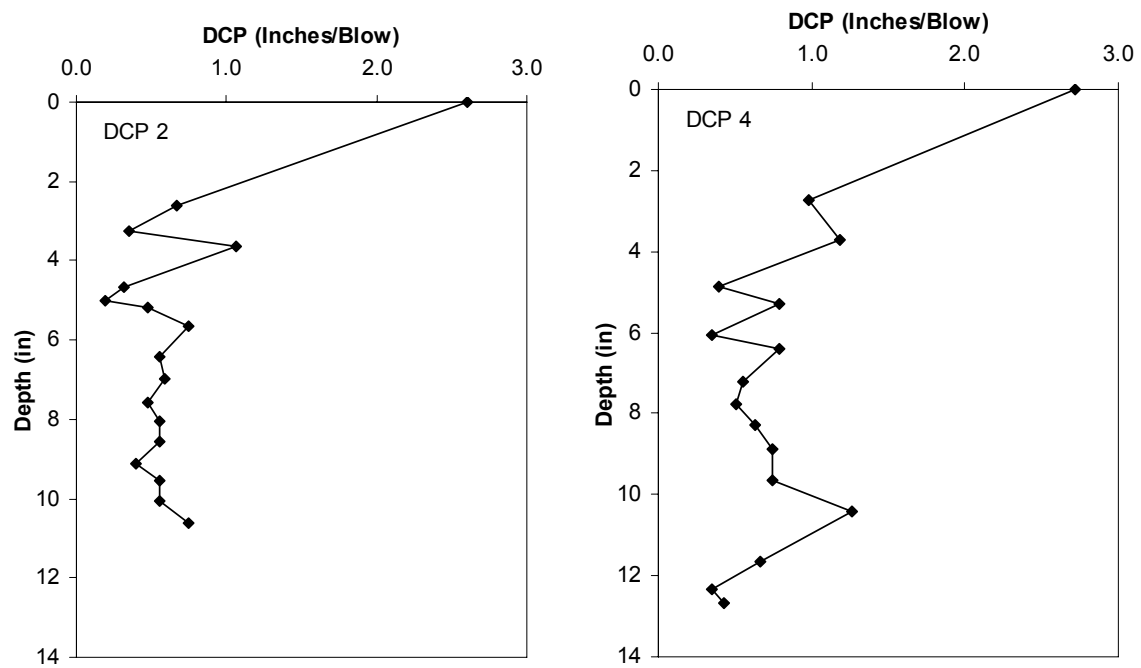


Figure 3.35. DCP profiles for Soil III at locations 4 and 8.

### 3.5.5 Soil V

Because Soil V (GP) contains a significant amount of large particles, only the nuclear gauge was used to measure unit weight and water content. Additionally, the presence of a significant amount of particles larger than 2 in. precluded the use of the PANDA or DCP for Soil V. Thus, only the CIV and PSPA were used in Soil V. Table 3.9 summarizes the results from the compaction control devices at the eight test locations for Soil V. The dry unit weights for the test locations ranged from 34 to 98 pcf, with all of the water contents around 1 percent. The dry unit weights of 34 and 70 pcf in Table 3.9 (locations 4 and 5) are obviously impossible and indicate a problem with nuclear gauge testing of materials with large particles. This result makes the other nuclear gauge measurements of dry unit weight somewhat suspect. In the results below, the data from locations 4 and 5 are not shown due to their unrealistic dry unit weights.

The measured CIV for Soil V are plotted versus dry unit weight in Figure 3.36. The CIV range from 7.7 to 19.5, but do not show a significant trend with increasing dry unit weight. No target CIV was defined for Soil V because the large particle sizes precluded laboratory evaluation of CIV. The measured average Young's Moduli from the PSPA for Soil V are plotted versus dry unit weight in Figure 3.37. The Young's Moduli range from about 34 ksi to more than 110 ksi, which are larger than the values measured for the other soils. There is significant scatter in the data in Figure 3.37, such that it is difficult to identify any trend with dry unit weight.

**Table 3.9. Results for Soil V from compaction control devices**

Test Location	$\gamma_d$ , Nuclear Gauge (pcf)	$W_{\text{nuclear gauge}}$ (%)	Average CIV	Average PSPA Young's Modulus (ksi)
1	94.6	1.3	11.8	68
2	98.0	1.3	19.5	75
3	92.2	0.9	14.5	110
4	69.6	0.9	18.7	87
5	33.6	1.1	18.9	58
6	86.9	1.1	15.9	90
7	88.6	1.2	14.1	41
8	90.5	1.2	7.7	34

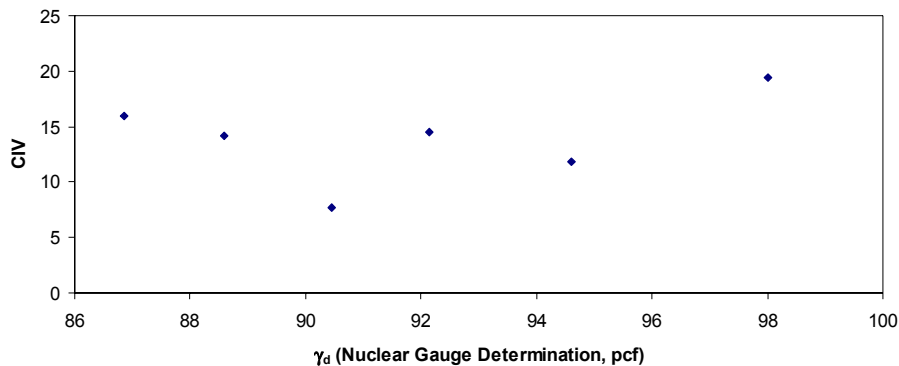


*Figure 3.36. CIV versus dry unit weight for Soil V.*

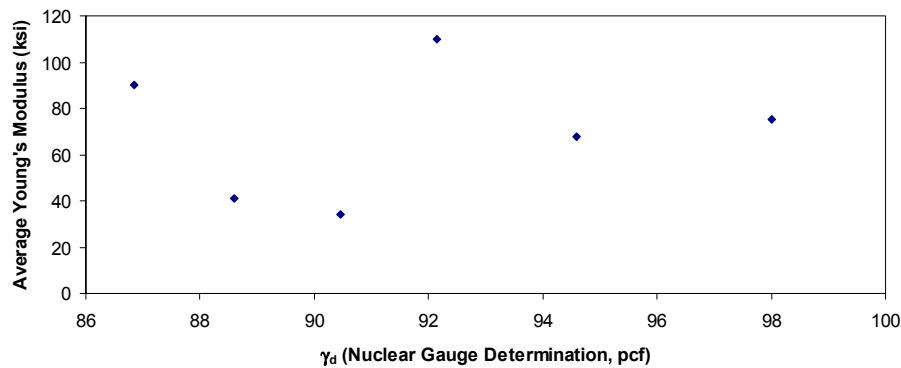


Figure 3.37. PSPA Young's Modulus versus dry unit weight for Soil V.

### 3.6 Summary

Field data using four new compaction control devices (Clegg Impact Hammer, PSPA, DCP, and PANDA) and two traditional methods (rubber balloon and nuclear gauge) were collected for five test soils. These soils included two clays (Soils I, II), one sand (Soil III), and two gravels (Soils IV, V).

For the clayey soils, it was observed that the CIV from the Clegg Impact Hammer and the average Young's Modulus from the PSPA were more influenced by the water content than the dry unit weight. The dynamic cone resistance profiles from the PANDA indicated that all of the clay locations were poorly compacted, which generally agreed with the dry unit weight measurements. The DCP generally distinguished between the locations with smaller and larger dry unit weights, but the MnDOT criterion for adequate compaction did not agree with the direct measurements of dry unit weight/relative compaction.

For the sandy soil (Soil III), the Clegg CIV and the PSPA Young's Moduli generally increased with increasing dry unit weight. However, there was significant scatter in these data. The PANDA and DCP generally distinguished between locations with smaller and larger dry unit weights, but the assessment of adequate compaction from these measurements did not always agree with the direct measurements of dry unit weight/relative compaction. For the fine gravel (Soil IV), there was no clear trend between dry unit weight and either the Clegg CIV or PSPA Young's Modulus. The PANDA and DCP did not provide accurate assessments of compaction when compared with direct measurements of dry unit weight. For the coarse gravel (Soil V), only the Clegg and PANDA devices could be used because of the large particle sizes. There was a large amount of scatter in the Clegg CIV and the PSPA Young's Moduli, such that it would be difficult to use them for compaction control in this type of material.

Table 3.10 summarizes the comparisons between the compaction assessments from the new devices and from direct measurement of dry unit weight/relative compaction. For these comparisons, relative compaction of 95 percent was considered acceptable and Table 3.10 notes whether there was agreement (A) or disagreement (D) between the different measurements. The disagreement locations were classified as  $D^P$  when the soil was poorly compacted but the device identified it as well compacted, and  $D^W$  when the soil was well compacted but the device identified it as poorly compacted. For the clayey soils (Soils I and II), the compaction assessments by the Clegg and PANDA mostly agreed with the direct measurements, while the

DCP mostly disagreed. None of the new devices measured water content, so water content measurements could not be compared. For Soil III (sand), the PANDA measurements consistently disagreed with the direct measurements of relative compaction, while the Clegg and DCP provided accurate assessments of compaction. Only the PANDA and DCP could be used in the fine gravel (Soil IV) and, their assessment of compaction only agreed with the direct measurements of relative compaction in about 50 percent of the cases.

The data in Table 3.10 indicate the Clegg Impact Hammer provided the most accurate assessments of compaction over all of the soils tested in Field Study 1. However, most of the test locations were poorly compacted at relative compaction values well below 95 percent. It is not clear if the same assessment of accuracy would have been obtained if the test pads had been better compacted.

**Table 3.10. Summary of results from Field Study 1**

	Soil I (Clay)			Soil II (Clay)			Soil III (Sand)			Soil IV (Gravel)	
	Clegg	PANDA	DCP	Clegg	PANDA	DCP	Clegg	PANDA	DCP	PANDA	DCP
<b>1</b>	A	A	D <sup>P</sup>	A	A	A	A	D <sup>P</sup>	A	A	D <sup>W</sup>
<b>2</b>	A	A	A	A	A	D <sup>P</sup>	A	D <sup>P</sup>	A	A	D <sup>W</sup>
<b>3</b>	A	A	A	A	A	D <sup>P</sup>	A	D <sup>P</sup>	A	A	D <sup>W</sup>
<b>4</b>	A	A	A	A	A	A	D <sup>P</sup>	D <sup>P</sup>	A	D <sup>P</sup>	A
<b>5</b>	A	A	D <sup>P</sup>	D <sup>W</sup>	D <sup>W</sup>	D <sup>W</sup>	A	A	A	A	D <sup>W</sup>
<b>6</b>	A	A	A	D <sup>W</sup>	D <sup>W</sup>	A	A	D <sup>P</sup>	A	D <sup>P</sup>	A
<b>7</b>	A	A	A	A	A	D <sup>P</sup>	A	D <sup>P</sup>	A	D <sup>P</sup>	A
<b>8</b>	D <sup>P</sup>	A	D <sup>P</sup>	A	A	D <sup>P</sup>	A	D <sup>P</sup>	A	D <sup>P</sup>	A

Notes: A: agreement between nuclear gauge assessment of dry unit weight and device assessment of compaction

D<sup>P</sup>: disagreement, soil poorly compacted but device identified it as well compacted

D<sup>W</sup>: disagreement, soil well compacted but device identified it as poorly compacted

## **4. Field Testing Program 2**

### **4.1 Introduction**

Field study 2 was conducted during the fall of 2005 and was intended to focus on the electrical devices (MDI, EDG) that became available during this project. However, problems were encountered in field testing with the EDG that prevented an evaluation of the device. To calibrate the EDG and develop a Soil Model (Chapter 2), independent field measurements of dry unit weight and water content are required at several field locations where EDG measurements are also obtained. Time constraints due to the field construction schedule precluded enough data from being collected to develop Soil Models for the field soils. Additionally, no signal was acquired by the EDG in the high plasticity clays tested during this field study due to significant attenuation. Because of these calibration issues, the EDG could not be evaluated during field testing. However, the EDG was used during the laboratory testing discussed in Chapter 5.

Testing was conducted at three construction sites in the central Texas region and focused on evaluating the devices for clayey soils used in Texas for highway embankments or as road subgrade. Field testing was not performed at sites of retaining wall construction because only gravelly materials were being used at these types of projects in the central Texas region during the time of field testing and the non-nuclear devices considered in this study are not suitable for gravelly materials. This chapter describes the field sites tested, and provides comparisons between measurements of dry unit weight and water content from traditional methods (rubber balloon, nuclear gauge, and oven drying) and the electrical devices.

### **4.2 Material Description**

Testing was conducted on three different soils at two field locations (Figure 4.1). The first soil was high plasticity Taylor clay (CH) being used to construct a landfill liner at a landfill located south of Austin, Texas. The landfill liner was being compacted in 6-in. lifts with a sheepsfoot roller to 95 to 100 percent Standard Proctor relative compaction at water contents around 23 percent. The other soils were tested at a site that is part of the construction of the Texas 130 toll road in an area east of Austin, Texas (Figure 4.1). One soil was low plasticity clay (CL) from an alluvial deposit from the Colorado River near the Texas 130 toll road. The section of soil tested was not compacted for use in the roadway, but served as an access road for heavy equipment to reach the actual construction site. The third soil consisted of high plasticity clay with sand (CH). The site for field testing of this soil was the compacted subgrade for the Texas 130 toll road.

The gradation curves for the three test soils are provided in Figure 4.2. The Taylor Clay contains more than 95 percent fines and has a plasticity index of 37, classifying it as high plasticity clay (CH). The low plasticity clay (CL) contains about 85 percent fines and has a plasticity index of 21. The sandy clay contains only 53 percent fines, but has a plasticity index of 34; thus classifying it as high plasticity clay (CH). Despite the similar classification (CH) of the Taylor Clay and sandy clay, the electrical properties of these two soils will differ because of the large percentage of sand and gravel-sized particles in the sandy clay.

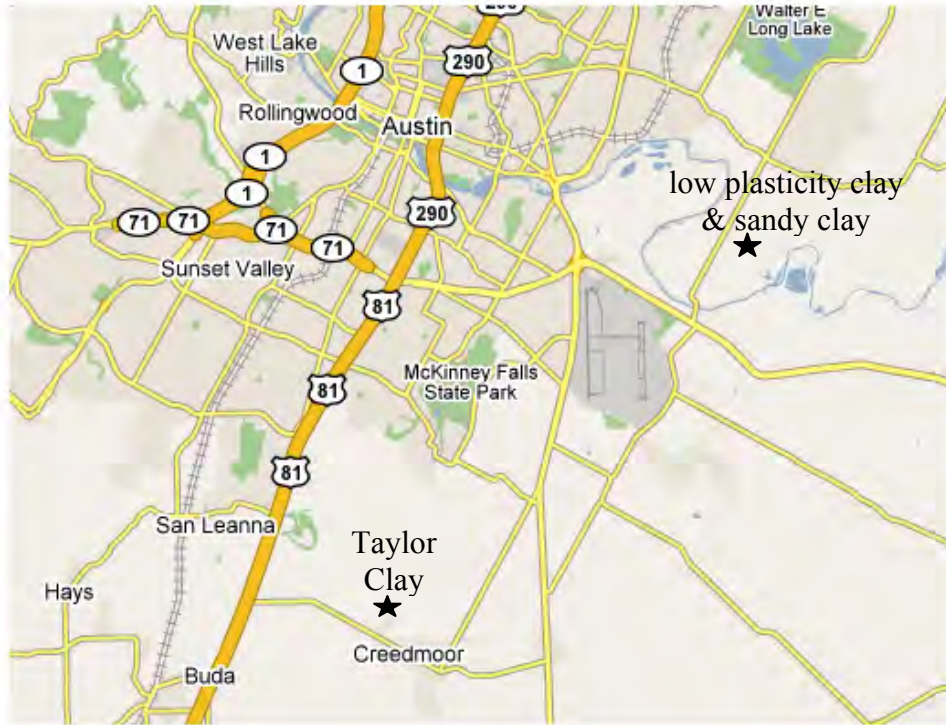


Figure 4.1. Locations of field testing (<http://maps.google.com>)

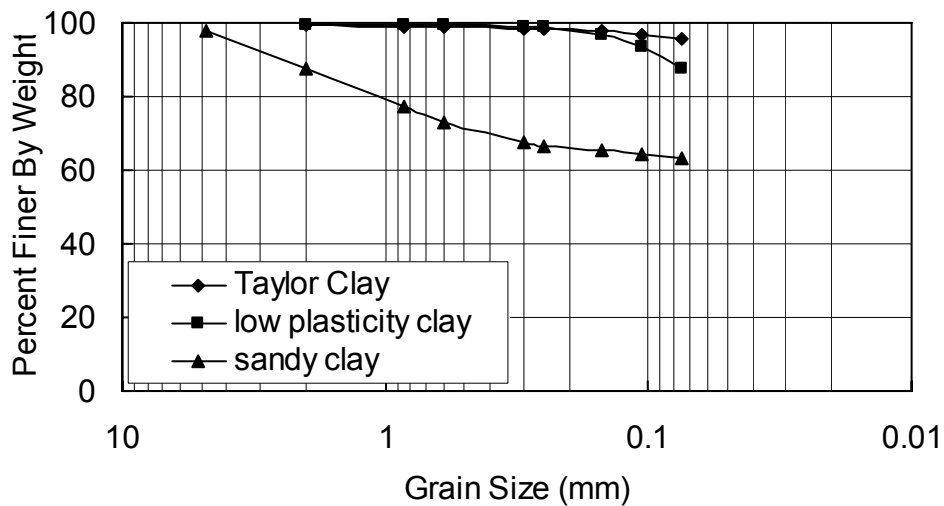


Figure 4.2. Grain size distributions of soils from Field Study 2

Standard Proctor compaction tests (ASTM D 698) were performed on the test soils to obtain compaction curves, maximum dry unit weights, and optimum water contents (Figure 4.3). The Taylor clay (CH) displays the smallest maximum dry unit weight and largest optimum water content, while the sandy clay (CH) displays the largest maximum dry unit weight and the smallest optimum water content due to its large percentage of sand and gravel-sized particles. The compaction curve for the low plasticity clay lies between the other two soils. The maximum dry unit weights and water contents for the Taylor Clay (CH), low plasticity clay (CL), and

sandy clay (CH) are approximately 105 pcf and 19.5 percent, 110 pcf and 17 percent, and 114.3 pcf and 15.2 percent, respectively. Each of these sets of values represents a degree of saturation of about 87 percent.

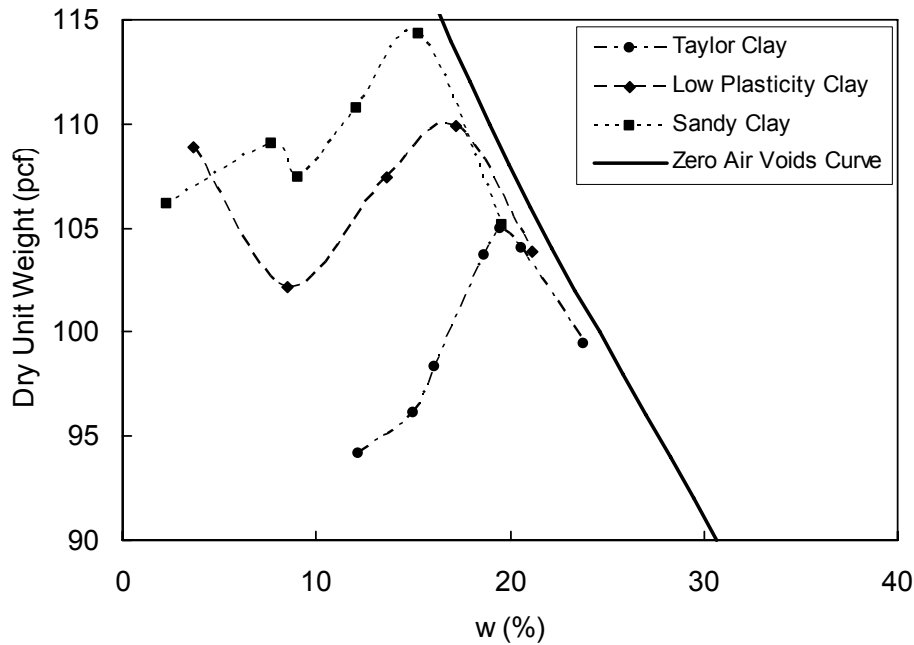


Figure 4.3. Standard Proctor compaction curves for the soils from Field Study 2

## 4.3 Equipment Calibration

### 4.3.1 Moisture-Density Indicator

Calibrations for the MDI are performed to obtain soil-specific constants used to predict the dry density ( $\rho_d$ ) and water content ( $w$ ) from the measured values of dielectric constant ( $K_a$ ) and bulk electrical conductivity ( $EC_b$ ). Soil constants  $a$ ,  $b$ ,  $c$ ,  $d$ ,  $f$ , and  $g$  (Chapter 2) are required for the calibration for each soil type. Recall that constants  $a$  and  $b$  relate  $\rho_d$  and  $w$  to  $K_a$ , while constants  $c$  and  $d$  relate  $\rho_d$  and  $w$  to  $EC_b$ . Constants  $f$  and  $g$  are used to correct for differences in pore fluid conductivity between the soil pore fluid used in laboratory calibration and the pore fluid present in the field.

The calibration of the MDI device is performed in conjunction with a set of compaction tests (ASTM D 698 or ASTM D 1557) using a 4-in. diameter stainless steel compaction mold and a non-conductive base (Figure 4.4). After compaction of the soil in the compaction mold, the center rod guide is placed on top of the mold and the 4-in. center rod is driven into the mold (Figure 4.4a). The center rod guide is removed, the mold collar is placed on top of the mold, and the multiple rod probe (MRP) head is placed on the mold collar and center rod (Figure 4.4b). The MRP must be in good contact with the mold collar and center rod probe.

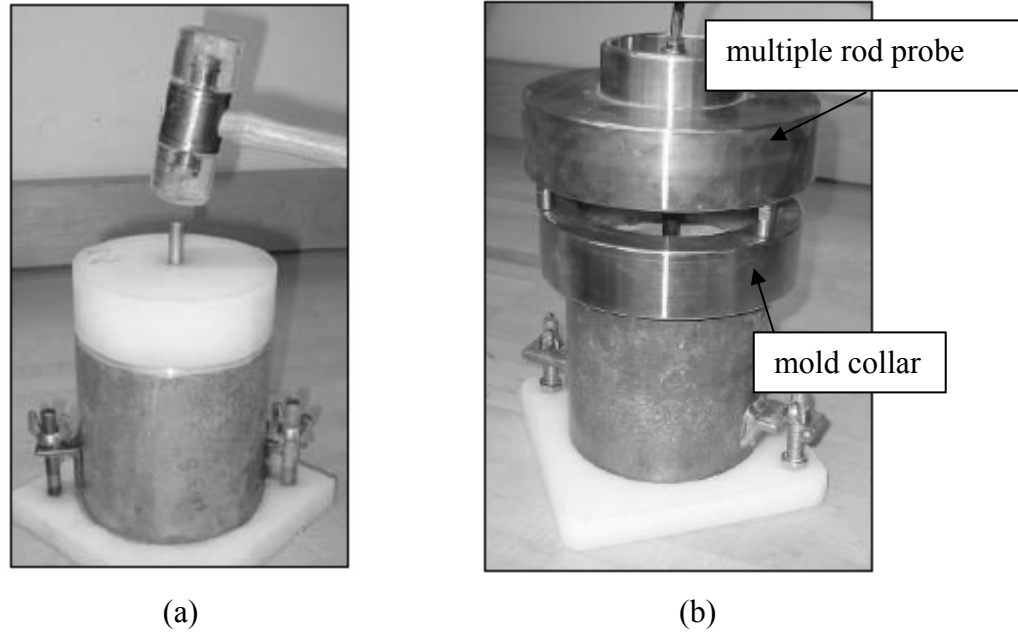


Figure 4.4. (a) Center rod being driven into the MDI calibration specimen, (b) MDI calibration specimen with the mold collar and multiple rod probe in place (Durham 2005).

Measurements of the dielectric constant ( $K_a$ ) and bulk electrical conductivity ( $EC_b$ ) are obtained using the MDI software that is operated on a PDA and connected to the MRP. A representative waveform produced during calibration for a poorly graded sand is shown in Figure 4.5. The waveform shows distinct first and second reflection points, which are indicated by arrows, and the scaled distance between these two points is used to calculate  $K_a$  (Equation 2.3). The initial ( $V_s$ ) and final ( $V_f$ ) voltages are also indicated in Figure 4.5 and these values are used to calculate  $EC_b$  (Equation 2.4). The water content of each compacted specimen is measured by oven drying after MDI testing, and the dry unit weight is determined from the total weight of soil in the mold and the measured water content. The procedure is repeated for five specimens of varying water content.

After measurements of  $K_a$ ,  $EC_b$ , dry unit weight, and water content are collected for five soil specimens at different water contents, the information is entered into the MDI calibration software. The following three graphs are generated by the MDI software:  $\sqrt{K_a} \cdot \rho_w / \rho_d$  versus  $w$ ,  $\sqrt{EC_b} \cdot \rho_w / \rho_d$  versus  $w$ , and  $\sqrt{EC_b}$  versus  $\sqrt{K_a}$ . Linear relationships are fit to the data of each plot, with the first graph providing soil constants  $a$  and  $b$ , the second graph providing  $c$  and  $d$ , and the third graph providing  $f$  and  $g$ . For most soil types, typical values of  $a$  are 0.7 to 1.85, and  $b$  is approximately 9 (Yu and Drnevich 2004). Typical ranges for soil constants  $c$ ,  $d$ ,  $f$ , and  $g$  have not been reported.

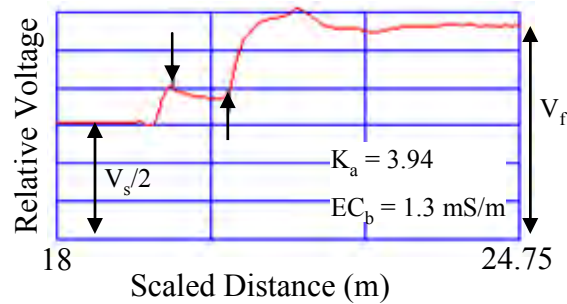
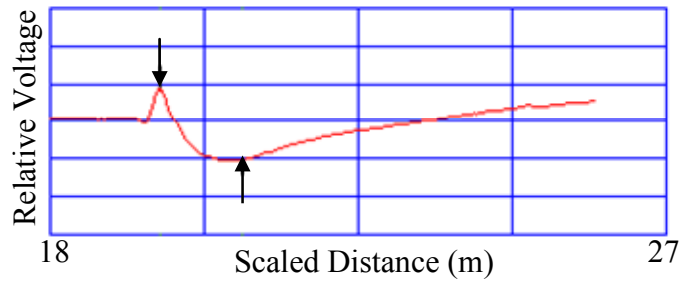


Figure 4.5. Representative MDI calibration waveform for poorly-graded sand.

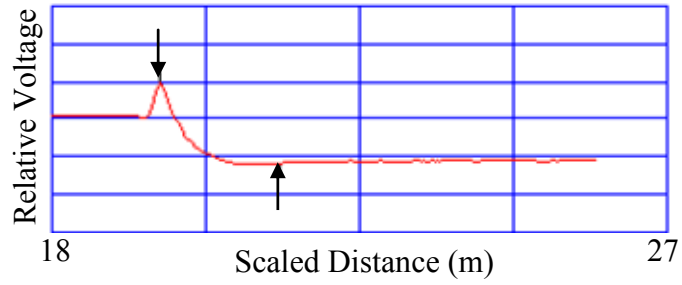
### Taylor Clay Calibration

MDI calibration data for the Taylor Clay were obtained using Standard Proctor compactive effort. The high PI Taylor Clay displayed distinctively different MDI waveforms than observed in sand. Three typical MDI waveforms for the Taylor Clay are shown in Figure 4.6. The arrows in Figure 4.6 indicate the first and second reflection points of the waveform determined by the MDI software. For the eight calibration tests on Taylor Clay, two waveforms displayed a relatively flat second reflection point and a voltage that slowly increased with distance to  $V_f$  (Figure 4.6a), two waveforms did not have a clearly visible second reflection point (Figure 4.6b), and four waveforms had a clear second reflection point and reached  $V_f$  relatively quickly (Figure 4.6c).

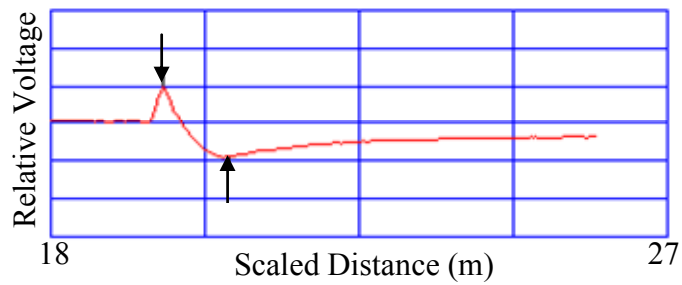
When the physical data ( $K_a$ ,  $EC_b$ ,  $\rho_d$ , and  $w$ ) were plotted to determine the MDI calibration constants (Figure 4.7), significant scatter was observed and at least three of the eight data points were assumed to be outliers. These apparent outliers are labeled 1 through 3 in Figure 4.7. Two of the outliers (points 1 and 3) correspond to waveforms similar to that in Figure 4.6a, while the third (point 2) corresponds to a waveform similar to that in Figure 4.6b. This result may indicate that MDI waveforms that do not display a clear second reflection point (Figure 4.6b) or do not reach  $V_f$  quickly (Figure 4.6a) are not reliable. Figure 4.7 includes the three calibration graphs for the Taylor Clay, as well as the computed calibration coefficients. The three outliers were not used to calculate the soil constants, yet there still was significant scatter in the data.



(a)



(b)



(c)

Figure 4.6. Representative MDI calibration waveforms for Taylor clay.

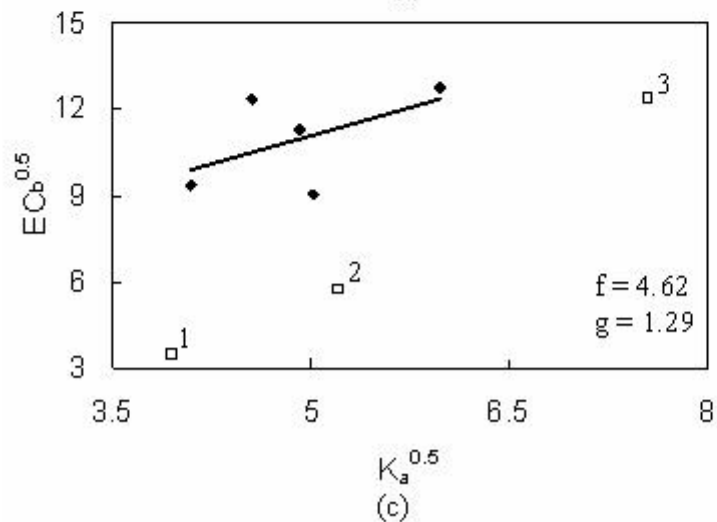
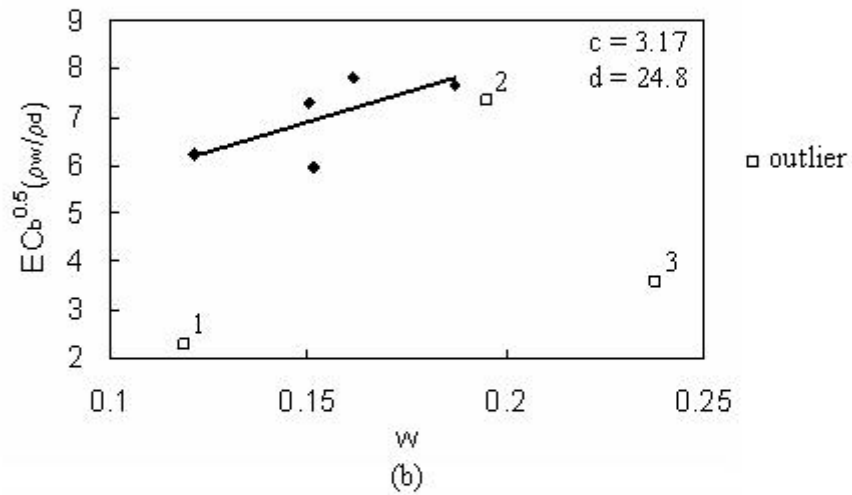
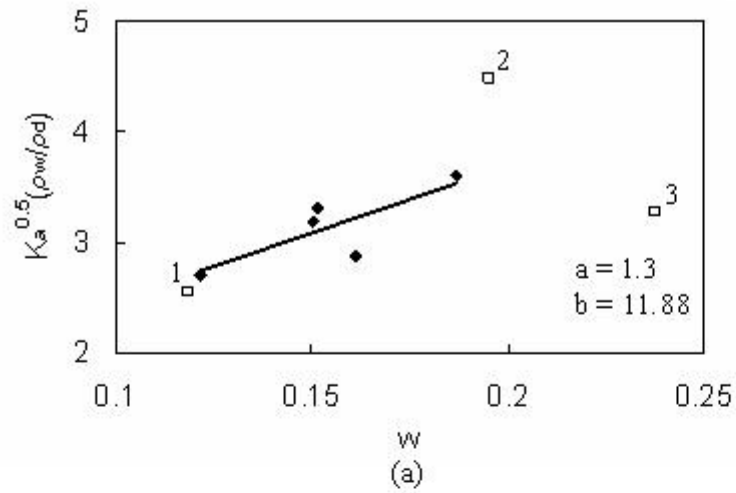


Figure 4.7. MDI calibration data for Taylor clay.

### Low Plasticity Clay Calibration

Figure 4.8 is a representative MDI calibration waveform for the low plasticity clay compacted at Standard Proctor compactive effort. All waveforms for this soil displayed a distinct second reflection point and rapidly reached  $V_f$ .

The calibration data for the low plasticity clay are plotted in Figure 4.9. The data for the dielectric constant ( $K_a$ ) show little scatter, while the data for the bulk electrical conductivity ( $EC_b$ ) show significantly more scatter. Because the data for  $K_a$  versus  $w$  exhibit a clear linear relationship, all data points were used to calculate the calibration coefficients shown in Figure 4.9.

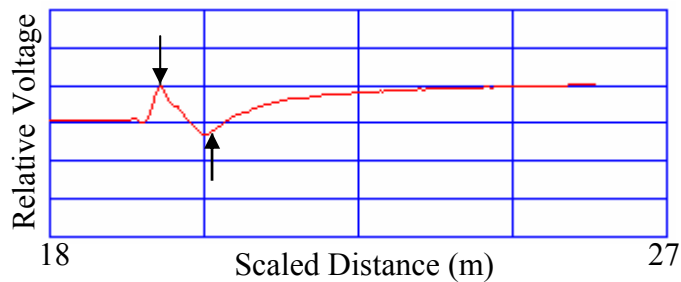


Figure 4.8. Representative MDI calibration waveforms for the low plasticity clay.

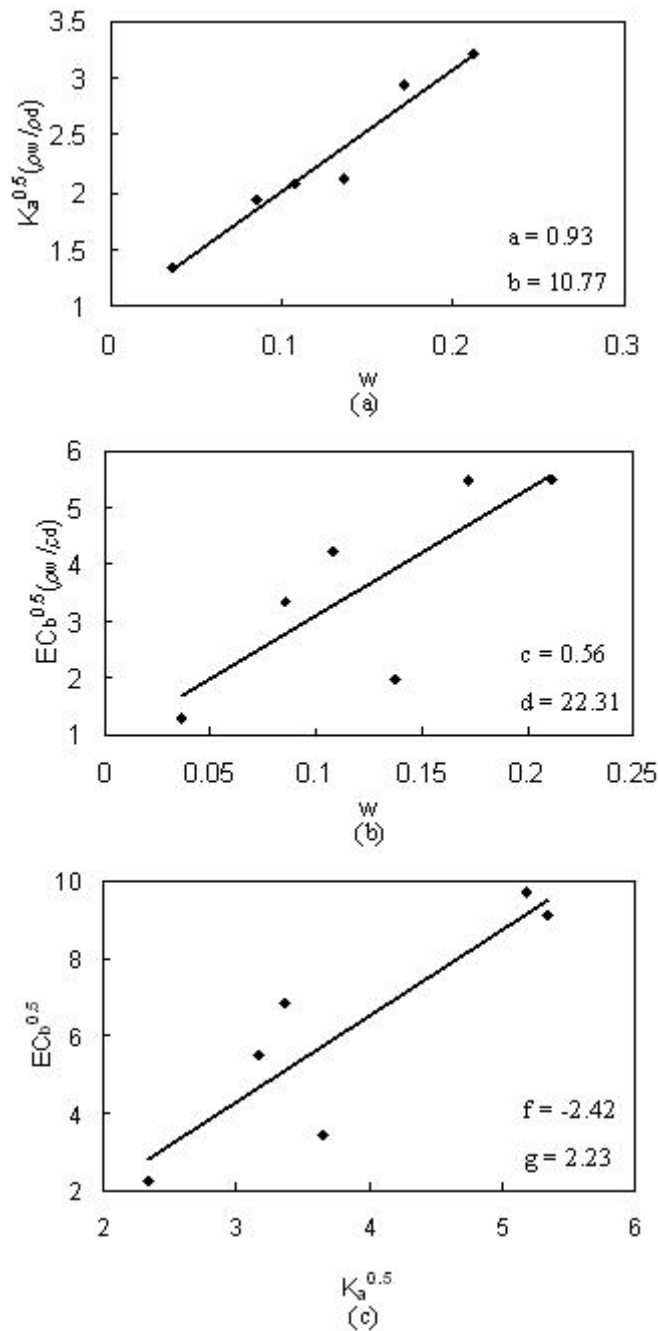


Figure 4.9. MDI calibration data for the low plasticity clay.

### Sandy Clay Calibration

The sandy clay was compacted using Standard Proctor compactive effort for the MDI calibration. The “best” and “worst” waveforms obtained during calibration are shown in Figure 4.10, with the arrows indicating the first and second reflection points identified by the MDI software. The “best” waveform (Figure 4.10a) displays a distinct second reflection and rapidly

reaches  $V_f$ . The “worst” waveform (Figure 4.10b) displays a distinct second reflection point but takes longer to reach  $V_f$ . The water contents of the specimens with the “best” and “worst” waveforms were 9.1 percent and 12.1 percent, respectively

The calibration data for the sandy clay are plotted in Figure 4.11. Again, the data for  $K_a$  display little scatter, while the data for  $EC_b$  exhibit much more scatter. Because none of the data points could be definitively identified as outliers based on anomalous  $K_a$  and  $EC_b$  values, all data points were used to calculate the calibration coefficients shown in Figure 4.11.

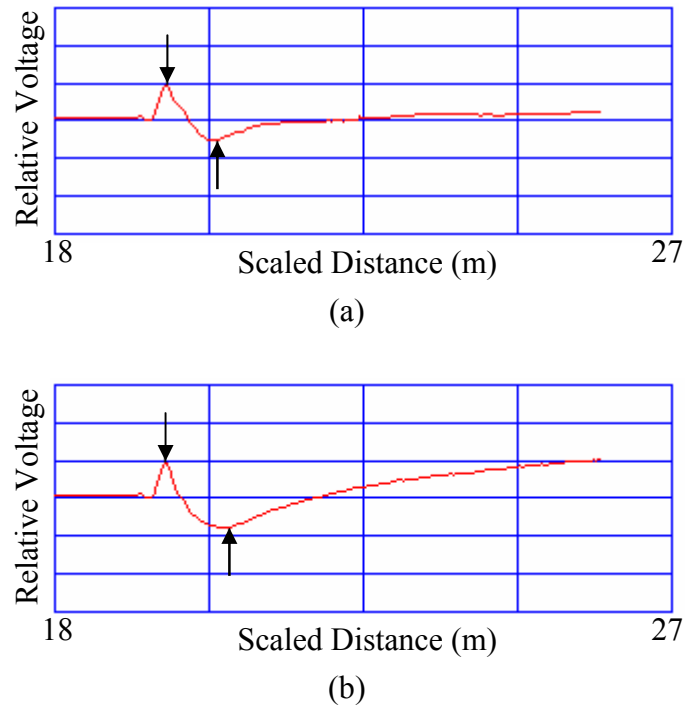


Figure 4.10. Representative MDI calibration waveforms for the sandy clay.

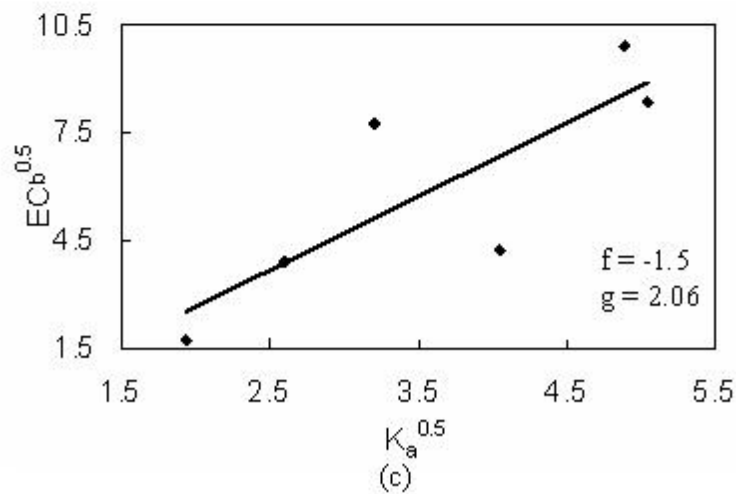
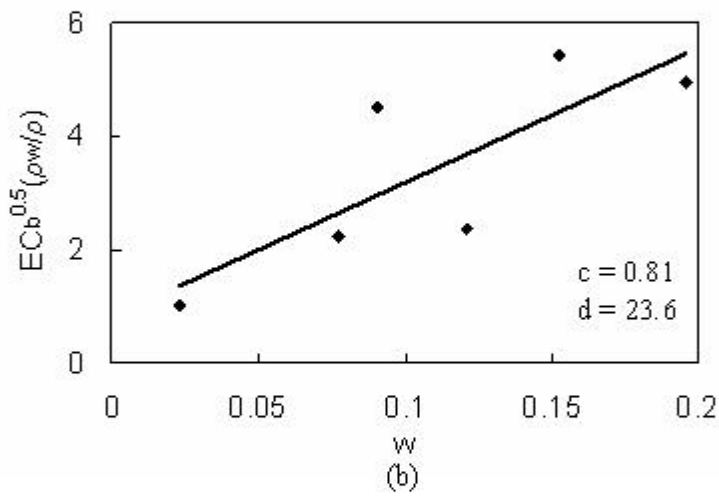
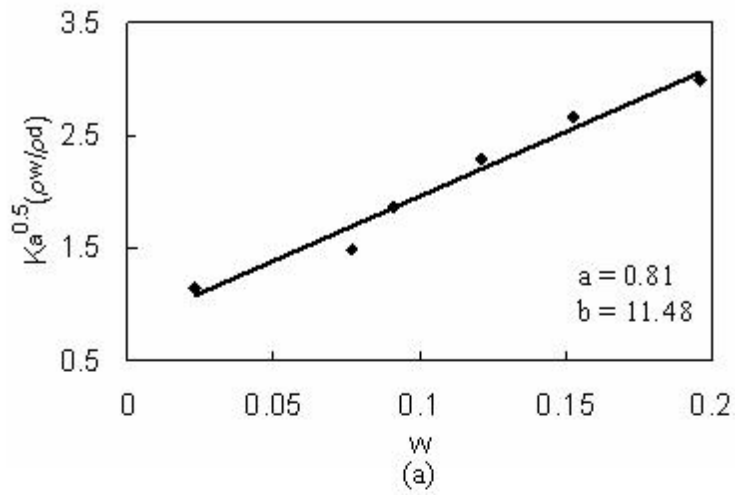


Figure 4.11. MDI calibration data for the sandy clay.

The calibration coefficients for each soil type are summarized in Table 4.1. Yu and Drnevich (2004) report typical values of  $a$  ranging from 0.7 to 1.85 and  $b$  equal to 9. The values of  $a$  and  $b$  determined for each soil are consistent with the typical values reported by Yu and Drnevich (2004). However, the scatter in the calibration data displayed in Figures 4.7, 4.9, and 4.11 will result in more uncertainty in the predicted values of dry unit weight and water content during field testing.

**Table 4.1. MDI calibration coefficients for soils from Field Study 2**

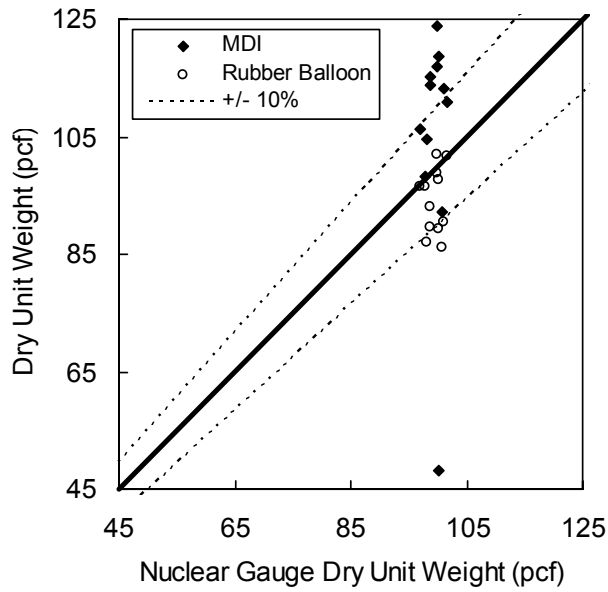
<b>Calibration Coefficient</b>	<b>Taylor Clay</b>	<b>Low Plasticity Clay</b>	<b>Sandy Clay</b>
$a$	1.3	0.93	0.81
$b$	11.88	10.77	11.48
$c$	3.17	0.56	0.81
$d$	24.8	22.31	23.6
$f$	4.62	-2.42	-1.5
$g$	1.29	2.23	2.06

## 4.4 Field Test Results

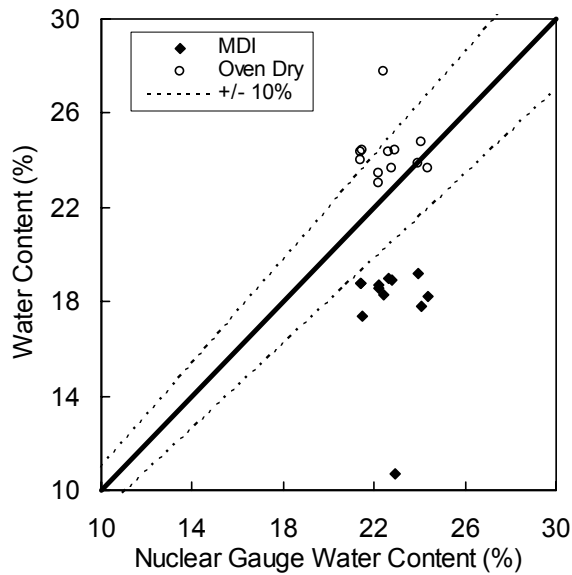
### 4.4.1 Taylor Clay

MDI measurements and traditional unit weight/water content measurements were performed at twelve locations at the landfill liner site in Taylor Clay. At each location an MDI, rubber balloon, and nuclear gauge measurement were obtained. Soil samples were obtained at each test location and transported back to the laboratory for water content determination by oven drying. Nuclear gauge measurements were performed by Kleinfelder, Inc. using a Troxler 3401 nuclear gauge operating in the direct transmission mode. The measurements obtained by the nuclear gauge were used as the standard for comparison with the MDI measurements. The nuclear gauge was chosen as the standard for comparison because it is currently the most widely used device in the field and was used in Field Study 1.

The MDI and rubber balloon dry unit weight and water content measurements for all twelve test locations are compared to the corresponding values measured by the nuclear gauge in Figure 4.12. The dry unit weights from the rubber balloon are slightly smaller than the nuclear gauge, which is a different result than obtained in Chapter 3. However, different personnel operated the rubber balloon devices in Field Tests 1 and 2. Most of the dry unit weight values from the MDI are larger than the corresponding values obtained by the nuclear gauge, while the values of water content from the MDI are generally smaller than those from the nuclear gauge. In general, the oven dry measurements of water content agree with those from the nuclear gauge. However, if one assumes that the water content of the Taylor clay was approximately 22 percent, based on the oven dry values in Figure 4.12b, the dry unit weights reported by the MDI are not realistic because they lie above the zero air voids curve (Figure 4.3). If one assumes that the water content of the Taylor clay was about 18 percent, based on the MDI values in Figure 4.12b, most of the dry unit weights reported by the MDI still lie above the zero air voids line.



(a)



(b)

Figure 4.12. Comparison of (a) dry unit weight and (b) water content measured by the MDI, rubber balloon, and nuclear gauge for Taylor Clay

One MDI measurement of dry unit weight is 48 pcf with a water content of 10.7 percent. The MDI waveform for this measurement differs from the shape of a typical MDI waveform because there is no measured drop in voltage after the first reflection point (Figure 4.13). Thus, this measurement is invalid, although the MDI device did not report an error message after obtaining this measurement.

All of the other MDI waveforms for measurements performed in the Taylor Clay showed a distinct first reflection point without a distinct second reflection point (e.g., typical waveform in Figure 4.6b), which may make the MDI data less accurate. Based on this observation and the unattainable dry unit weights reported, it appears that the MDI cannot provide reliable data in high plasticity Taylor clay.

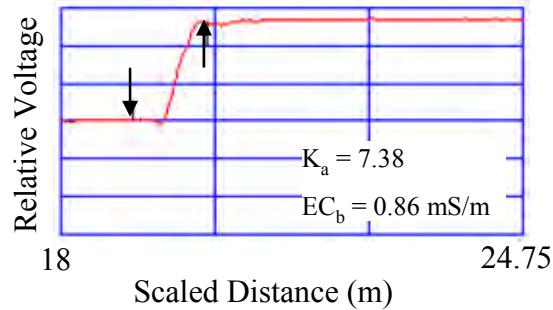


Figure 4.13. MDI waveform for measurement in Taylor Clay that resulted in a value of 48 pcf for dry unit weight and a water content of 10.7%.

#### 4.4.2 Low Plasticity Clay

For the low plasticity clay (CL), dry unit weight and water content measurements were performed by the MDI and nuclear gauge measurements at eight locations, while rubber balloon tests were performed at only six locations. The MDI and rubber balloon data for all test locations are compared to the corresponding nuclear gauge measurements in Figure 4.14.

MDI measurements of dry unit weight ranged from 102 to 107 pcf, with an average of about 105 pcf. These values were smaller than the nuclear gauge measurements by 5 to 15 pcf (Figure 4.14a), although five out of the eight measurements were within 10 percent of the nuclear gauge measurement. As opposed to the results in the Taylor clay, in the low plasticity clay the MDI underpredicts dry unit weight relative to the nuclear gauge. The rubber balloon dry unit weight measurements were significantly more variable (103 pcf to 137 pcf) and are mostly greater than the corresponding nuclear gauge measurement (Figure 4.14a). However, problems were encountered when performing the rubber balloon test in the low plasticity clay. These problems include difficulty excavating the test hole and the presence of a non-horizontal ground surface. These difficulties may have affected the accuracy of the rubber balloon unit weight measurements.

The water content comparisons are displayed in Figure 4.14(b). The MDI values are generally larger than the nuclear gauge values, with five values of MDI water content over 10 percent larger than the corresponding values from the nuclear gauge. The water content values measured by oven drying are closer to the values from the nuclear gauge. In the Taylor Clay, the MDI water contents were smaller than the water content values from the nuclear gauge. In the low plasticity clay, the opposite is true.

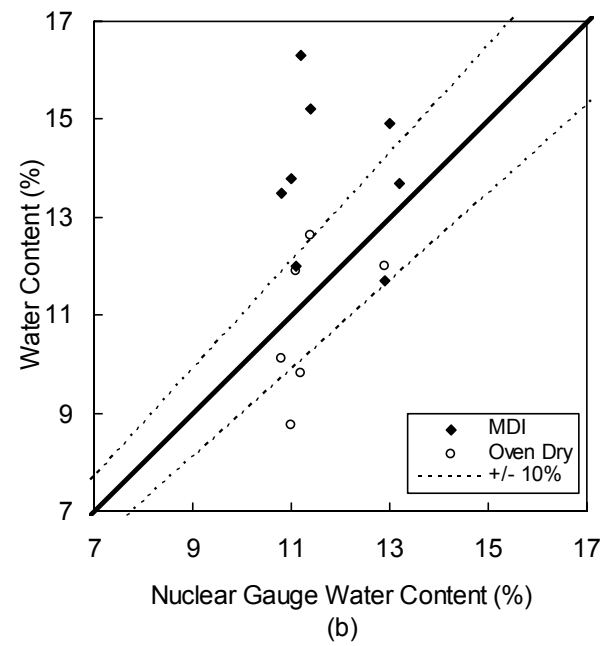
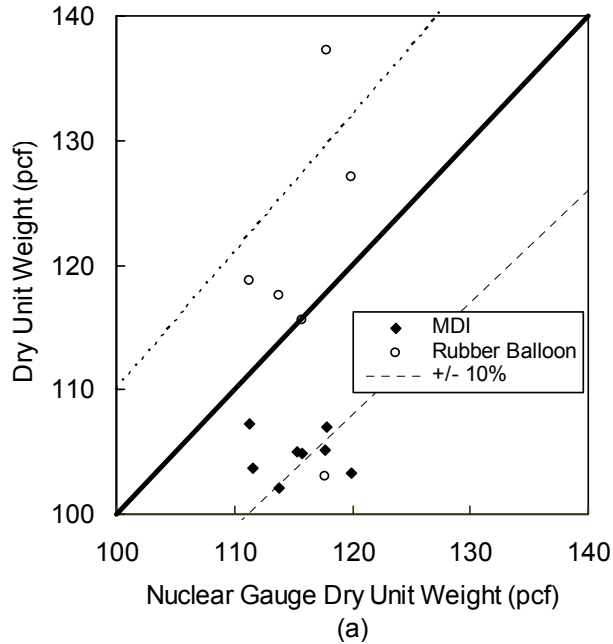


Figure 4.14. Comparison of (a) dry unit weight and (b) water content measured by the MDI, rubber balloon, and nuclear gauge for low plasticity clay.

#### 4.4.3 Sandy Clay

Three measurements were performed with the MDI, rubber balloon, and nuclear gauge devices at the sandy clay site. Only three measurements were performed at this site due to time constraints imposed by the construction schedule. The MDI and rubber balloon data for all test locations are compared to the corresponding nuclear gauge measurements in Figure 4.15.

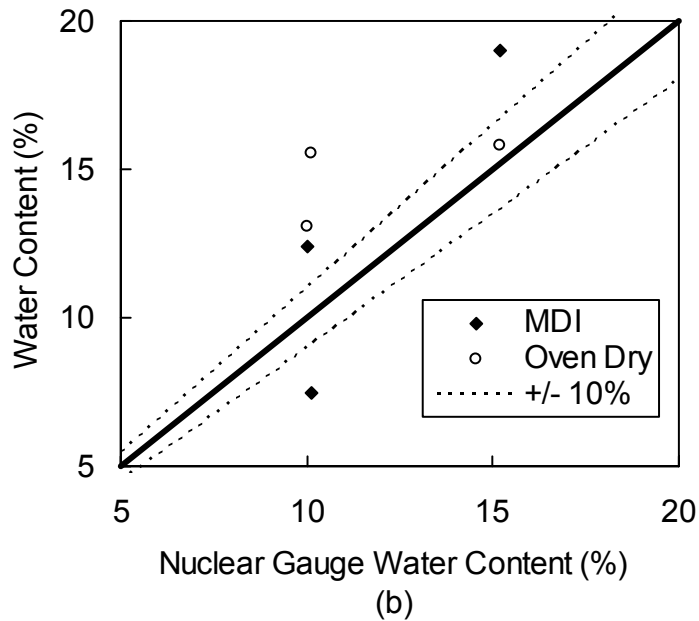
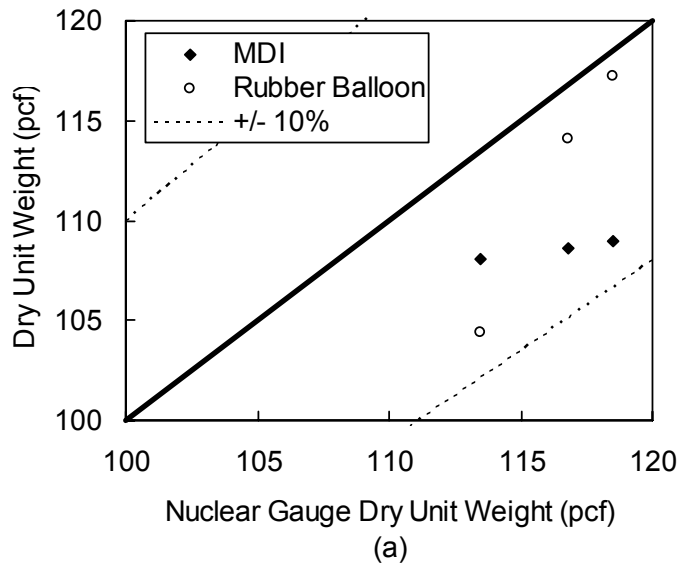


Figure 4.15. Comparison of (a) dry unit weight and (b) water content measured by the MDI, rubber balloon, and nuclear gauge for the sandy clay.

All measurements for dry unit weight from the MDI and rubber balloon tests were within 10 percent of the nuclear gauge measurements. However, all three MDI measurements of dry unit weight were very similar (~108.5 pcf). All of the MDI water contents differed from the nuclear gauge by more than 10 percent, with two points larger and one point smaller than the nuclear gauge. The oven dry water content values were all larger than the values obtained by the nuclear gauge. It is hard to draw a definitive conclusion regarding the accuracy of the MDI in the sandy clay because there are only three data points. Nonetheless, the comparisons in Figure 4.15 are not favorable.

## 4.5 Summary

Dry unit weight and water content measurements were obtained at three different test sites, each consisting of a different soil. These sites were all construction sites in Central Texas. The first site consisted of Taylor Clay (CH), the soil at the second site was low plasticity clay (CL), and the third site consisted of sandy clay (CH). MDI, rubber balloon, and nuclear gauge measurements were made at each site. EDG measurements were attempted in the Taylor Clay but the device was unable to acquire an electrical signal. Time constraints at the other sites precluded development of a Soil Model for the EDG, and thus testing with the EDG was abandoned.

The dry unit weights indicated by the MDI device did not agree favorably with the dry unit weights measured by either the nuclear gauge or rubber balloon. In the Taylor Clay, dry unit weights indicated by the MDI device were larger than those from the nuclear gauge and rubber balloon, while in the low plasticity clay the dry unit weights indicated by the MDI device were smaller. In the sandy clay, all dry unit weights indicated by the MDI were within 10 percent of the nuclear gauge readings. However, because only three measurements were obtained in the sandy clay, generalized conclusions cannot be drawn.

The water contents indicated by the MDI did not agree favorably with values measured by either of the traditional methods (nuclear gauge, oven drying). The MDI values of water content in the Taylor Clay were all smaller than the water contents measured by the nuclear gauge and oven drying. In the low plasticity clay, the water content values indicated by the MDI were larger than the water content values from the nuclear gauge and oven drying. MDI water contents for the sandy clay were significantly different than the water content values obtained from the nuclear gauge, but they were not consistently larger or smaller. However, with only three data points it is difficult to make generalized conclusions regarding the MDI accuracy for the sandy clay.

Table 4.2 provides a summary of the comparison between the dry unit weights and water contents measured by the MDI and the nuclear gauge.

**Table 4.2. Summary of results from Field Study 2**

	$\gamma_d$	Water content
<b>Taylor Clay (CH)</b>	MDI larger than nuclear gauge	MDI smaller than nuclear gauge
<b>Low Plasticity Clay (CL)</b>	MDI smaller than nuclear gauge	MDI larger than nuclear gauge
<b>Sandy Clay (CH)</b>	Not enough data	Not enough data



## 5. Laboratory Testing Program

### 5.1 Introduction

Laboratory evaluation of several of the compaction control devices was performed in an effort to test the devices under controlled laboratory conditions. Laboratory testing involved compacting large-scale soil specimens to a known dry unit weight and water content and using each device to assess the compaction of the soil. The compaction control devices that were evaluated in the laboratory are the Moisture Density Indicator (MDI), the Electrical Density Gauge (EDG), the PANDA dynamic cone penetrometer, and the Clegg Impact Hammer.

### 5.2 Material Description

Laboratory testing was performed using sand that represents a material that would be used as select backfill for a retaining wall. The grain size distribution for this sand is shown in Figure 5.1. Based on its gradation, the USCS classification for this soil is poorly graded sand, while the TxDOT backfill type for this soil is Type B (Table 3.2).

Standard Proctor (ASTM D698) and Modified Proctor (ASTM D1557) compaction tests were performed to obtain compaction curves for the poorly graded sand (Figure 5.2). The Standard Proctor tests did not show significant variation of dry unit weight with water content, with all values close to 109 pcf. The Modified Proctor tests showed more variation in dry unit weight, with a maximum value of 117 pcf obtained at 7.5 percent water content. It was difficult to compact specimens of sand at water contents larger than about 8 to 10 percent because the soil was so freely draining.

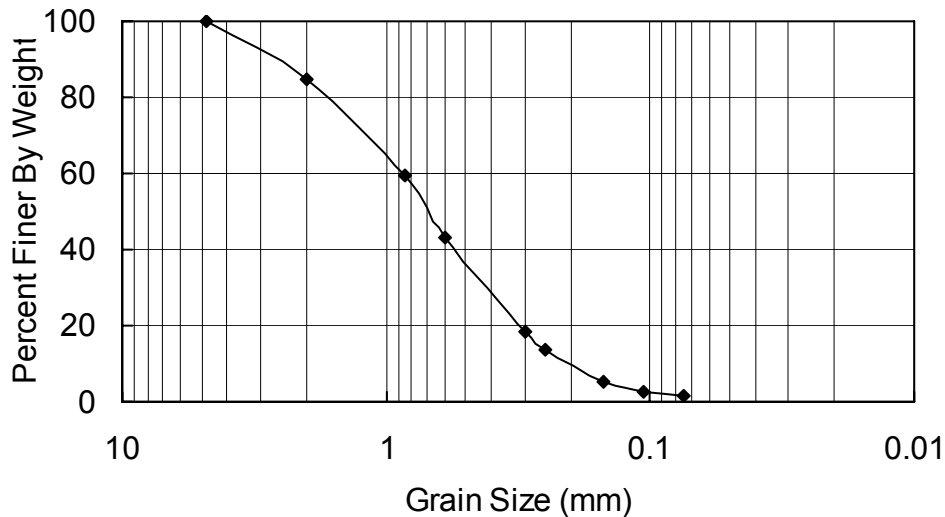


Figure 5.1. Grain size distribution of poorly graded sand used in laboratory testing.

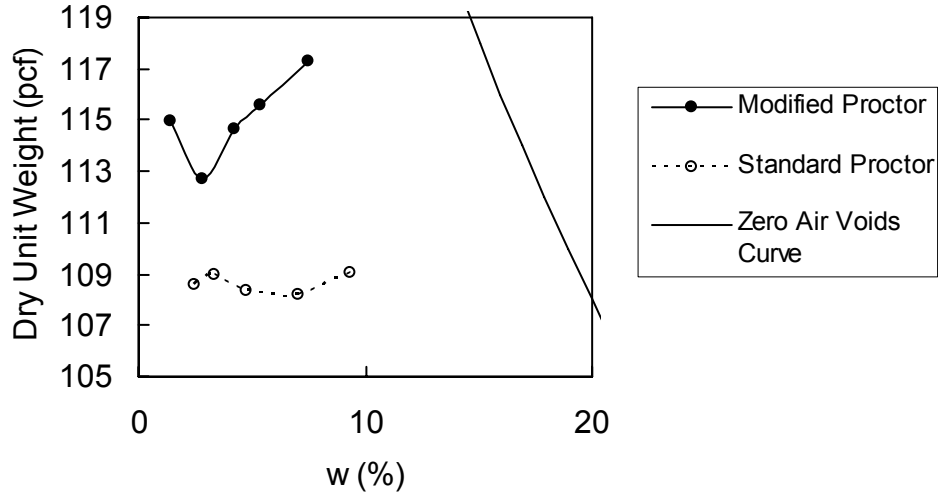


Figure 5.2. Grain size distribution of poorly graded sand used in laboratory testing.

### 5.3 Laboratory Testing Procedures

The laboratory tests were performed in boxes constructed of 0.75 in. plywood with dimensions of 18 in. by 26 in. by 18 in (Figure 5.3). The boxes were assembled using 2 in. drywall screws spaced 6.5 in. apart. The boxes were lined with a 0.15 mil-thick water proof tarp to prevent the wood from absorbing moisture from the test soil. The water proof tarp was held in place with packaging tape.

Sand specimens 12 in. high were compacted in the laboratory test boxes. For each box, approximately 400 lb of sand was mixed in preparation for compaction. After the soil was well mixed, the moisture content of the soil was determined using microwave oven heating (ASTM D 4643) and adjusted until its water content reached the target value. Based on the selected target dry unit weight and target water content for each box, the total weight of soil required to build the specimen was determined and the specimen constructed. The soil was compacted in six, 2-in. lifts using a vibratory hand compactor (Bosch 11316EVS). The undercompaction method (Ladd 1978) was used to build the specimens in an effort to minimize the variation of dry unit weight with depth. Nonetheless, some variations were still observed (Tobin 2006). Specimen preparation and testing of the compaction control devices were completed within eight hours to limit evaporation of water from the top of the specimen and to minimize moisture migration to the bottom of the specimen.

Six specimens were constructed to evaluate the compaction control devices. Table 5.1 lists the target values of water content, total unit weight, dry unit weight, and relative compaction for each test specimen. All of the specimens were compacted at a water content of about 3 percent, and the relative compaction varied from 95 to 107 percent of standard Proctor.

**Table 5.1. Target compaction conditions for laboratory test specimens**

Specimen	w (%)	Target Total Unit Weight (pcf)	Target Dry Unit Weight (pcf)	Target Standard Proctor Relative Compaction
1	3.1	107.2	104.0	95 %
2	3.4	111.7	108.0	99 %
3	3.1	115.5	112.0	103 %
4	3.0	112.2	109.1	100 %
5	3.0	115.9	112.5	103 %
6	2.8	119.6	116.4	107 %

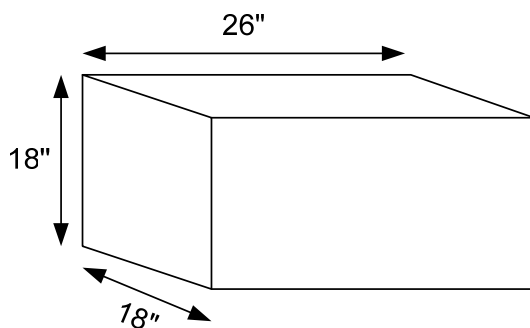


*Figure 5.3. Laboratory test box*

Within each test specimen, one MDI, one EDG, three rubber balloon, two PANDA dynamic cone penetrometer, and three Clegg Impact Hammer tests were performed. The approximate lateral location of each test within the test specimen is shown in Figure 5.4. The order of the tests was: EDG, MDI, rubber balloon, PANDA (trial 1), Clegg Impact Hammer (trial 1), PANDA (trial 2), Clegg Impact Hammer (trial 2), and Clegg Impact Hammer (trial 3). After all of these tests were performed, 4 in. of soil was removed from the top of the box and another rubber balloon measurement was performed to determine the unit weight at mid-height of the specimen. Finally, an additional 4 in. of soil was excavated for a final rubber balloon unit weight measurement near the bottom of the specimen. The additional rubber balloon measurements allowed for an assessment of the variation of dry unit weight with depth within the specimen.

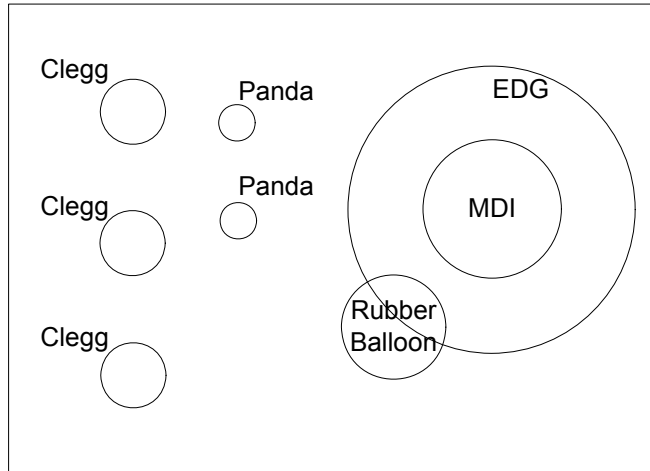


Figure 5.4. Location of compaction control tests within test specimens

## 5.4 Equipment Calibration

### 5.4.1 Moisture-Density Indicator Calibration

The calibration procedure for the MDI discussed in Section 4.3.1 was also used to develop soil-specific calibration coefficients (*a*, *b*, *c*, *d*, *f*, and *g*). Calibration curves ( $\sqrt{K_a} \cdot \rho_w / \rho_d$  versus *w*,  $\sqrt{EC_b} \cdot \rho_w / \rho_d$  versus *w*, and  $\sqrt{EC_b}$  versus  $\sqrt{K_a}$ ) for the poorly graded sand are shown in Figure 5.5, along with the derived calibration coefficients. Calibrations were performed on sand compacted with Standard and Modified Proctor compaction energies. There is little scatter observed in the  $\sqrt{K_a} \cdot \rho_w / \rho_d$  vs. *w* data, with slightly more scatter observed in the  $\sqrt{EC_b} \cdot \rho_w / \rho_d$  vs. *w* and  $\sqrt{EC_b}$  vs.  $\sqrt{K_a}$  data. The scatter in the calibration data that incorporates  $EC_b$  (Figure 5.5b, 5.5c) is significantly less than observed for the clayey materials discussed in Chapter 4 (Figures 4.7, 4.9, 4.11). Because the calibration data in Figure 5.5 display only moderate scatter, there is confidence in the soil calibration parameters for the test soil.

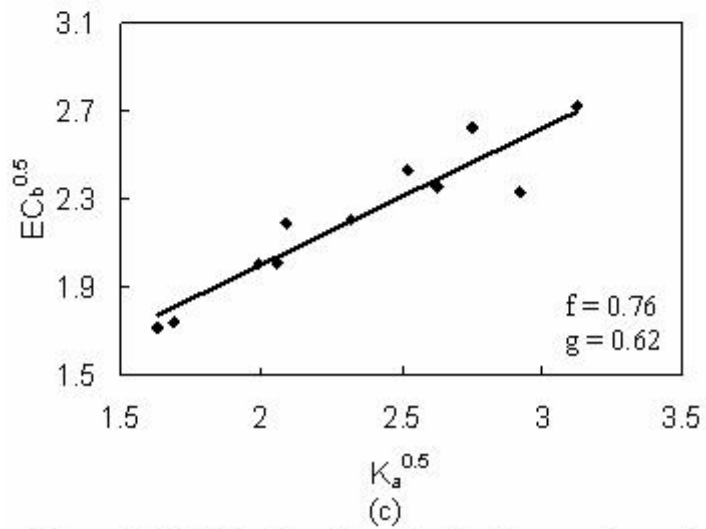
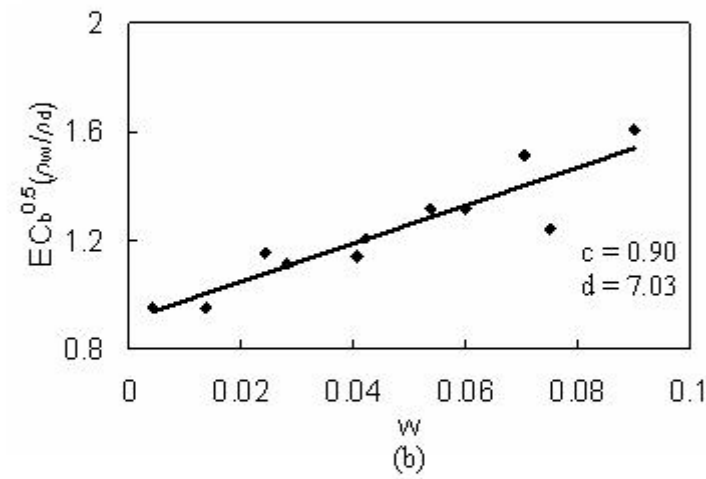
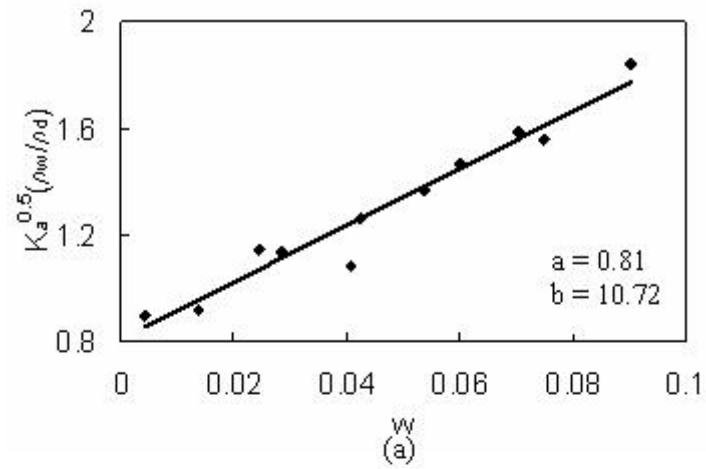


Figure 5.5. MDI calibration data for the poorly graded sand

### 5.4.2 Electrical Density Gauge Calibration

The recommended EDG calibration involves selecting a number of test locations with known, but different, values of dry unit weight and water content. A set of EDG measurements is performed at each location, followed by a rubber balloon test to determine the dry unit weight and water content of the soil. The values of dry unit weight and water content associated with each EDG measurement are entered into the EDG equipment to develop a soil model. The EDG fits its model to the data and reports a fit parameter, with a better soil model indicated by a fit parameter closer to 1.0. The EDG manufacturer (Electrical Density Gauge, LLC 2004) recommends for calibration the following values of percent relative compaction and water content for sandy soil (Table 5.2).

**Table 5.2. Recommended values of relative compaction and water content for EDG calibration in sandy soil (Electrical Density Gauge, LLC 2004)**

% Relative Compaction	w %
98	5
98	7.5
98	10
92	5
92	7.5
92	10

**Table 5.3. Data set used to develop EDG soil model for the poorly graded sand**

% Relative Compaction (Standard Proctor)	w %
98	5.2
104	6.6
107	6.2
104	4.6
73	4.8

The soil model for the poorly graded sand was generated by compacting soil to different dry unit weights and water contents in the laboratory test boxes. Dry unit weights and water contents were evaluated from rubber balloon tests and microwave oven drying. The values of percent relative compaction (based on Standard Proctor) and water content for the compacted soil specimens used to create the soil model for the poorly graded sand are shown in Table 5.3.

The range of water contents (4.6 percent to 6.6 percent, Table 5.3) used to develop the soil model for the poorly graded sand is narrower than those listed for the ideal soil model in Table 5.1 (5 percent to 10 percent) because the sand could not hold more than about 8 percent water content before free water accumulated in the bottom of the specimen. The fit parameter given by the EDG for the soil model of the poorly graded sand was 0.802. The EDG does not provide the user with any additional information regarding soil parameters determined from the calibration.

### 5.4.3 PANDA Dynamic Cone Penetrometer Calibration

As discussed in Section 3.4.1, the PANDA provides failure and tolerance lines for the dynamic cone resistance ( $q_d$ ) based on the general classification of the soil. The gradation of the poorly graded sand (Figure 5.1) and the French soil classification system (Figure 3.7) was used to define the soil type of the test soil. The poorly graded sand is classified as soil type D<sub>1</sub> because less than 12 percent passes the #200 sieve, more than 70 percent passes the #10 sieve, and the soil is non plastic. The resulting failure and tolerance lines for the PANDA for the poorly graded sand are shown in Figure 5.6.

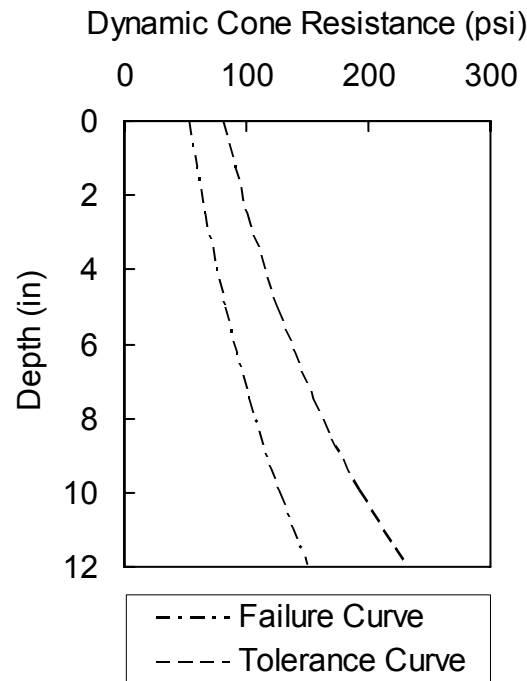


Figure 5.6. Failure and tolerance lines for the poorly graded sand obtained from the PANDA soil library (Sol-Solution 2006)

### 5.4.4 Clegg Impact Hammer Calibration

ASTM D5784 describes the procedure to determine the target Clegg Impact Value (CIV) for a given soil. To obtain the target CIV, soil is compacted using Standard Proctor effort in a 6-in. diameter mold. After the soil has been compacted, the Clegg Impact Hammer is placed on top of the mold and the CIV value is recorded. The procedure is repeated for specimens compacted

to a range of water contents. The target CIV is the maximum CIV value obtained from the compacted soil specimens. The CIV responds to changes in physical characteristics in the soil that influence its strength. Generally, the CIV remains constant dry of optimum or reaches a peak and rapidly decreases as water content increases beyond the optimum water content.

The Clegg calibration curves for the poorly graded sand were obtained by varying the soil water content and using Modified Proctor and Standard Proctor compaction effort. The measured CIV as a function of water content for the two compaction energies are shown in Figure 5.7. The Standard Proctor target CIV value is 18.4 and the Modified Proctor target CIV value is 21.4 based on these data.

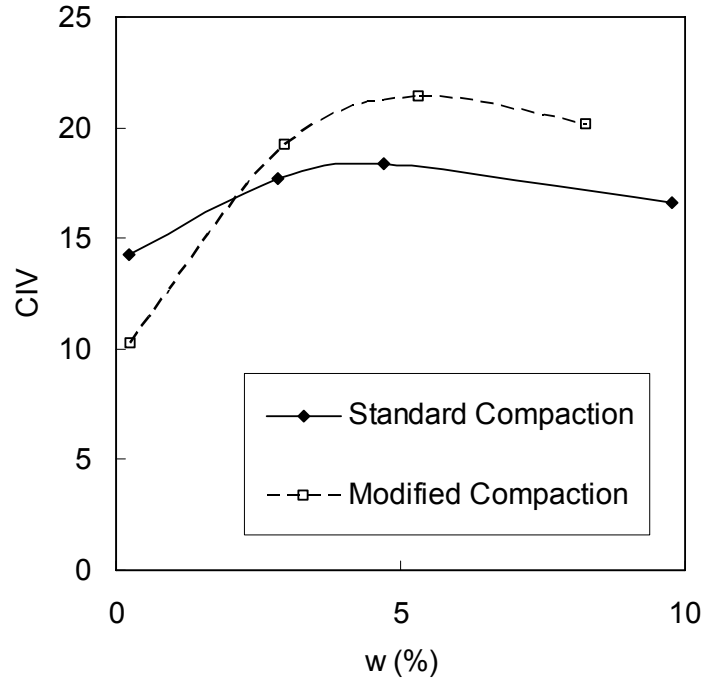


Figure 5.7. Variation of CIV with water content for poorly graded sand

## 5.5 Laboratory Test Results

### 5.5.1 Unit Weight and Moisture Content Variations within Test Specimens

Before testing of the compaction control devices, two specimens were prepared to investigate the uniformity of the unit weight and moisture content throughout the compacted specimens when using the under-compaction technique. Specimen A was compacted to a target total unit weight of 111.2 pcf at a water content of 2.95 percent. This corresponds to a relative compaction of 98 percent Standard Proctor. Specimen B was compacted to a target total unit weight of 115.4 pcf at a water content of 2.9 percent, corresponding to a relative compaction of 102 percent Standard Proctor. Unit weight measurements were obtained at the corners and center of the specimen using the rubber balloon method, and the water content was measured at each of these locations using the microwave oven dry method. To observe how the unit weight and moisture content varied with depth, measurements were obtained at the top, middle, and bottom of the specimen for all five test locations, for a total of 15 measurements per specimen. The

effective depths of the unit measurements were 2 in., 6 in., and 10 in. below the specimen surface.

Figure 5.8 shows the variation of total unit weight with depth and horizontal location for both samples. Figure 5.8 also shows the bulk total unit weight obtained by dividing the total weight of soil used to form the specimen by the volume of the specimen. The theoretical under-compacted values of  $\gamma_t$  ( $\gamma_{t,initial}$ ) for each layer, which represents the unit weight of the soil immediately after compaction of the lift, are shown in Figure 5.8 for comparison.

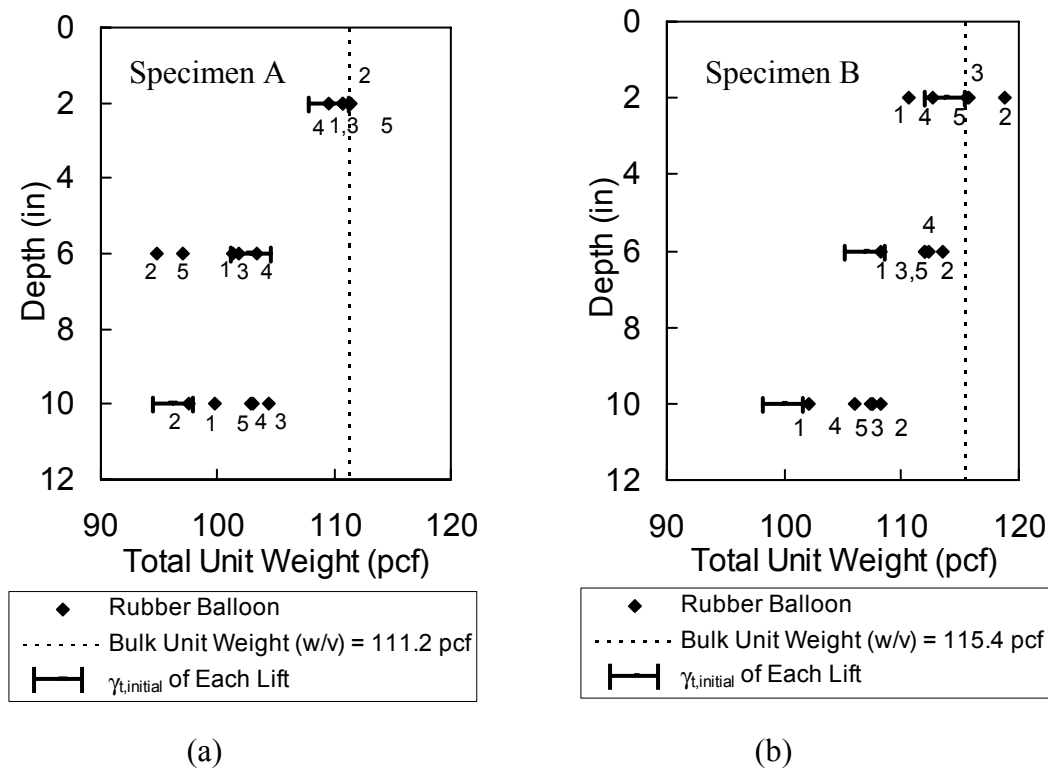


Figure 5.8. Variation of total unit weight with depth and horizontal location (points 1, 2, 4, and 5 are at the corners, point 3 is at the center)

For both specimens the total unit weight measured by the rubber balloon at the top of the specimen corresponds well to the bulk total unit weight calculated by dividing the weight of soil by the volume of the specimen ( $w/v$ ). By comparing the initial under-compaction total unit weights with those measured after compaction of the entire specimen, it can be seen that the final unit weights of the deeper layers are larger than  $\gamma_{t,initial}$  but not as large as the final target unit weight values. This result indicates that the deeper layers did not get compacted to the target final unit weight, implying that the percent under-compaction used to build the specimens may have been too large. The data in Figure 5.8 also show that the bottom and middle layers of Specimen A, and all of Specimen B, experienced significant horizontal variations in the unit weight. For specimen A there does not seem to be consistency for the horizontal locations of the minimum and maximum unit weights. For example, test location 4 in Specimen A was the location of the minimum unit weight in the top layer, but this location was the location of the maximum unit weight for the middle layer. However, for specimen B, the locations of the

minimum and maximum unit weight were consistent throughout the depth of the box. Based on these measurements, the total unit weight within a layer can vary by as much as 9 pcf and the total unit weight between layers can vary by as much as 16.7 pcf.

The average measured water content for specimen A was 2.8 percent with a standard deviation of 0.1 percent. This is reasonably close to the target water content of 2.95 percent. The average measured water content for Specimen B was 2.7 percent with a standard deviation of 0.1 percent. The bottom layer of Specimen B displayed the largest range of water contents, with values varying from 2.5 percent to 2.9 percent; however the measured average water content is only 0.2 percent less than the target water content of 2.9 percent. The maximum difference in water content was 0.4 percent within layers and 0.4 percent between layers. The variation in water content is minimal compared to the variation in total unit weight.

Analysis of the measured total unit weights and water contents of Specimens A and B shows that it was difficult to produce a uniform unit weight throughout the large, compacted specimens. For the analysis of the compaction control equipment being tested in this study, measured rubber balloon values were averaged corresponding to the depth of influence for each device. However, rubber balloon measurements were performed only once per layer in the soil specimen. This accounts for some vertical variations within the sample, but does not account for any horizontal variations that are present. Therefore, it is possible that the unit weights from the rubber balloon are not representative of the dry unit weights at locations tested by the other devices. This procedure is described more fully in the next sections. The water content was easier to control both horizontally and vertically.

### 5.5.2 MDI Results

Dry unit weights and water contents derived from rubber balloon total unit weight and microwave oven water content measurements are used as the standard for comparison with the measurements obtained by the MDI. The MDI provides an average value for the soil dry unit weight and water content over the length of its probes, which are 8 in. long. Because the dry unit weight can vary considerably over this depth (Figure 5.8), the MDI measurements are compared with values from the rubber balloon averaged over the top and middle layers of the specimens.

Two measurements were made with the MDI for each test specimen. These measurements were averaged to represent a single dry unit weight and water content per test specimen. For test specimens 1, 2, 3, 4, and 6, the two MDI dry unit weight measurements were within 1 pcf, and the two MDI water content measurements were within 1 percent of each other. For test specimen 5, the two MDI measurements were very different; one measurement was  $\gamma_d = 114$  pcf and  $w = 3.3\%$ , while the other measurement was  $\gamma_d = 104$  pcf and  $w = 12\%$ . This discrepancy indicates less confidence in the MDI measurements for test specimen 5, as a water content of 12 percent is not possible for this specimen. Thus, this second value should be discarded.

The dry unit weight and water content measurements from the MDI for all six test specimens are compared with the averaged values from rubber balloon testing / oven drying in Figure 5.9. In this figure, each specimen is labeled and two data points are shown for test specimen 5 (5a and 5b); point 5b represents the average of the two measurements and point 5a represents only the realistic measurement ( $\gamma_d = 114$  pcf,  $w = 3.3\%$ ).

The dry unit weight values measured by the MDI were all approximately 115 pcf (Figure 5.9a), while the measurements from the rubber balloon ranged from 100 to 115 pcf. The target dry unit weights ranged from 104 pcf to 116 pcf (Table 5.1), thus the rubber balloon values

appear to be more reasonable. Some of the difference between the MDI and rubber balloon values of dry unit weight may be due to variability within the soil specimen not accounted for by the rubber balloon measurements. However, it is suspect that the MDI reported approximately the same dry unit weight for all test specimens. The MDI measurements of water content show good agreement with the microwave oven measurements of water content (Figure 5.9b), although the water content did not vary considerably between test specimens. For test specimen 5, good agreement is only obtained when considering the first reading (data point 5a). In general, the MDI shows relatively accurate measurements of water content, but less accurate measurements of dry unit weight for the laboratory test specimens of sand.

### **5.5.3 EDG Results**

The EDG provides an average value for the soil dry unit weight and water content over the length of its probes, which are 6 in. long. Thus, the EDG measurements were compared with a weighted average of the measurements from the top and middle layers of the specimen (2/3 of top layer plus 1/3 of middle layer) using the rubber balloon and oven drying methods.

The EDG measurements of dry unit weight and water content for all six test specimens are compared with the appropriately averaged rubber balloon dry unit weight and microwave oven water content measurements in Figure 5.9. The dry unit weight measurements from the EDG were approximately 90 pcf for all soil specimens (Figure 5.9a), while the rubber balloon indicated values of 100 to 115 pcf. The EDG consistently measured water content values of 5 percent for all specimens (Figure 5.9b), while the values obtained by the microwave oven ranged from 2.9 to 3.4 percent. These results indicate a less favorable agreement between EDG measurements of dry unit weight and water content as compared with traditional methods of measurement.

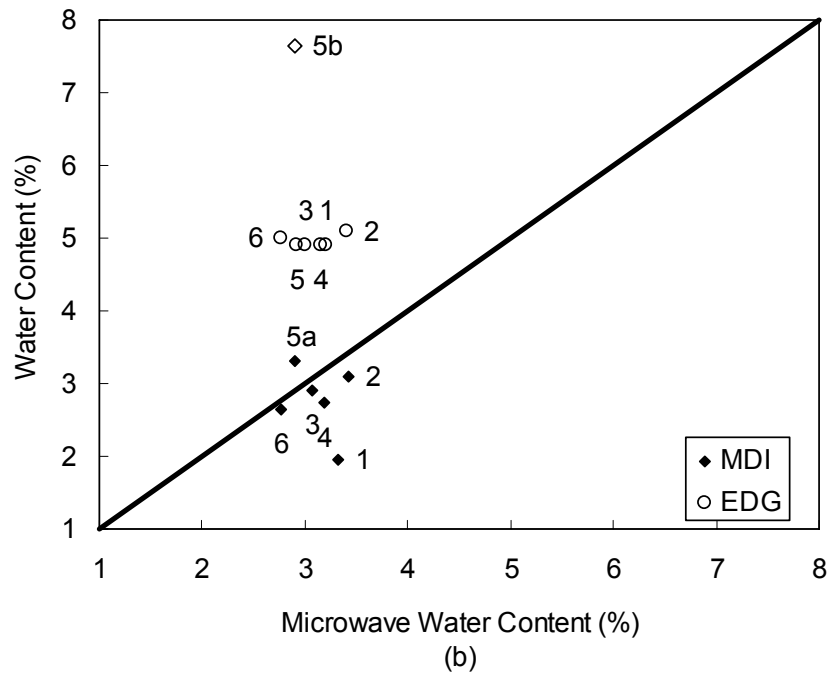
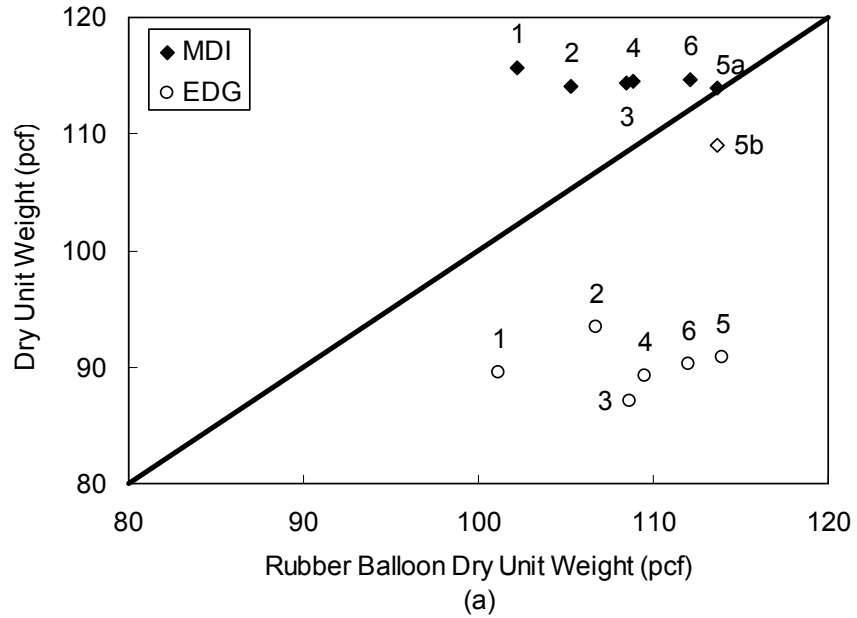


Figure 5.9. Comparison of (a) dry unit weight and (b) water content from rubber balloon testing, microwave oven, MDI, and EDG.

### 5.5.4 PANDA Results

The PANDA Dynamic Cone Penetrometer measures the dynamic cone resistance ( $q_d$ ) with depth. Two PANDA profiles of dynamic cone resistance versus depth were obtained in each test specimen. One PANDA profile from test specimen 1 and one PANDA profile from test

specimen 6 are shown in Figure 5.10. These profiles, shown by the solid lines, are representative of the measurements obtained by the PANDA and demonstrate how the dynamic cone resistance increases with dry unit weight ( $\gamma_d \sim 104$  pcf for specimen 1,  $\gamma_d \sim 116$  pcf for specimen 6). The dashed lines in Figure 5.10 are the failure line (92 percent Standard Proctor) and the tolerance line (95 percent Standard Proctor), as generated by the PANDA software and French soil class D<sub>1</sub> (Section 5.4.3).

The PANDA dynamic cone resistance profile for specimen 1, test 1 (Figure 5.10a) lies well below the failure line, indicating the sample has a relative compaction below 92 percent Standard Proctor. The PANDA  $q_d$  profile for specimen 6, test 1 (Figure 5.10b) lies mostly above the tolerance line, indicating a relative compaction greater than 95 percent Standard Proctor. Based on the average dry unit weight measured by the rubber balloon, specimen 1 had a relative compaction of 94 percent Standard Proctor and specimen 6 had a relative compaction of 105 percent Standard Proctor. Thus, the PANDA profiles are consistent with the relative compaction values for these test specimens.

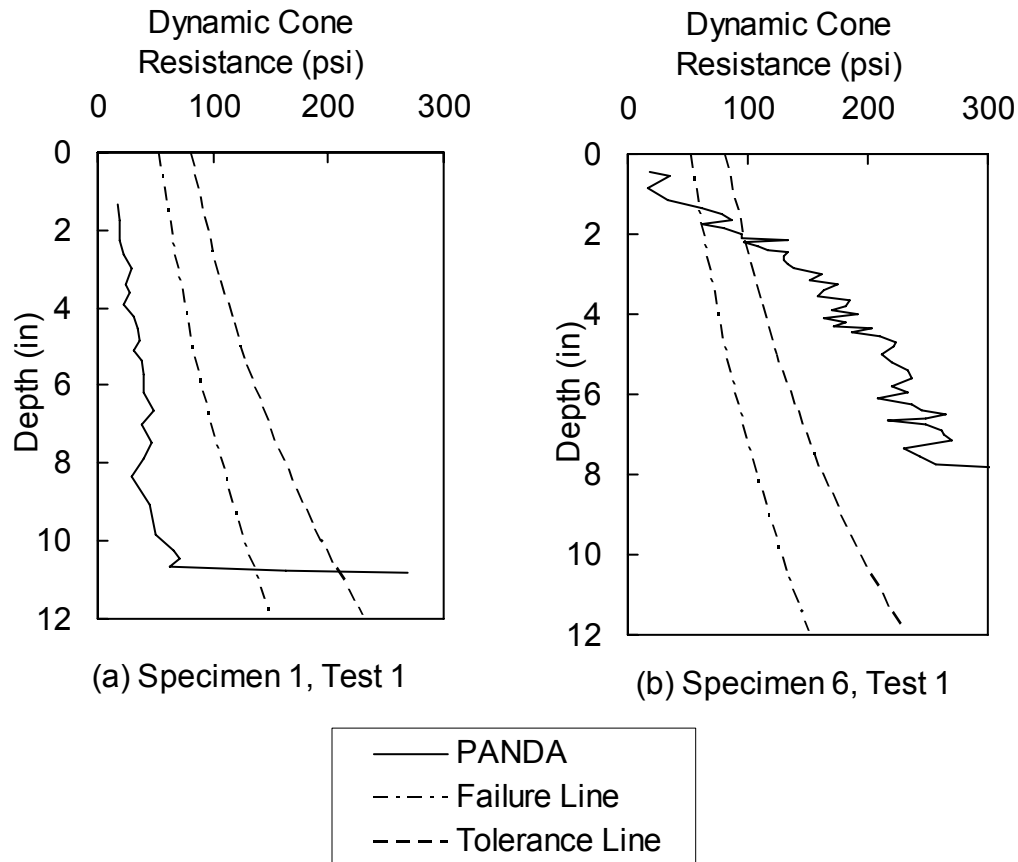


Figure 5.10. PANDA  $q_d$  profiles for (a) specimen 1, test 1 and (b) specimen 6, test 1.

Table 5.4 lists the percent relative compaction for the six test specimens as determined from the PANDA  $q_d$  profiles. These values of relative compaction were obtained by visual examination of the measured  $q_d$  profiles as compared with the failure and tolerance lines. Also listed in Table 5.4 are the values of relative compaction measured by the rubber balloon. The PANDA measurements indicate that specimens 1 through 3 have a relative compaction of less

than 92 percent, and that specimens 4 through 6 have a relative compaction larger than 92 percent. Although the PANDA relative compaction values do not exactly correspond with the measured values of relative compaction, the PANDA does track the increasing dry unit weight from specimens 1 through 6.

**Table 5.4. Summary of PANDA measurements from laboratory test specimens**

Specimen	PANDA % Standard Compaction	Rubber Balloon % Standard Compaction
1	< 92	94
	< 92	
2	< 92	96
	< 92	
3	< 92	99
	92	
4	92 - 95	100
	92	
5	> 95	102
	92 - 95	
6	> 95	105
	> 95	

### 5.5.5 Clegg Impact Hammer Results

Three measurements of the Clegg Impact Value (CIV) were obtained for each soil specimen. The CIV values from each test are listed in Table 5.5. For the specimens compacted a smaller values of relative compaction, the Clegg hammer often compressed the underlying soil so much that it hit the stops such that no CIV reading was obtained (Table 5.5). Only test specimen 6, the densest specimen, provided CIV for all trials.

The CIV values obtained for all of the trials and test specimens are below the target CIV value of 18.4, which corresponds to 100 percent Standard Proctor relative compaction. Thus, the Clegg results indicate that all of the specimens are well below 100 percent Standard Proctor relative compaction. However, the data in Table 5.4 indicate that specimens 4, 5, and 6 were compacted at or above 100 percent relative compaction. Therefore, the Clegg did not accurately distinguish between poorly compacted and well-compacted specimens.

**Table 5.5. CIV measurements from laboratory test specimens**

Specimen	Trial Number	CIV	Rubber Balloon % Relative Compaction
1	1	No Reading	94
	2	No Reading	
	3	No Reading	
2	1	No Reading	96
	2	No Reading	
	3	No Reading	
3	1	4.1	99
	2	No Reading	
	3	No Reading	
4	1	4.2	100
	2	No Reading	
	3	No Reading	
5	1	5.4	102
	2	3.1	
	3	No Reading	
6	1	4.6	105
	2	5.1	
	3	3.2	

## 5.6 Summary

The MDI, EDG, PANDA Dynamic Cone Penetrometer, and Clegg Impact Hammer devices were tested on laboratory-compacted specimens of poorly graded sand. To minimize the variability of dry unit weight within the specimens, the under-compaction technique was used to build the test specimens. Analysis of the total unit weight and water content variability within specimens prepared using the under-compaction method showed that the total unit weight within a given layer varied by as much as 9 pcf and the total unit weight between layers varied by as much as 16.7 pcf. The water content varied less than the total unit weight, with a maximum difference of 0.4 percent within the specimens.

Measurements of dry unit weight and water content by the MDI and EDG were compared to weighted average measurements from rubber balloon and microwave oven dry tests. The MDI consistently reported the same dry unit weight for each specimen, and this value did not agree with the rubber balloon measurements. The MDI water content measurements showed good

agreement with the microwave oven measurements of water content. The EDG also consistently reported the same dry unit weight for each specimen (although this value was different than the MDI value), and again this value did not agree with the rubber balloon measurements. The EDG consistently indicated water contents of 5 percent, which did not agree with the oven dry values. The PANDA Dynamic Cone Penetrometer accurately tracked the variation of dry unit weight across specimens, but did not always accurately identify the level of relative compaction. The Clegg Impact Hammer CIV values indicated a relative compaction of less than 100 percent for all specimens, although two specimens were compacted above 100 percent relative compaction.

The results from the laboratory study can be compared with those from the two field studies. In Field Study 2, the MDI device was used at clay sites, while sandy soil was used in the laboratory study. The MDI more accurately assessed water content in the sand than in the clay soils, but the dry unit weights were not very accurately assessed by the MDI for either type of soil. The dry unit weights from the MDI were not consistently larger or smaller than the values measured by standard methods. However, it should be noted that the nuclear gauge was not available for laboratory testing and thus the rubber balloon method was used to measure unit weight in the laboratory. Previous field testing (Chapters 3 and 4) showed some differences between the dry unit weights from the nuclear gauge and rubber balloon methods, and thus the conclusions from laboratory testing may have been different if the nuclear gauge was available.

As for the Clegg Impact Hammer and PANDA, the laboratory tests revealed that these devices either accurately measured or underestimated the level of compaction of sand as compared with the rubber balloon measurements of dry unit weight. These results are slightly different than those for the sand from Field Study 1 (Chapter 3, Table 3.10, Soil III). In the field study, the Clegg mostly agreed with the direct measurement of dry unit weight, while the PANDA mostly disagreed.

## **6. Practical Issues**

### **6.1 Introduction**

This chapter discusses various practical issues related to each compaction control device used in this study, based on the experimental programs performed as part of this study and the experience of using the compaction control devices in a construction setting. The advantages and disadvantages of each device are compared and contrasted.

### **6.2 Impact Methods**

The impact methods evaluated in this study were the PANDA dynamic cone penetrometer, the standard dynamic cone penetrometer (DCP), and the Clegg Impact Hammer. Each of these methods measures the resistance to impact and empirically correlates this resistance to the “compactness” of the soil. A measurement of dry unit weight is not obtained, nor is there a theory that directly relates the measured resistance to dry unit weight. None of these methods provides a measure of water content and, thus, if construction specifications require the as-compacted water content to be measured another device is needed.

#### **6.2.1 PANDA**

The PANDA was developed in France and it has been used there for compaction control. A French standard exists for its use. The PANDA equipment itself is relatively light and manageable in size. However, the transportation case for the PANDA is slightly cumbersome because it contains multiple extension rods for deeper profiling.

Compaction level is assessed by the PANDA by comparing the dynamic cone resistance profile with failure and tolerance profiles provided by the manufacturer. These profiles are based on the soil type and moisture condition of the fill, and thus are not based on any soil-specific compaction information. Additionally, the soil classification used by the PANDA is a French system, not the Unified Soil Classification System (USCS), such that it is somewhat difficult for an operator in the United States to use. New versions of the PANDA are expected to include the USCS.

The PANDA is best-suited for profiling compaction over a depth of several feet. Because of poor confinement near the ground surface, it does not provide accurate estimates of compaction in the top few inches. Thus, it would be difficult to use the PANDA for lift-by-lift compaction control when the lifts were smaller than about 6 in.

#### **6.2.2 Standard Dynamic Cone Penetrometer**

The DCP is relatively easy to use and requires minimal training. An ASTM standard exists that describes its use (ASTM D 6951). However, it is a cumbersome device to use and transport in the field. A minimum of two persons is required to operate and record data for the DCP, because of the weight of the device and because there is no data acquisition system for the standard device. Electronic data collectors are available but are generally very expensive.

Compaction is assessed with the DCP by measuring the penetration rate in in./blow. No standardized relationship between penetration rate and compaction level exists, although one has

been proposed by MnDOT (Burnham 1997). The DCP penetration rate also has been correlated with the California Bearing Ratio (CBR) for pavement design.

Similar to the PANDA, the DCP is best-suited for profiling compaction over a depth of several feet. Because of poor confinement near the ground surface, it does not provide accurate estimates of compaction in the top few inches. Also, in soft clay soils, the DCP may actually advance under its own self-weight.

### **6.2.3 Clegg Impact Hammer**

The Clegg Impact Hammer is very small in size and lightweight, especially compared to the other impact devices tested. Minimal training is required to operate the device. The test time is very rapid, with the ability to determine a CIV in less than one minute. An ASTM standard exists to govern the use of the Clegg Impact Hammer, and it is relatively inexpensive to purchase.

Compaction is assessed by the Clegg Impact Value (CIV), which is the maximum acceleration, in tens of gravity, of the hammer as it impacts the surface of the compacted soil. The depth of influence of this measurement is unknown. Soil-specific calibration is required to specify the target CIV for a given compaction condition. This target CIV is assessed by measuring the CIV of laboratory-compacted specimens in a Proctor compaction mold. For soft clay soils or uniform sand, the hammer body may penetrate the soil during testing to the point that the hammer handle strikes the guide tube. In these cases, no readings are obtained.

## **6.3 Electrical Methods**

The electrical methods evaluated in this study were the Moisture Density Indicator (MDI), the Electrical Density Gauge (EDG), and the Soil Quality Indicator (SQI). Each of these methods measures the electrical properties of the compacted soils and relates these properties to the dry unit weight and moisture content of the soil. Thus, these methods provide essentially the same data ( $\gamma_d$  and  $w$ ) as current compaction control devices (e.g. nuclear gauge), and could be easily implemented into current construction specifications.

### **6.3.1 MDI**

The MDI was relatively simple to use in the field and has a sound theoretical basis. An ASTM standard exists that describes its use (ASTM D 6780). However, in stiffer soils it is difficult to hammer the four probes into the soil. In these cases it can take up to 20 minutes to perform a single measurement. At times, the device was unable to detect a signal immediately after setup. In these cases, the “Get Signal” button was selected several times or the cables reconnected until the device would take a reading. Additional problems were experienced when using the device to test high plasticity clays.

The MDI measures a time domain reflectometry (TDR) waveform from which the electrical properties of the soil are determined. The device requires soil-specific calibration to develop the model parameters that relate the electrical properties of the soil to its dry unit weight and water content. This calibration is not difficult to perform, as it can be performed using the same laboratory specimens used to develop a compaction moisture-density curve.

### **6.3.2 EDG**

The EDG is somewhat cumbersome to use in the field. After the probes are placed in the soil, four readings are taken with the electrical connectors placed on four different combinations of probes. The switching of connectors to and from different probes takes some time. Similar to the MDI, the probes can be difficult to insert into stiff soils. Also, the device will not operate on high plasticity clays.

The EDG measures the dielectric properties of the soil and relates them to the dry unit weight and water content of the soil. The soil-specific calibration for the EDG is performed by performing electrical measurements in the field for the soil compacted over a range of known dry unit weights and water contents. The dry unit weight and moisture content of each soil sample used in the calibration are measured by other methods, such as the rubber balloon test for unit weight and oven drying for water content. This calibration is difficult to perform at a field site, because of time constraints and because a range of unit weights and water contents is required. Also, it may be difficult on site to find soil less than fully compacted at water contents far from optimum.

### **6.3.3 SQI**

The SQI is lightweight, easy to use in the field, and ideal for lift-by-lift compaction control. Little training is necessary for the operator. The test block and accompanying laptop computer make transportation and handling of the SQI and its accessories somewhat cumbersome. As the SQI exists now, in prototype form, it is necessary to use a laptop computer in the field for data acquisition and reduction. However, the manufacturer anticipates that the software eventually will be coupled directly with the device for retail sale. Careful preparation of the testing surface is important for the SQI.

Similar to the other electrical devices, soil-specific calibration is required for the SQI. However, at this time the manufacturer has not developed a standard calibration method. Thus, this device cannot be used at this time.

## **6.4 Stiffness Methods**

The only stiffness method tested in the field in this study was the Portable Seismic Property Analyzer (PSPA). The PSPA uses surface wave methods to measure the average Young's Modulus over the top few inches of soil.

### **6.4.1 PSPA**

The PSPA device is small and easy to handle. It is currently necessary to use a laptop computer in the field for data acquisition and reduction; however, the manufacturer anticipates that soon the software will be coupled directly with the device. Extensive training is required of the operator to address ideal soil-to-receiver coupling, data analysis, and data selection for the PSPA. Also, the device is expensive, relative to the other devices considered in this study.

Again, soil-specific calibration is necessary to identify the stiffness required to ensure a desired level of compaction. This calibration requires sophisticated resonant column-torsional shear laboratory testing which is not commonplace in geotechnical laboratories. Also, the PSPA does not provide a measure of water content, which is a concern because soil stiffness of partially saturated, fine-grained soils is affected significantly by water content (Chapter 7).

## **6.5 Summary**

This chapter discussed the various practical issues related to the field use and calibration of the compaction control devices investigated in this study. Table 6.1 provides a comparison of the various devices in terms of these practical issues.

**Table 6.1. Comparison of Practical Issues for Compaction Control Devices**

	<b>Nuclear Gauge</b>	<b>PANDA</b>	<b>DCP</b>	<b>MDI</b>	<b>EDG</b>	<b>SQI</b>	<b>PSPA</b>	<b>Clegg</b>
<b>Test Method</b>	Nuclear	Impact	Impact	Electrical	Electrical	Electrical	Stiffness	Impact
<b>Reported Test Parameters</b>	$\gamma_d, w$	Dynamic cone resistance ( $q_d$ )	Penetration rate (in/blow)	$\gamma_d, w$	$\gamma_d, w$	$\gamma_d, w$	Young's Modulus (E)	Clegg Impact Value (CIV)
<b>ASTM Standard</b>	D 2922, D 3017	None	D 6951	D 6780	None	None	None	D 5874
<b>Soil-Specific Calibration</b>	Not required	Identification of soil type	Provided by manufacturer based on soil type	Laboratory testing in Proctor mold	Field calibration using direct measurement of $\gamma_d, w$	Required but no standard method yet developed	Laboratory stiffness testing	Laboratory testing in Proctor mold
<b>Operator Training</b>	Extensive	Moderate	Minimal	Moderate	Moderate	Moderate	Extensive	Minimal
<b>Ease of Use</b>	Moderate	Moderate	Difficult	Difficult	Difficult	Potentially Easy	Moderate	Easy
<b>Approx. Cost of Device</b>	\$5,000	\$10,000	\$1,000	\$6,000	\$7,500	Not yet available	\$30,000	\$2,500



## 7. Stiffness of Compacted Soil Specimens

### 7.1 Introduction

Some of the compaction control devices considered in this study, such as the PSPA, measure the stiffness of the soil in an effort to assess its compactness. While dry unit weight certainly affects the stiffness of soil, the stiffness is also affected by the negative pore water pressures (i.e., soil suction) present in these partially saturated materials. Accordingly, an experimental study was conducted to investigate whether soil stiffness is a suitable parameter to assess the compactness of compacted fills. The soil suction was measured, as well as the soil stiffness as characterized by the shear wave velocity and compression wave velocities, for clay specimens compacted at different water contents and dry unit weights.

### 7.2 Background

A literature review was performed to investigate the impact of compaction conditions on matric suction, the effect of compaction conditions on soil stiffness as measured by stress wave velocities, and the relationship between matric suction and wave velocity.

Before continuing, the terms soil suction and matric suction need to be defined. Soil suction has two components, namely, matric and osmotic suctions. The matric suction component is mainly associated with the capillary phenomenon resulting from the surface tension of water. The difference between the air and water pressures across the air-water interface is the matric suction. In the field, the pore-air pressure is assumed to be equal to the atmospheric pressure, and thus the matric suction is equal to the negative pore water pressure in the soil. The osmotic suction basically results from the concentration of the dissolved salts in the pore-water. Generally, the initial compaction water content of compacted soils appears to have a direct relation with the developed matric suction, while the osmotic suction is not sensitive to the changes in the compaction water content (Fredlund and Rahardjo, 1993).

Many researchers (e.g., Olson and Langfelder 1965, Fredlund and Rahardjo 1993, Sivakumar and Wheeler 2000, Agus and Schanz 2006) have shown that the matric suction of compacted soils is primarily dependent on the compaction water content and almost independent of the dry unit weight. An example of a matric suction—water content relationship is shown in Figure 7.1. Here, the matric suction was measured in specimens compacted at different values of water content and dry density. The matric suction measurements vary considerable with water content, but they do not vary between the specimens compacted at different dry densities.

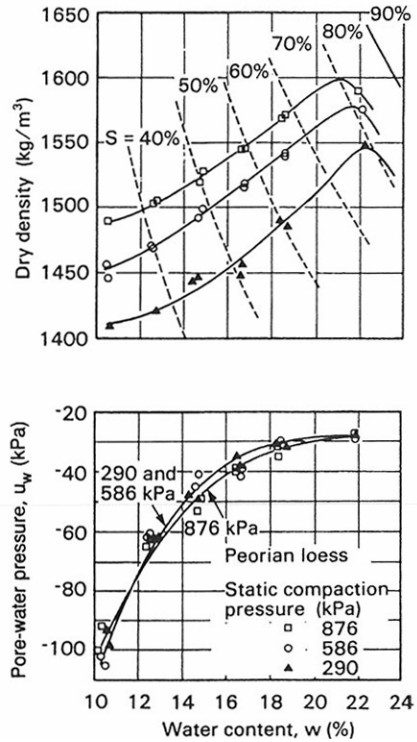


Figure 7.1. Effect of compaction water content and dry density on matric suction for compacted Goose Lake clay (Olson and Langfelder, 1965).

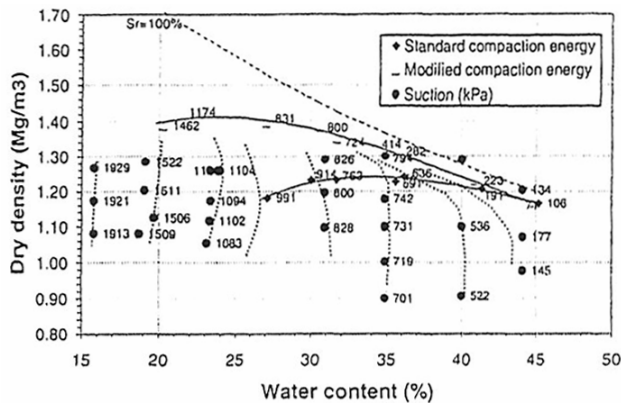


Figure 7.2. Matric suction values for specimens compacted at different dry unit weights and water contents (Gonzalez and Colmenares, 2006).

Gonzalez and Colmenares (2006) measured the matric suction for kaolin specimens compacted at different dry unit weights and water contents. The Proctor compaction curve and measured suctions are presented in Figure 7.2. The authors plotted contours of constant suction and concluded that the suction contours were nearly vertical at small dry unit weights and tended to curve to the left at large dry unit weights. Above the Standard Proctor optimum water content, the contours became asymptotic to the line of 100 percent degree of saturation. The authors

concluded that the matric suction depends mainly on the water content, with a much lesser influence of the dry unit weight.

The effect of compaction conditions (compaction water content, dry unit weight, and degree of saturation) on the stiffness of compacted soils at small strains has been investigated in several studies. The stiffness at small strains has been evaluated in terms of the shear wave velocity ( $V_s$ ), which is related to the maximum shear modulus ( $G_{max} = \rho V_s^2$ ), and the compression wave velocity ( $V_p$ ), which is related to the constrained modulus ( $M_{max} = \rho V_p^2$ ).

Stephenson (1978) measured shear and compression wave velocities of compacted low plasticity silty clay. The influence of void ratio and degree of saturation on  $V_s$  and  $V_p$  was the primary concern of this study. The wave velocities decreased with increasing void ratio for a given degree of saturation. At a constant void ratio, the wave velocities increased with increasing degree of saturation for degrees of saturation ranging between 35 and 85 percent.

Wu et al. (1984) and Qian et al. (1991) studied the effect of the degree of saturation on the shear modulus at small strains of a non-plastic silt (Figure 7.3). The shear modulus reached a maximum value at degrees of saturation ranging between 4 and 20 percent, and this maximum value was as much as twice as large as the value for dry or fully saturated conditions. Marinho et al. (1995) studied the effect of the degree of saturation on the shear modulus at small strains of compacted London clay. The authors reported peak values for the shear modulus at degrees of saturations ranging between 75 and 85 percent.

Ooi and Pu (2002, 2003) investigated the effect of the compaction water content, dry unit weight, and degree of saturation on the stiffness at small strains of fine-grained pavement geomaterials (Figure 7.4). The stiffness was measured using the GeoGauge device, and thus the authors only reported the foundation stiffness,  $K$  (equation 2.16). The stiffness reached a maximum value at water contents slightly dry of optimum and decreased with further increases in water content (Figure 7.4c). All the stiffness values peaked within degrees of saturation between 66 percent and 76 percent (Figure 7.4d). The authors concluded that the stiffness is not directly related to dry unit weight.

The results from these studies indicate that compaction water content, dry unit weight, and degree of saturation all may affect the stiffness of compacted soil. However, the degree to which each variable impacts the stiffness has not been assessed.

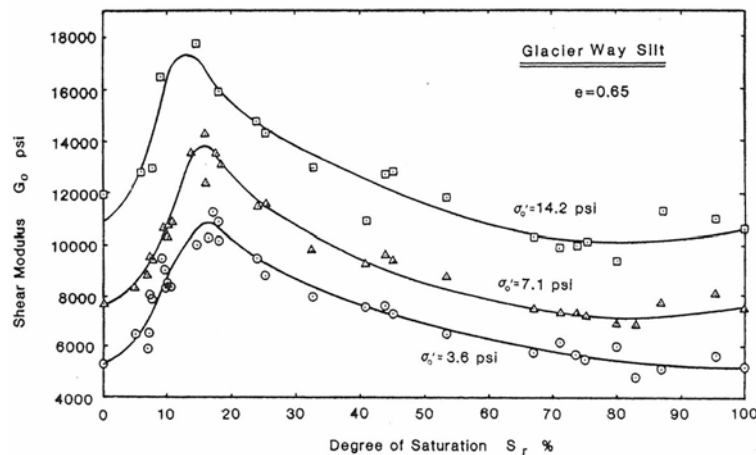


Figure 7.3. Effect of degree of saturation on the small-strain shear modulus (Wu et al. 1984).

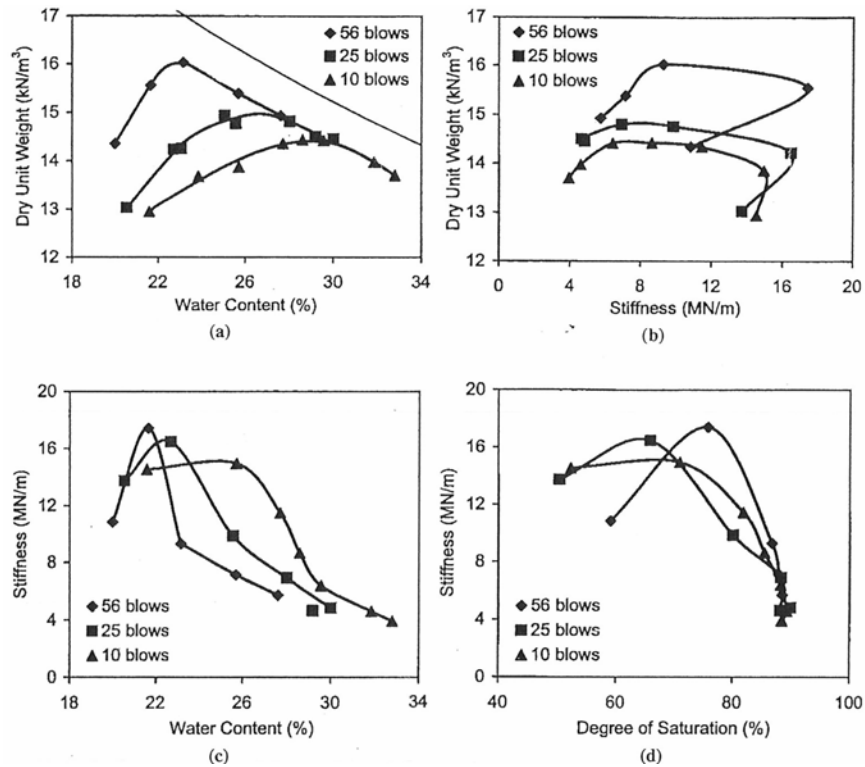


Figure 7.4. Results of stiffness testing on compacted Waipio silt: (a) compaction curves, (b) dry unit weight versus stiffness, (c) stiffness versus water content, and (d) stiffness versus degree of saturation (Ooi and Pu 2003).

Only a few studies have investigated the effect of matric suction on the shear modulus at small strains of compacted soils. Marinho et al. (1995) studied the effect of matric suction on the small strain shear modulus of London clay compacted at different water contents and void ratios. The specimens were compacted and then allowed to dry gradually, and shear wave velocity and matric suction were measured at various stages of the drying process. Soil stiffness increased with increasing suction up to a certain suction value, beyond which soil stiffness either decreased or stopped increasing (Figure 7.5). Similar results were found by Picornell and Nazarian (1998) for a coarse sand, fine sand, silt, and clay, and by Vinale et al. (1999), Vassalo and Mancuso (2000), and Mancuso et al. (2002) for compacted silty sand. Other studies (Marinho et al. 1995) have found that the soil stiffness may decrease at larger values of matric suction. Mendoza et al. (2005), Leong et al. (2006), Mendoza and Colmenares (2006), and Sawangsuriya et al. (2006) showed a continuous increase of soil stiffness with increasing matric suction. These inconsistencies may be related to the different soils tested and the range of matric suction values in the tests. Nonetheless, the studies do not provide a clear picture on the impact of matric suction on soil stiffness.

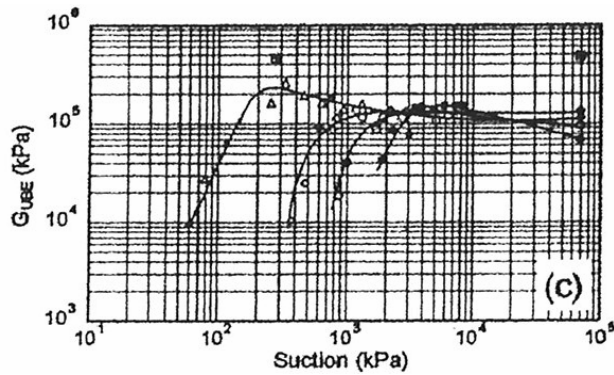


Figure 7.5. Shear stiffness versus matric suction for London clay (Marinho et al., 1995).

### 7.3 Experimental Program

An experimental test program was conducted on a soil that represents a typical material used by TxDOT for construction of embankments. The soil was obtained from an active TxDOT construction site in June, 2004. The soil was classified as low plasticity clay according to the Unified Soil Classification System (USCS) with a liquid limit of 38 percent, plasticity index of 17 percent, and clay fraction of 27 percent. Standard Proctor compaction tests revealed that the clay had an optimum water content of 19 percent and a maximum dry unit weight of 106 pcf.

Test specimens were prepared by kneading compaction using an air piston that applies constant pressure. An aluminum rod, 0.5 inch in diameter, was pushed into the soil under the applied air pressure to perform the kneading action. The specimens were compacted in six lifts of approximately equal height (ASTM D 2850). A series of tests was performed to determine the combination of number of blows per lift and kneading pressure required to reach the desired dry unit weights. Twenty five blows per lift were used. A constant kneading pressure ranging between 10 and 40 psi was selected to prepare specimens at different dry unit weights. The compacted specimens were 2-in. diameter and 4.6-in. tall.

Wave velocities were measured using piezoelectric transducers that transmit a wave from one end of the specimen and receive the wave at the other end of the specimen. By measuring the travel time of the wave over the known distance between transducers, the wave velocity can be computed. The instrumentation required for supporting piezoelectric transducers include: a function generator to produce the excitation signal, an amplifier to amplify the signal before sending it to the transducer, and an oscilloscope to display the excitation signal and the amplified received signal. A schematic diagram of the piezoelectric transducers and the associated electronics required during testing is shown in Figure 7.6. For the generation of compression (P) waves, the piezoelectric transducer is a disk that faces perpendicular to the end platen and displaces into the specimen to generate a P-wave (Figure 7.7). The piezoelectric element required for the generation of shear (S) waves, usually referred to as a bender element, consists of a plate that protrudes into the soil and displaces laterally to generate an S-wave (Figure 7.7). A schematic of the end platens designed for this study, which contain both piezoelectric disks and bender elements, are shown in Figure 7.7.

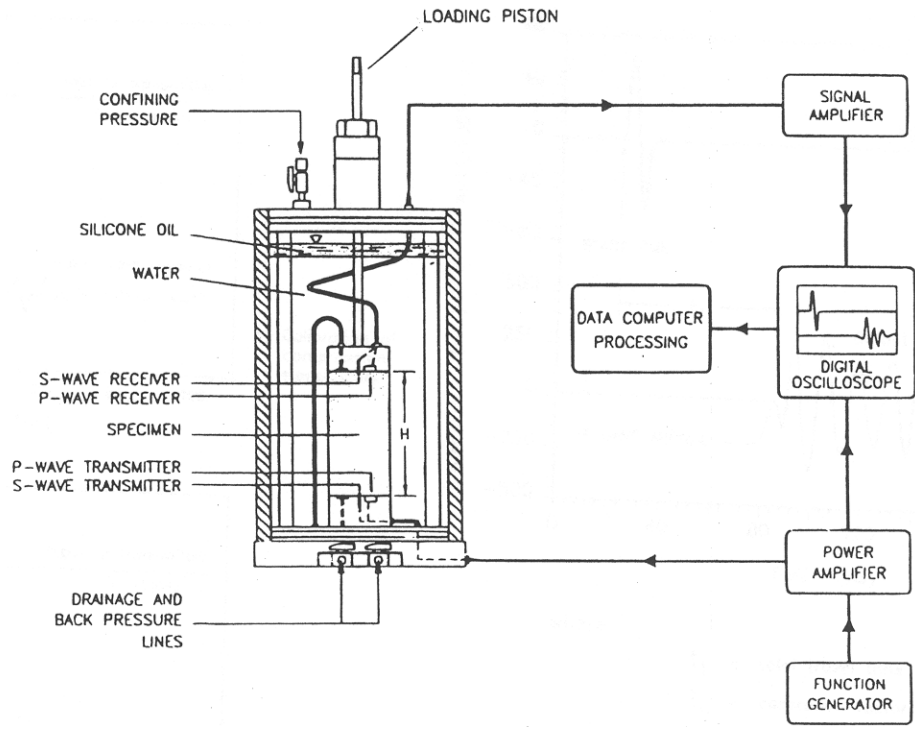


Figure 7.6. Schematic of piezoelectric transducer test up (Bringoli et al. 1996).

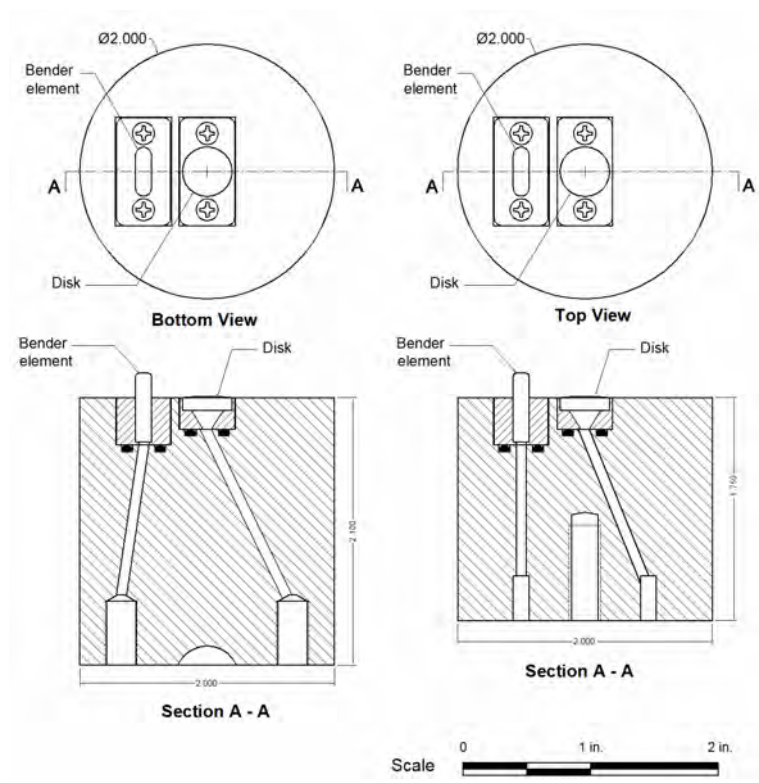


Figure 7.7. Triaxial end platens designed for the test specimens.

A total of 28 specimens compacted at different water contents ranging from approximately 12 to 25 percent and dry unit weights ranging from approximately 92 and 112 pcf were tested (Figure 7.8). Wave velocities were measured at a confining pressure of 15 psi under unconsolidated-undrained (UU) conditions (i.e., no drainage). Additionally details regarding the procedures used for the velocity measurements (e.g., excitation frequency) can be found in Salem (2007).

In addition to the wave velocity measurements, a series of tests was performed to determine the effect of the compaction water content, dry unit weight, and degree of saturation on the soil matric suction. The soil matric suction was measured using a pressure plate apparatus. Again, details can be found in Salem (2007).

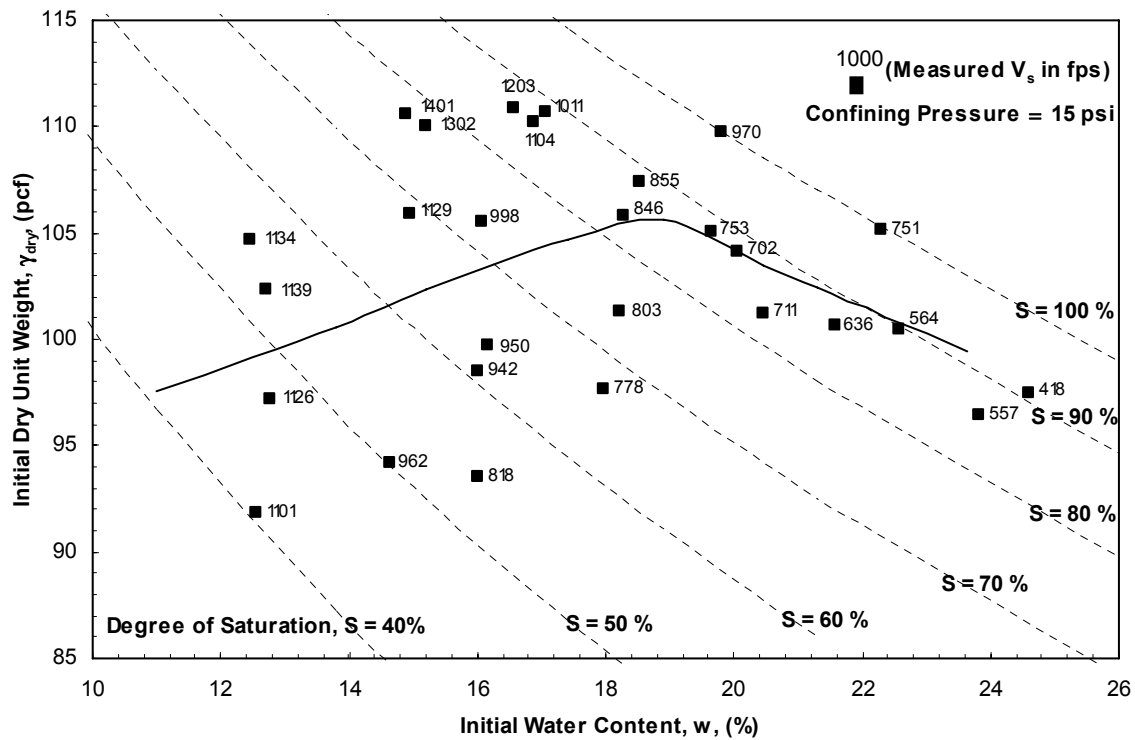


Figure 7.8. Measured shear wave velocities for specimens compacted at different values of water content and dry unit weight.

## 7.4 Experimental Results

### 7.4.1 Effect of compaction conditions on wave velocity

The as-compacted values of dry unit weight and water content are plotted in Figure 7.8 with the measured shear wave velocities at a confining pressure of 15 psi listed next to each data point. The shear wave velocities shown in Figure 7.8 are plotted versus as-compacted (i.e., initial) water content, dry unit weight, and degree of saturation in Figure 7.9. For approximately the same dry unit weight (i.e., within a range of 5 pcf), the shear wave velocity increased with decreasing water content (Figure 7.9a). For approximately the same water content (i.e., within a range of 3 percentage points), the shear wave velocity increased slightly with increasing the dry

unit weight as shown in Figure 7.9b. For water contents less than 22 percent, the data in Figure 7.9b reveals that the dry unit weight has little effect on the shear wave velocity, except perhaps at dry unit weight values greater than 105 pcf. Figure 7.9b also indicates that for a given dry unit weight, the shear wave velocity may vary by a factor of two depending on the water content. Figure 7.9c displays the measured shear wave velocities versus initial degree of saturation. Generally, the shear wave velocities decrease with increasing degree of saturation. The shear wave velocity data for specimens with  $\gamma_d$  less than 105 pcf follow a single trend, while the data for specimens with  $\gamma_d$  greater than 105 pcf follow another trend

Compression wave velocities were measured on the same specimens that were used for the shear wave velocity measurements (Figure 7.8). The compression wave velocities are plotted versus as-compacted (i.e., initial) water content, dry unit weight, and degree of saturation in Figure 7.10. In contrast to the results for shear wave velocity, for compression wave velocity the effect of dry unit weight was more pronounced than the effect of water content (Figure 7.10a, b). At approximately the same dry unit weight, the compression wave velocity decreased slightly with increasing water content as shown in Figure 7.10a. However, for approximately the same water content (Figure 7.10b), the compression wave velocities increased significantly with increasing dry unit weight, particularly at dry unit weights above 100 pcf. The variation of the compression wave velocity with the degree of saturation is shown in Figure 7.10c. Although there is significant scatter, the compression wave velocity generally increases with saturation. For fully saturated specimens (not shown in Figure 7.10c), the compression wave velocity was measured to be between 5,100 and 6,000 fps, which represents the compression wave velocity of water.

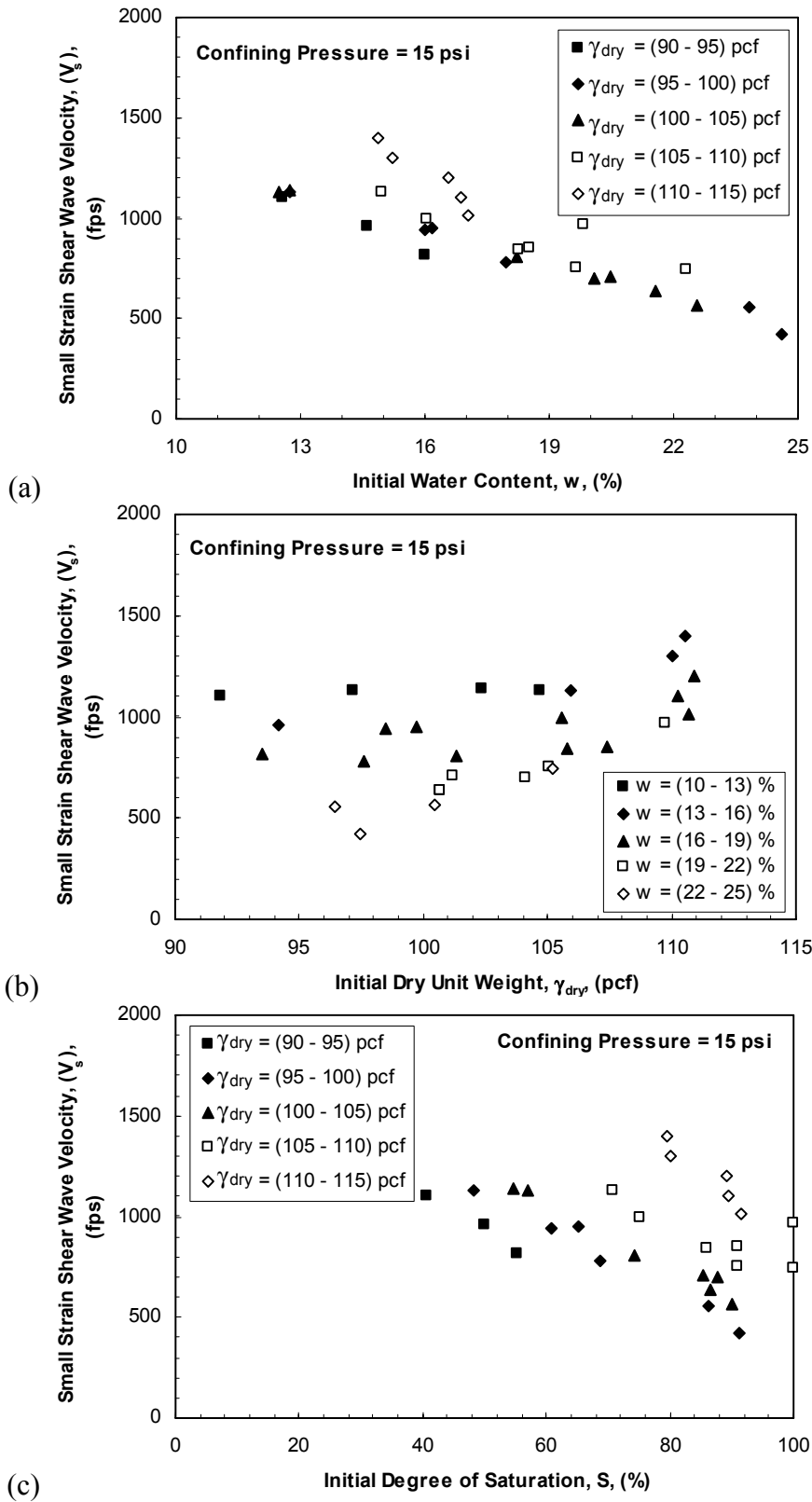


Figure 7.9. Measured shear wave velocity versus (a) water content, (b) dry unit weight, and (c) degree of saturation.

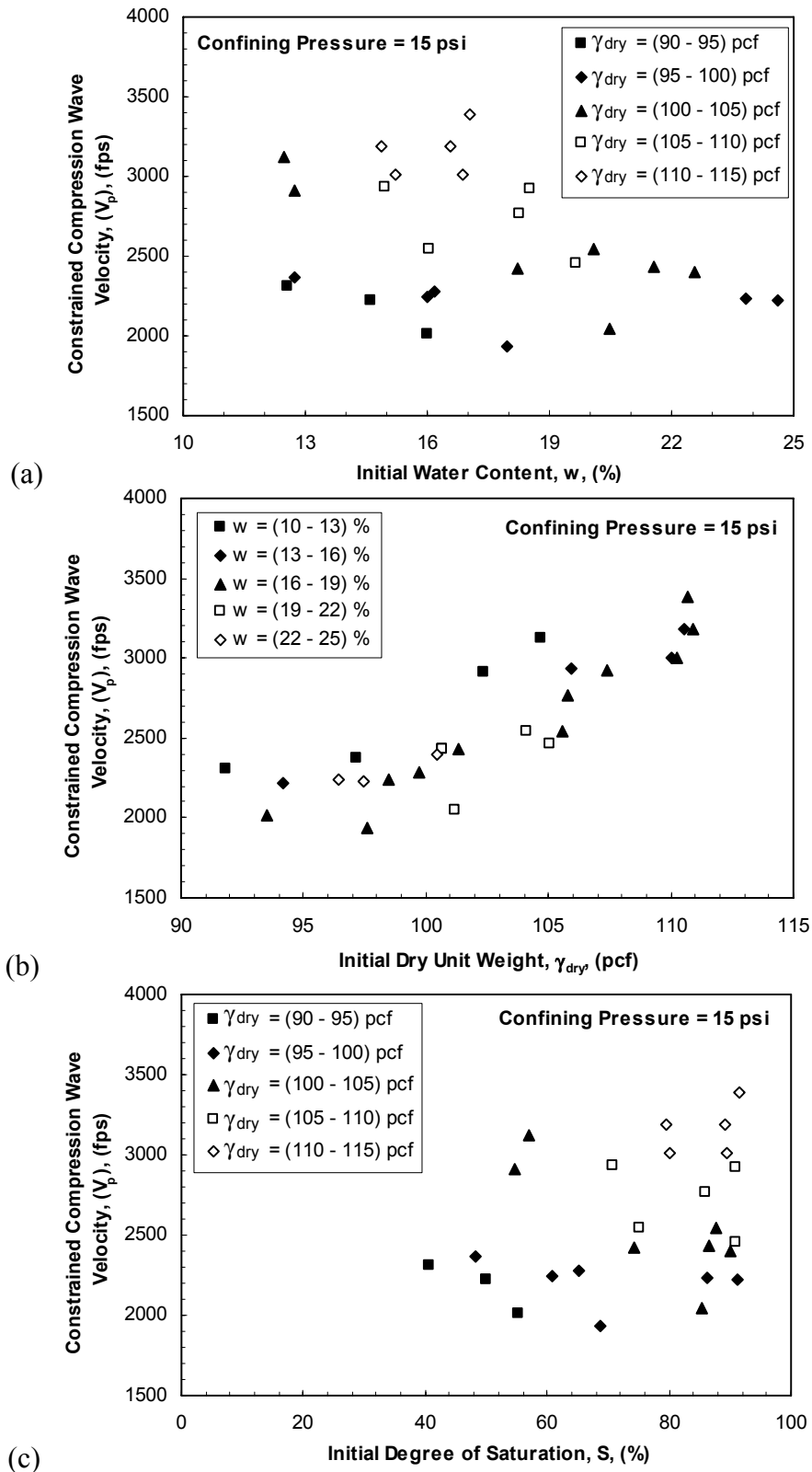


Figure 7.10. Measured compression wave velocity versus (a) water content, (b) dry unit weight, and (c) degree of saturation.

### 7.4.2 Effect of compaction conditions on matric suction

Over 40 tests were performed to determine the effect of the compaction water content, dry unit weight, and degree of saturation on the soil matric suction. The soil matric suction was measured using a pressure plate apparatus. The as-compacted values of dry unit weight and water content are plotted in Figure 7.11 with the measured matric suction listed next to each data point. Generally, the matric suction decreased as the water content increased. Nearly vertical contours of constant suction were observed (Figure 7.11). Thus, the matric suction was observed to be primarily dependent on the compaction water content and almost independent of the dry unit weight as shown in Figure 7.12. The matric suction decreased from over 80 psi at water contents less than 12 percent to less than 5 psi at water contents greater than 23 percent. The matric suction also decreased with increasing saturation (not shown), but the scatter in the matric suction-saturation relationship was more significant than for the matric suction–water content relationship shown in Figure 7.12.

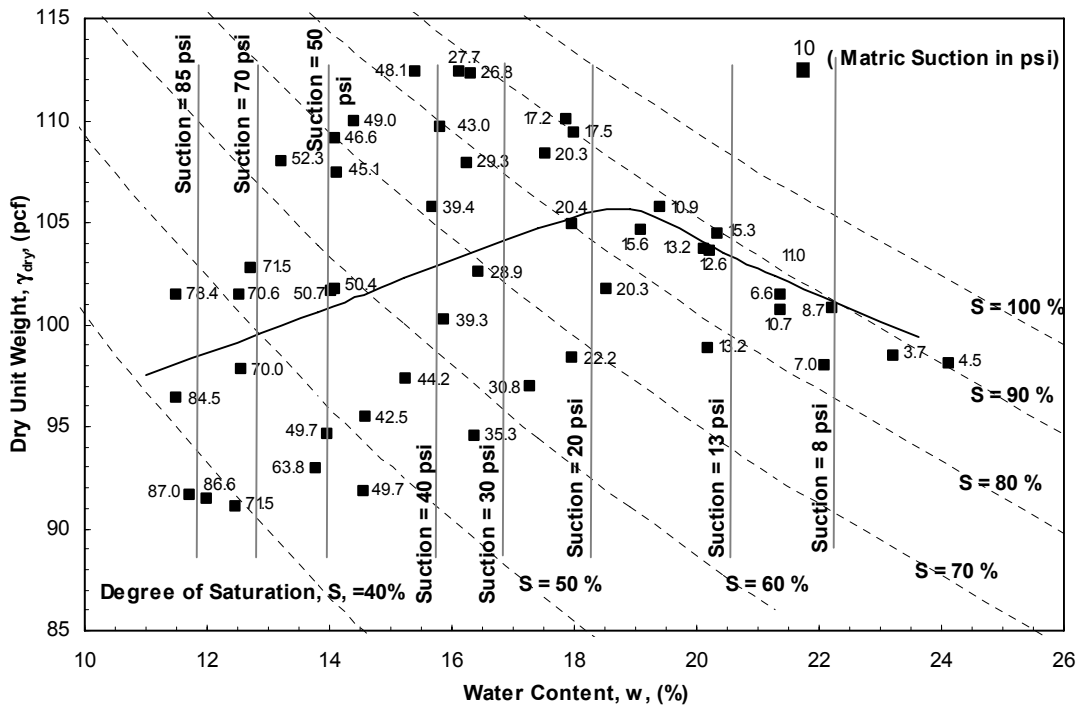


Figure 7.11. Measured matric suction for specimens compacted at different values of water content and dry unit weight.

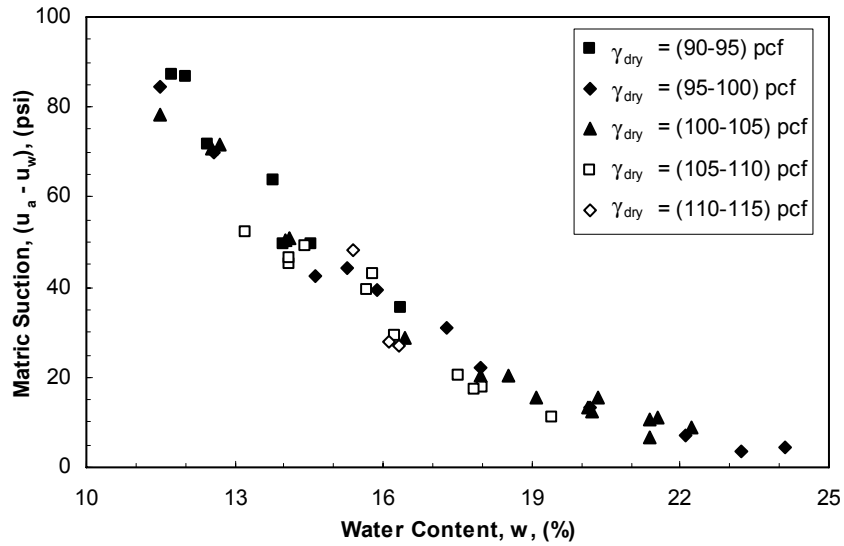


Figure 7.12. Measured values of matric suction versus water content.

### 7.4.3 Relationship between stiffness and matric suction

To study the relationship between stiffness and matric suction, the results from the matric suction tests (Figure 7.12) were used to estimate the initial matric suction for each of the 28 specimens for which the shear and compression wave velocities were measured (Figure 7.8). For these comparisons, the shear and compression wave velocities were converted into shear modulus ( $G_{\max}$ ) and constrained modulus ( $M_{\max}$ ) values.

The measured shear and constrained moduli are plotted versus matric suction in Figure 7.13. A significant increase in shear modulus ( $G_{\max}$ ) was observed when the initial matric suction increased from 4 to 20 psi (Figure 7.13a). At larger values of matric suction, the shear moduli values were scattered and no clear trend could be defined. For the constrained modulus, a slight increase was observed when the matric suction increased from 4 to 20 psi (Figure 7.13b). At larger values of matric suction, the constrained moduli values were also scattered and no clear trend could be defined. Note that because the data in Figures 7.13 are plotted in log-log space, the range of moduli values is larger than may visually appear.

One issue that must be considered is the effect of the void ratio, or dry unit weight, on the measured stiffnesses. To remove the effect of the dry unit weight from the stiffness–matric suction relationships, the shear and constrained moduli were normalized by dividing the values by the quantity,  $F(e)$ , that has been used to describe the effect of void ratio ( $e$  = void ratio) on the stiffness of clays (Hardin and Black 1968). The expression for  $F(e)$  is:

$$F(e) = \frac{(2.97 - e)^2}{(1 + e)} \quad (7.1)$$

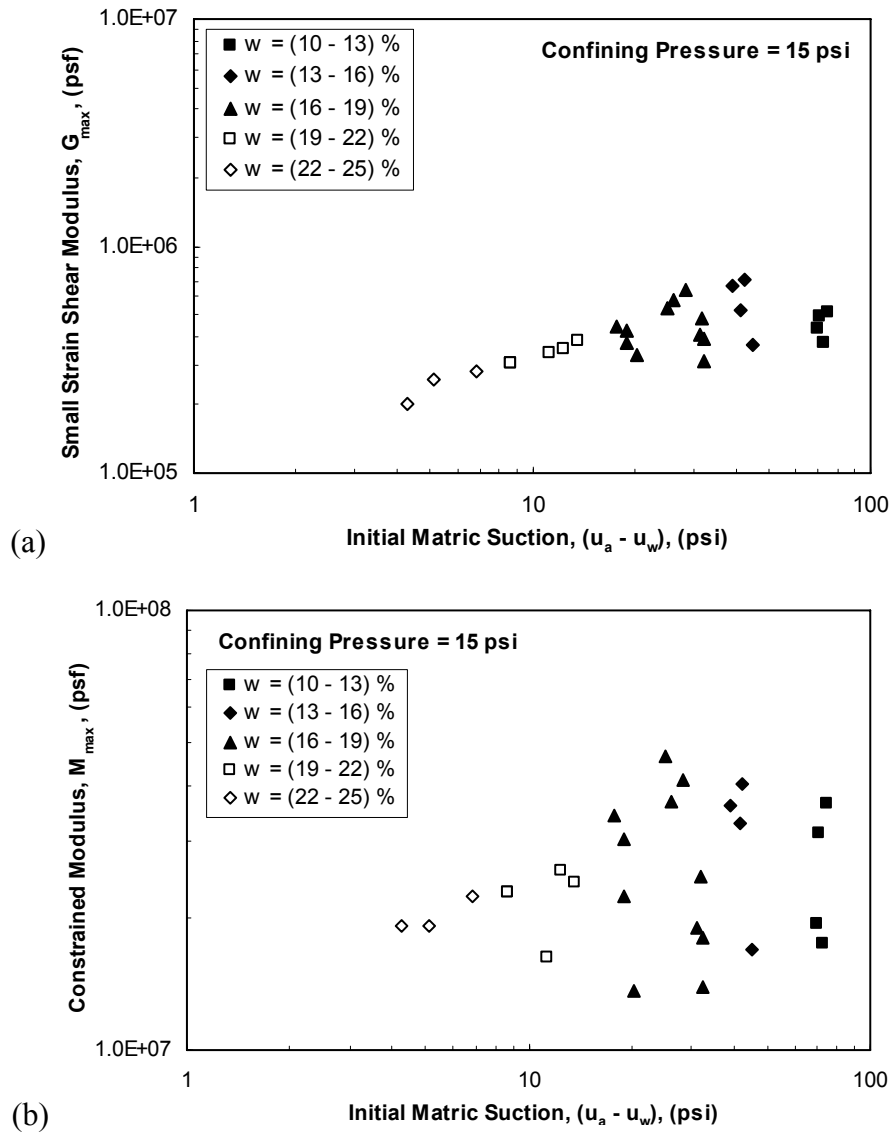


Figure 7.13. Measured values of (a) shear modulus and (b) constrained modulus vs matric suction.

Figure 7.14 displays the normalized moduli,  $G_{\max}/F(e)$  and  $M_{\max}/F(e)$ , versus matric suction. As the matric suction increases, the normalized shear modulus increases (Figure 7.14a), and with less scatter than the un-normalized values of  $G_{\max}$  (Figure 7.13a). The normalized constrained modulus slightly increases as the matric suction increases (Figure 7.14b), again with less scatter than the un-normalized values (Figure 7.13b).

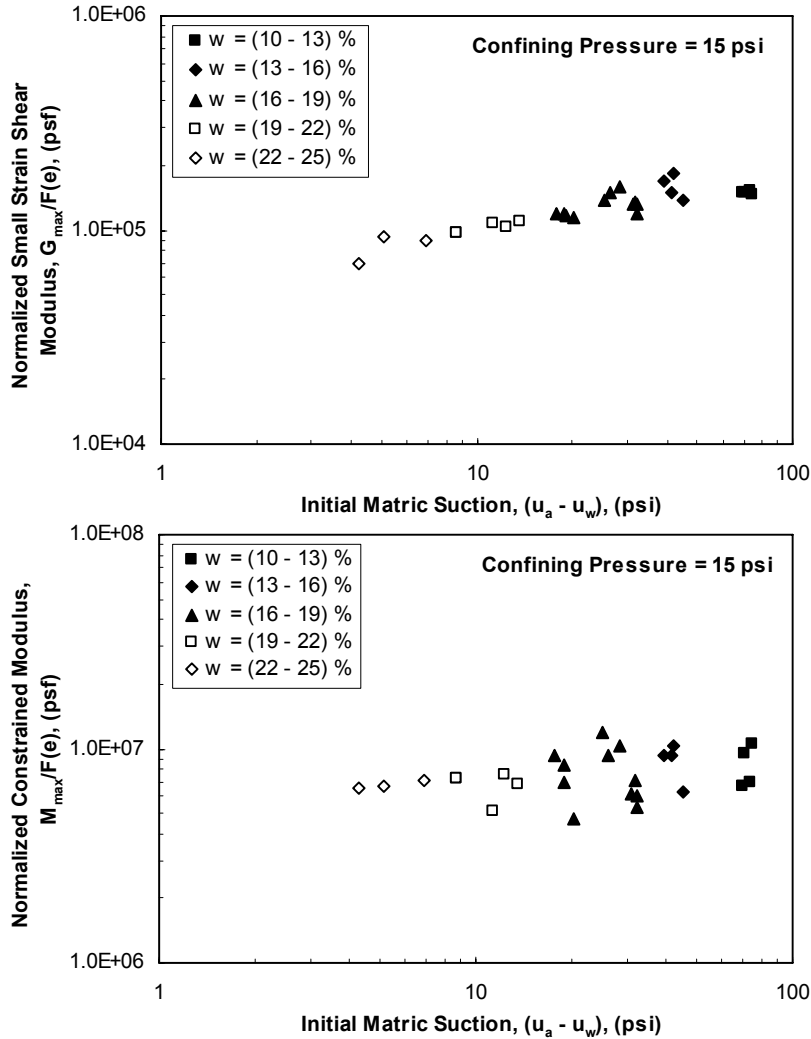


Figure 7.14. Normalized values of (a) shear modulus and (b) constrained modulus vs matric suction.

## 7.5 Summary

The suitability of using the stiffness at small strains to assess the compactness of fill materials was investigated. An experimental study was performed to consider the effect of the compaction water content and dry unit weight on the shear wave velocity, compression wave velocity, and matric suction of compacted clays. In addition, the variations of the small-strain shear and constrained moduli with matric suction were studied.

The results from this study indicate that the effect of the compaction water content on the shear wave velocity is more pronounced than that of the dry unit weight. At approximately the same dry unit weight, the shear wave velocity increased with decreasing water content. For compression wave velocity, the effect of the dry unit weight was more pronounced than that of the water content. At approximately the same dry unit weight, the compression wave velocity decreased slightly with increasing water content.

The matric suction measurements indicated that matric suction was primarily dependent on the compaction water content and almost independent of the dry unit weight. The shear modulus,  $G_{\max}$ , and constrained modulus,  $M_{\max}$ , increased with increasing matric suction for matric suction values ranging between 4 and 20 psi. At larger values of matric suction, the moduli values were scattered. However, the normalized moduli,  $G_{\max}/F(e)$  and  $M_{\max}/F(e)$ , which account for variations in void ratio, displayed less scatter when plotted versus matric suction.

This experimental study revealed that the stiffness of compacted clay is affected significantly by matric suction and less so by dry unit weight. Without fully characterizing the complex relationship between matric suction, dry unit weight, and stiffness, field measurements of stiffness alone are not suitable for evaluating the compactness of soil.



## 8. Conclusions and Recommendations

### 8.1 Summary and Conclusions

This study identified nine currently available devices as potential replacements for the nuclear gauge for soil compaction control. Three devices are based on impact testing: the PANDA dynamic cone penetrometer, the Clegg Impact Hammer, and the standard dynamic cone penetrometer (DCP). Three devices are based on measuring the electrical properties of the soil: the Moisture Density Indicator (MDI), the Electrical Density Gauge (EDG), and the Soil Quality Indicator (SQI). Three devices measure the stiffness properties of the soil: the Portable Seismic Property Analyzer (PSPA), the GeoGauge, and the Soil Compaction Supervisor (SCS). Generally, the electrical devices report measurements of dry unit weight and water content, while the impact and stiffness methods provide only an assessment of general compactness that can be related to relative compaction. After assessing the technical basis of each compaction control method and reviewing results from previous investigations, seven of the nine identified devices were selected for use in the experimental program in this study. The two devices that were not selected for further study were the GeoGauge and the SCS. The GeoGauge was not selected because of previously identified technical problems related to seating of the device and repeatability of measurements. The SCS was not selected because of its weak theoretical basis and lack of prior success.

The selected compaction control devices were evaluated through two field studies and one laboratory study. Field Study 1 focused on evaluating the five devices that were available during the first year of this study (PANDA, Clegg, DCP, SQI, and PSPA), while Field Study 2 focused on two electrical devices (MDI, EDG) that became available during the second year of this study. The Laboratory Study investigated two electrical devices (MDI, EDG), as well as the PANDA and Clegg Impact Hammer, under controlled compaction conditions in laboratory specimens. For each of these experimental studies, the measurements from the compaction control devices were compared with traditional measurements of dry unit weight and water content performed by the nuclear gauge, the rubber balloon method, and oven drying.

Field Study 1 produced data for three impact devices (PANDA, Clegg, and DCP) and one stiffness device (PSPA) on five different soils ranging from high plasticity clay to gravel. Data were collected with the SQI, but the required soil-specific calibration was not available from the manufacturer, and thus the data could not be converted into dry unit weight and water content. For the clayey soils, it was observed that the Clegg CIV and PSPA Young's Moduli were more influenced by water content than dry unit weight. The PANDA and DCP distinguished between locations with relatively low and relatively high dry unit weights, but the specific level of compaction could not be accurately assessed. For the sandy soil, the Clegg CIV and PSPA Young's Moduli generally increased with increasing dry unit weight. However, there was significant scatter in these data. The PANDA and DCP generally distinguished between locations with smaller and larger dry unit weights, but the assessment of adequate compaction from these measurements did not always agree with the direct measurements of dry unit weight and relative compaction. For the gravel soils, there was significant scatter in the Clegg CIV and the PSPA Young's Moduli, such that it would be difficult to use these devices for compaction control. The PANDA and DCP could only be used in the fine gravel and, again the assessment of compaction

from these devices did not always agree with the dry unit weight/relative compaction measurements from the nuclear gauge.

Field Study 2 focused on evaluating two electrical devices (MDI, EDG) at three construction sites in the Austin area. These sites encompassed CH, CL, and sandy clay (CH) soils. Because of time constraints in the field, the EDG could not be field-calibrated and was not used further in the field study. For dry unit weight, the MDI did not agree favorably with the dry unit weights measured by the nuclear gauge or rubber balloon. In the CH soil, dry unit weights measured with the MDI device were 10 to 20 percent larger than those from the nuclear gauge and rubber balloon, while in the CL soil the dry unit weights measured with the MDI device were about 10 percent smaller. In the sandy clay, all dry unit weight measurements by the MDI were within 10 percent of the nuclear gauge readings. For water content, the MDI did not agree favorably with either of the traditional methods (nuclear gauge, oven drying). The MDI measurements of water content in the CH soil were all smaller than the water contents measured by the nuclear gauge and oven drying. In the CL soil, the water content values measured by the MDI were larger than the water content values from the nuclear gauge and oven drying. MDI water contents for the sandy clay were significantly different than the water content values obtained from the nuclear gauge and oven drying. Because of issues related to electrical conductivity in clays (Yu and Drnevich 2004), it is not surprising that the MDI did not perform well in these materials.

The laboratory study of the compaction devices focused on evaluating four of the devices (MDI, EDG, PANDA, and Clegg) on laboratory-compacted specimens of poorly graded sand. The MDI consistently reported the same dry unit weight for each specimen, and this value did not agree with the rubber balloon measurements. The MDI water content measurements showed good agreement with the microwave oven measurements of water content. The EDG also consistently reported the same dry unit weight for each specimen (although this value was different than the MDI value), and again this value did not agree with the rubber balloon measurements. The EDG consistently measured a water content of 5 percent, which did not agree with the oven dry values. The Clegg Impact Hammer CIV values indicated a relative compaction of less than 100 percent for all specimens, although two specimens were compacted above 100 percent relative compaction. The PANDA Dynamic Cone Penetrometer accurately tracked the variation of dry unit weight across specimens, but did not always accurately identify the level of relative compaction.

Because some of the compaction control devices considered in this study, such as the PSPA, measure the stiffness of the soil in an effort to assess its compactness, an additional experimental laboratory study was performed to investigate whether soil stiffness is a suitable parameter to assess the compactness of compacted fills. In these experiments, the soil stiffness of compacted clay was characterized by the shear wave velocity and compression wave velocities. The matric suction was measured on additional specimens. These measurements were used to assess the effect of the compaction water content and dry unit weight on the shear wave velocity, compression wave velocity, and matric suction of compacted clays.

The results from the laboratory study of wave velocities indicate that the effect of the compaction water content on shear wave velocity is more pronounced than that of dry unit weight for clays. At approximately the same dry unit weight, the shear wave velocity increased with decreasing water content. For compression wave velocity, the effect of the dry unit weight was more pronounced than that of the water content. At approximately the same dry unit weight, the compression wave velocity decreased slightly with increasing water content. The matric

suction measurements indicated that matric suction was primarily dependent on the compaction water content and almost independent of the dry unit weight. The shear modulus and constrained modulus increased with increasing matric suction for matric suction values ranging between 4 and 20 psi.

## **8.2 Recommendations**

None of the non-nuclear devices examined in this study is currently feasible for replacing the nuclear gauge for field compaction control. Several of the devices (DCP, Clegg, PSPA) may provide a general assessment of compaction dry unit weight, but do not provide the precision required for compaction control. Many of the devices, including the DCP, Clegg, PANDA, and PSPA, do not provide a measure of water content, and thus require an additional means to measure water content. This issue is most important for the compaction control of clays, where water content is an important parameter.

While none of the devices examined in this study is currently ready to replace the nuclear gauge, two stand out as potential replacements if they are improved. First, the MDI has a sound theoretical basis in relating the dielectric constant and electrical conductivity to dry unit weight and water content. While there are issues using this device in clayey soils, and the device did not always provide accurate results in sandy soils, it is being improved and may be acceptable in the future. Second, the SQI also appears to have a good theoretical basis for relating electrical soil properties to dry unit weight and water content. If the manufacturer can develop a robust calibration procedure, this device may also be useful in the future. Finally, at least one additional device is currently being developed by researchers at the University of Wisconsin (Fratta et al. 2005). This device combines measurements of the electrical properties of the soil with compression wave velocity measurements to provide values of dry unit weight and water content for the soil. If this device becomes commercially available, it should also be considered for replacement of the nuclear gauge.



## References

- Adams, A. (2004), "Assessment of Rapid Methods for Density Control of MSE Walls and Embankments," M.S. thesis, Department of Civil, Architectural, and Environmental Engineering, University of Texas, Austin, TX.
- Agus, S.S., and Schanz, T. (2006). "Drying, wetting, and suction characteristic curves of a bentonite-sand mixture," Geotechnical Special Publication, No. 147, Vol. 2, pp. 1405-1414.
- ASTM (1994), "D 2167-94, Standard Test Method for Density and Unit Weight of Soil in Place by the Rubber Balloon Method," American Society of Testing and Materials, West Conshohocken, PA.
- ASTM (1999), "D 2216-99, Standard Test Method for Laboratory Determination of Water (Moisture) Content of Soil and Rock by Mass," American Society of Testing and Materials, West Conshohocken, PA.
- ASTM (1999), "D 3017-99, Standard Test Method for Water Content of Soil and Rock in Place by Nuclear Methods (Shallow Depth)," American Society of Testing and Materials, West Conshohocken, PA.
- ASTM (2000), "D 4643-00, Standard Test Method for Determination of Water (Moisture) Content of Soil by the Microwave Oven Heating," American Society of Testing and Materials, West Conshohocken, PA.
- ASTM (2000), "D 698-00, Standard Test Method for Laboratory Compaction Characteristics of Soil Using Standard Effort," American Society of Testing and Materials, West Conshohocken, PA.
- ASTM (2001), "D 2922-01, Standard Test Method for Density of Soil and Soil-Aggregate in Place by Nuclear Methods (Shallow Depth)," American Society of Testing and Materials, West Conshohocken, PA.
- ASTM (2002), "D 1557-02, Standard Test Methods for Laboratory Compaction Characteristics of Soil Using Modified Effort (56,000 ft-lbf/ft<sup>3</sup> (2,700 kN-m/m<sup>3</sup>)," American Society of Testing and Materials, West Conshohocken, PA.
- ASTM (2002), "D 5874-02, Standard Test Method for Determination of the Impact Value (IV) of a Soil," American Society of Testing and Materials, West Conshohocken, PA.
- ASTM (2003) "D 2850, Standard test method for unconsolidated-undrained triaxial compression test on cohesive soils," American Society of Testing and Materials, West Conshohocken, PA.

- ASTM (2005), "D 6780-05, Standard Test Method for Water Content and Density of Soil in Place by Time Domain Reflectometry (TDR)," American Society of Testing and Materials, West Conshohocken, PA.
- Ayers, P. and Bowen, H. (1988), "Laboratory Investigation of Nuclear Density Gauge Operation," Transactions of the American Society of Agricultural Engineers, Vol. 31, May.
- Bringoli, E.G.M., Gotti, M., and Stokoe, K.H. (1996). "Measurement of shear waves in laboratory specimens by means of piezoelectric transducers," *Geotechnical Testing Journal*, Vol. 19, No. 4, pp. 384-397.
- Burnham, T.R., 1997, "Application of the Dynamic Cone Penetrometer to Minnesota Department of Transportation Pavement Assessment Procedures," Report No. MN/RD - 97/19, Mn Dept. of Trans., Maplewood, MN, 37 pp.
- Cardenas, R. (2000), "Soil Compaction Meter Verification Testing—Summary Report," prepared for Gas Research Institute by Foster-Miller, Inc., Waltham, MA, [http://www.mbw.com/scm2000\\_prnt.htm](http://www.mbw.com/scm2000_prnt.htm), Accessed 11/03.
- Chen, D., Wu, W., He, R., Bilyeu, J., and Arrelano, M. (1999), "Evaluation of In-Situ Resilient Modulus Testing Techniques," *Geotechnical Special Publication*, n 89, p 1-11.
- Drnevich, V.P., Lin, C., Yi, Q., Yu, X., Lovell, J. (2001), "Real-Time Determination of Soil Type, Water Content, and Density Using Electromagnetics," Joint Transportation Research Program Final Report FHWA/IN/JTRP-2000/20, August.
- Durham, G. (2005), "Using TDR Technology for Earthwork Compaction Quality Control," Presentation to the California Geotechnical Engineers Association, January 15, [http://www.durhamgeo.com/pdf/m\\_test-pdf/paper/CGEA%20CA%20Jan%202005.pdf](http://www.durhamgeo.com/pdf/m_test-pdf/paper/CGEA%20CA%20Jan%202005.pdf), Accessed March 2006.
- Electrical Density Gauge, LLC (2004), "Electrical Density Gauge For Compacted Soil Users Manual," August.
- Ellis, R., and Bloomquist, D. (2003), "Development of Compaction Quality Control Guidelines that Account for Variability in Pavement Embankments in Florida," University of Florida Department of Civil and Coastal Engineering, [http://www.dot.state.fl.us/research-center/Completed\\_Proj/Summary\\_SMO/FDOT\\_BC287\\_rpt.pdf](http://www.dot.state.fl.us/research-center/Completed_Proj/Summary_SMO/FDOT_BC287_rpt.pdf), accessed 9/03.
- Evelt, S. (2000), "Nuclear Gauge Train-the-Trainer Course," USDA-Radiation Safety Staff, <http://www.cprl.ars.usda.gov/wmru/pdfs/gauge-1.pdf>.
- Fratta, D., Alshibli, K., Tanner, W., and Roussel, L. (2005) "Combined TDR and P-wave velocity measurements for the determination of in situ soil density-experimental study," *Geotechnical Testing Journal*, v 28, n 6, November, 2005, p 553-563.
- Fredlund, D.G., and Rahardjo H. (1993). "Soil mechanics for unsaturated soils."

- Geneq Inc. (2006), <http://www.geneq.com/catalog/en/edg/html>, Accessed May 2006.
- GTI (2004), "Evaluation of Soil Compaction Measuring Devices," Prepared by Distribution and Pipeline Technology Divisions, Gas Technology Institute, April.
- Gonzalez, N.A., and Colmenares, J.E. (2006). "Influence of matric suction on the volume change behaviour of a compacted clayey soil," *Geotechnical Special Publication*, No. 147, Vol. 1, pp. 825-836.
- Gucunski, N., and Maher, A. (2002), "Evaluation of Seismic Pavement Analyzer For Pavement Condition Monitoring," Department of Civil & Environmental Engineering at Rutgers University, May.
- Hardin, B.O., and Black, W.L. (1968), "Vibration modulus of normally consolidated clay," *Journal of Soil Mechanics and Foundations Division, ASCE*, Vol. 94, No. SM2, pp. 353-369.
- Heitzler, F., Cardenas, R., George, D., Pasch, K., and Deguire, D. (1995), United States Patent 5426972, June 1995, <http://patft.uspto.gov/netacgi/nph-parser?Sect1=PTO1&Sect2=HITOFF&d=PALL&p=1&u=/netahtml/srchnum.htm&r=1&f=G&l=50&s1=5426972.WKU.&OS=PN/5426972&RS=PN/5426972>, Accessed 11/03.
- Humboldt Mfg. Co. (1999a), "GeoGauge User Guide, version 3.1," Norridge, IL, September.
- Juran, I., and Rousset, A. (1999), "A Soil Compaction Control Technology Assessment and Demonstration," *Proceedings of the APWA International Public Works Congress and Exhibition*, Denver, CO, September 19-22, <http://irc.nrc-cnrc.gc.ca/fulltext/apwa/apwacompaaction.pdf>, Accessed September 2003.
- Ladd, R.S. (1978), "Preparing Test Specimens Using Undercompaction," *Geotechnical Testing Journal*, GTJODJ, Vol. 1, No. 1, March, pp. 16-23.
- Langton, D. (1999), "The Panda Lightweight Penetrometer for Soil Investigation and Monitoring Material Compaction," Soil Solution Ltd, [http://www.solution.com/telechargement/article\\_doug\\_ground\\_engineering1.pdf](http://www.solution.com/telechargement/article_doug_ground_engineering1.pdf), Accessed Sept. 03.
- Lenke, L., Grush, M., and McKeen, R. (1999), "Evaluation of the Humboldt GeoGauge™ on Dry Cohesionless Silica Sand in a Cubical Test Bin," ATR Institute, University of New Mexico, [http://www.hanmicorp.net/MFG/Humboldt/GeoGauge/GeoGauge--Reports/ATR\\_Report\\_GeoGauge.PDF](http://www.hanmicorp.net/MFG/Humboldt/GeoGauge/GeoGauge--Reports/ATR_Report_GeoGauge.PDF), accessed 9/03.
- Leong, E.C., Cahyadi, J., and Rahardjo, H. (2006). "Stiffness of a compacted residual soil," *Geotechnical Special Publication*, No. 147, Vol. 1, pp. 1169-1180.
- Mancuso, C., Vassallo, R., and d'Onforio, A. (2002). "Small strain behavior of a silty sand in controlled-suction resonant column–torsional shear tests," *Canadian Geotechnical Journal*, Vol. 39, No. 1, pp. 22-31.

- Marinho, E.A.M., Chandler, R.J., and Crilly, M.S. (1995). "Stiffness measurements on an unsaturated high plasticity clay using bender elements," Proceedings of the 1<sup>st</sup> International Conference on Unsaturated Soils, Paris, Vol. 1, pp. 535-539.
- MBW, Inc. (2003), "Soil Compaction Supervisor," Publication # L16489, June.
- Mendoza, C.E., Colmenares, J.E., (2006). "Influence of the suction on the stiffness at very small strains," Geotechnical Special Publication, No. 147, Vol. 1, pp. 529-540.
- Mendoza, C.E., Colmenares, J.E., and Merchan, V.E. (2005). "Stiffness of an unsaturated compacted clayey soil at very small strains," Advanced Experimental Unsaturated Soil Mechanics—Trento, Italy, 27-29 June, pp. 199-204.
- Miller, H., and Mallick, R. (2003), "Field Evaluation of a New Compaction Monitoring Device," prepared for the New England Transportation Consortium.
- Nazarian S., Baker, M., and Crain, K. (1997), United States Patent 5614670, March, <http://patft.uspto.gov/netacgi/npharser?Sect1=PTO1&Sect2=HITOFF&d=PALL&p=1&u=/netahtml/srchnum.htm&r=1&f=G&l=50&s1=5,614,670.WKU.&OS=PN/5,614,670&RS=PN/5,614,670> Accessed 2/15/04.
- Nelson, C, and Sondag, M. (1999), "Comparison of the Humboldt GeoGauge<sup>TM</sup> with In-Place Quasi-Static Plate Load Tests," CNA Consulting Engineers, Minneapolis, MN.
- Olson, R.E., and Langfelder, L.J. (1965). "Pore water pressures in unsaturated soils," Journal of Soil Mechanics and Foundations Division, ASCE, Vol. 91, No. SM4, pp. 127-150.
- Ooi, P.S.K., and Pu, J. (2002). "Evaluating compaction of tropical soils using soil stiffness," Bearing capacity of roads, railways and airfields: Proceedings of the 6<sup>th</sup> International Conference on the Bearing Capacity of Roads and Airfields, Lisbon, Portugal, pp. 1143-1149.
- Peterson, A., and Wiser, D. (2003), "What Measures Backfill Compaction Best?," Gas Utility Manager Magazine, January, <http://www.gasindustries.com/articles/jan03b.htm>, Accessed 11/03.
- Picornell, M., and Nazarian, S. (1998). "Effect of soil suction on the low-strain shear modulus of soils," Proceedings of the 2<sup>nd</sup> International Conference on Unsaturated Soils, Beijing, China, Vol. 2, pp. 102-107.
- Qian, X., Gray, D.H., and Woods, R.D. (1991). "Resonant column tests on partially saturated sands," Geotechnical Testing Journal, Vol. 14, No. 3, pp. 266-275.
- Rivat, F. (2005), personal communication, August 22.
- Salem, M. (2007) "Stiffness of unsaturated compacted clays at small strains," Ph.D. Dissertation, University of Texas at Austin.

- Sawanguriya, A., Edil, T.B., Bosscher, P.J., and Wang, X. (2006). "Small-strain stiffness behavior of unsaturated compacted subgrade," *Geotechnical Special Publication*, No. 147, Vol. 1, pp. 1121-1132.
- Simmons, C. (2000) "Letter of Finding: Memorandum to the Missouri Department of Transportation Research, Development and Technology Division," July 25.
- Sivakumar, V., and Wheeler, S.J. (2000). "Influence of compaction on the mechanical behaviour of an unsaturated compacted clay. Part 1: wetting and isotropic compression," *Geotechnique*, Vol. 50, No. 4, pp. 359-368.
- Sol-Solution (2006), [www.sol-solution.com/pandaa.html](http://www.sol-solution.com/pandaa.html), Accessed March 2006.
- Stephenson, R.W. (1978). "Ultrasonic testing for determining dynamic soil moduli," *Dynamic Geotechnical Testing*, ASTM STP 654, ASTM International, West Conshohocken, PA, pp. 179-195.
- Texas Department of Transportation (2004a), "Standard Specifications for Construction and Maintenance of Highways, Streets, and Bridges: Item 132: Embankment," Adopted by the Texas Department of Transportation, June 1.
- Texas Department of Transportation (2004b), "Standard Specifications for Construction and Maintenance of Highways, Streets, and Bridges: Item 423: Retaining Walls," Adopted by the Texas Department of Transportation, June 1.
- Tobin, R.E. (2006) "Assessment of Rapid, Non-nuclear Compaction Control Devices," M.S. Thesis, Department of Civil, Architectural, and Environmental Engineering, University of Texas, Austin, TX.
- TransTech Systems (2003), "Measurement of the Density and Water Content of Soil Using Impedance Spectroscopy," Technical Note 0303, February 26.
- Vassallo, R., and Mancuso, C. (2000). "Soil behavior in the small and the large strain range under controlled suction conditions," *International Workshop on Unsaturated Soils—Trento, Italy*, 10-12 April.
- Vinale, F., D'Onofrio, A., Mancuso, C., Santucci de Magistris, F., Tatsuoka, F. (1999). "The pre-failure behaviour of soils as construction materials," *Pre-Failure Deformation Characteristics of Geomaterials*, pp. 955-1007.
- Wu, S., Gray, D.H., and Richart, F.E. (1984). "Capillary effects on dynamic modulus of sands and silts," *Journal of Geotechnical Engineering*, Vol. 110, No. 9, pp. 1188-1203.
- Yu, X. and Drnevich, V.P. (2004), "Soil Water Content and Dry Density by Time Domain Reflectometry," *Journal of Geotechnical and Geoenvironmental Engineering*, Vol. 130, No. 9, September.